THE UNIVERSITY
of EDINBURGH

The role of Prolyl Hydroxylase Domain enzymes in normal and malignant haematopoiesis

Hannah Lawson

A thesis submitted in fulfilment of the requirements for the degree of Doctor of Philosophy

University of Edinburgh

Author's Declaration

I declare that this thesis has been composed solely by myself and that it has not been submitted, in whole or in part, in any previous application for a degree. Except where states otherwise by reference or acknowledgment, the work presented is entirely my own.

Hannah Lawson

May 2019

Abstract

Acute Myeloid Leukaemia (AML) arises from a dysregulation in haematopoietic stem and progenitor cells (HSPCs), leading to the production of highly proliferative blast cells. Current chemotherapies can eliminate these cells but fail to eradicate the leukaemic stem cell (LSC) source. There has been increasing interest in the microenvironment in which LSCs, as well as their haematopoietic stem cell (HSC) counterparts reside, with particular focus on the hypoxic nature of the niche. As such, this led us to investigate Hypoxia Inducible Factors (HIFs) in leukaemia development where our previously published data shows that HIFs are tumour suppressors in AML.

This thesis builds on this work, investigating the therapeutic potential of Prolyl Hydroxylases Domain (PHD) inhibition, which stabilises HIFs. Results show that deletion of the *Phd* isoforms *Phd1* and *Phd2* reduces leukaemic transformation and development *in vitro.* Additionally, when leukaemic cells deficient in *Phd1* and *Phd2* were transplanted into syngeneic lethally irradiated recipient mice, there was a reduction in leukaemic engraftment, resulting in an increase in disease latency when compared to the control cells. In addition, I further validated this result by using a doxycycline-inducible shRNA model to knockdown levels of *Phd2* in leukaemic cells. Mirroring the results of the gene deletion study, *Phd2* knockdown led to a regression of leukaemia both *in vitro* and *in vivo.*

To further validate PHDs as therapeutic targets in AML, I investigated the impact of deletion of *Phd1* and *Phd2* specifically in the hematopoietic system using *Vav-iCre*. Steady state analysis of the HSPC and differentiated cell compartments found there were no significant differences when compared to control mice. Moreover, further utilising the inducible shRNA model, I acutely deleted Phd2 *in vivo*, discovering a decrease in the frequency and functionality of the HSC compartment, with no other discernible phenotypes. Given there were no significant detrimental effects on normal haematopoiesis, this study provides a strong rationale for studying the inhibition of *Phds* in combination with current chemotherapeutic regimes, aiming to provide targeted therapies for AML.

Lay Summary

Acute Myeloid Leukaemia (AML) is an aggressive blood cancer, with poor long-term survival outcomes due to high rates of fatal disease relapse. Importantly these problematic disease relapses are caused by leukaemic stem cells (LSCs), which are highly mutated forms of normal haematopoietic stem and progenitor cells (HSPCs) that sustain blood production throughout life. Both HSPCs and their LSC counterparts reside in bone marrow microenvironment, which is very low in oxygen, known as hypoxia. Cells adapt to this low oxygen condition through the HIF (Hypoxia Inducible Factor) pathway. Deleting HIF, the orchestrator of this pathway, increased the potency of LSCs, making the disease more aggressive. This thesis found that stabilising HIF levels, through deletion of the HIF-inhibitor PHD, decreased LSC potency, reducing the disease burden in mice. Using a PHD inhibitor in collaboration with current chemotherapies holds great promise for effective AML treatment.

Table of Contents

Table of Figures

Table of Tables

Related Publications

Vukovic M., Sepulveda C., Subramani C., Guitart A. V., Mohr J., Allen L., Panagopoulou T. I., Paris J., **Lawson H**., Villacreces A., Armesilla-Diaz A., Gezer D., Holyoake T. L., Ratcliffe P. J. and Kranc K. R. (2016). Adult hematopoietic stem cells lacking Hif-1α self-renew normally. *Blood*, *127*(23), 2841–2846.

Guitart A., Panagopoulou P., Villacreces A., Vukovic M., Sepulveda C., Allen L., Carter R., van de Lagemaat L., Morgan M., Giles P., Sas Z., Gonzalez M., **Lawson H**., Paris J., Edwards-Hicks J., Schaak K., Subramani C., Gezer D., Armesilla-Diaz A., Wills J., Easterbrook A., Coman D., So C., O'Carroll D., Vernimmen D., Rodrigues N., Pollard P., Morton N., Finch A and Kranc K. R. (2017). Fumarate hydratase is a critical metabolic regulator of haematopoietic stem cell functions. *JEM*, *214* (3), 719.

O'Duibhir O., Paris J., **Lawson H**., Vukovic M., Sepulveda C., Shenton D., Carragher N and Kranc K. R. (2018). Machine learning enables live label-free phenotypic screening in three dimensions. *ASSAY and Drug Development Technologies*, *16*(1).

Abbreviations

ABBREVIATION	MEANING
2OG	2-oxoglutarate
AGM	Aorta-gonad mesonephros
AML	Acute myeloid leukaemia
ALL	Acute lymphocytic leukaemia
BM	Bone marrow
bp	base pairs
CAG	Cytomegalovirus early enhancer element and chicken β-actin
CAR	CXCL12-abundant reticular cells
CFC	Colony-forming cell
CFU-S	Colony-forming unit spleen
cKit	Tyrosine-protein kinase (mast/stem cell growth factor receptor (SCFR) or CD117)
CLP	Common lymphoid progenitor
CMP	Common myeloid progenitor
Cola1	Collagen type I gene
CXCL12	CXC motif chemokine 12
DMEM	Dulbecco's modified eagle's medium
Dox	Doxycycline
DPC	Days post cotium
E	Embryonic day
EDTA	Ethylenediaminetetraacetic acid
FACS	Fluorescence-activated cell sorting
FBS	Foetal bovine serum
FCS	Foetal Calf Serum
FIH	HIF-inhibitory protein
FL	Foetal liver
FLT3	Fms related tyrosine kinase 3
FSC	Forward Scatter
GATA2	GATA binding protein 2
GFP	Green fluorescent protein
GM	Granulocyte/macrophage
GM-CSF	Granulocyte-macrophage colony-stimulating factor
GMP	Granulocyte/macrophage progenitor
Gy	Gray
h	hours
HET	Heterozygous
HIF	Hypoxia inducible factor
HOXA9	Homeobox A9
HPC-1	Haematopoietic progenitor cell-1
HPC-2	Haematopoietic progenitor cell-2
HRE	Hypoxia response element
HSC	Haematopoietic stem cell
HSPC	Haematopoietic stem and progenitor cell
iCre	Improved Cre recombinase

IL	Interleukin
IMDM	Iscove's modified dulbecco's medium
IT-HSC	Intermediate-term haematopoietic stem cell
KO	Knockout
LDA	Limiting dilution assay
Lineage (Lin^-)	Haematopoietic cell population that does not express mature haematopoietic marker
LK	$Lineage^-$ $cKit^+$
LMO2	LIM domain only 2
LMPP	Lymphoid-primed multipotent progenitors
LSC	Leukaemic stem cell
LSK	$Lineage^-$ $Sca\text{-}1^+$ $cKit^+$
LT-HSC	Long-term haematopoietic stem cell
MEIS	Myeloid ectropic insertion site
MEP	Megakaryocyte/erythroid progenitors
Mk	Megakaryocyte
MLL	Mixed lineage leukaemia
MLL-AF9	Mixed lineage leukaemia translocated AF9 protein
MPP	Multipotent progenitor
MSC	Mesenchymal stem cells
MSCV	Murine stem cell virus
O_2	Molecular oxygen
ON	Overnight
P300/CBP	P300/Creb-binding protein
PB	Peripheral blood
PBS	Phosphate-buffered saline
PHD	Prolyl hydroxylase domain
Pre-LSCs	Pre-leukaemic stem cells
PU.1	Purine-rich sequence 1
qPCR	Quantitative Polymerase Chain Reaction
RBC	Red blood cells
RT	Room temperature
RT-PCR	Reverse Transcriptase Polymerase Chain Reaction
rtTA	Tetracycline-dependent transactivator
RUNX1	Runt-related transcription factor 1
SCA-1	Stem cell antigen-1
SCF	Stem cell factor
SCL	Stem cell leukaemia
shRNA	short-hairpin RNA
SLAM	Signalling lymphocyte activation molecule
SSC	Side scatter
ST-HSC	Short-term haematopoietic stem cell
Tet	Tetracycline
TF	Transcription factor
VEGF	Vascular endothelial growth factor
VHL	Von Hippel-Lindau
WT	Wild type

Acknowledgements

I'd like to thank Professor Kamil Kranc for all the valued support and mentorship.

The 'Kranquinhos' for teaching me a lot about science, but even more about life and friendship. I have you all to thank for this thesis and pretty much everything else in my life.

All present & past lab members & SCRM staff for their kindness, guidance & company. Even on the worst days, I truly had the best time with all of you.

My Hamilton and Glasgow girls, so many years of friendship, and many more to come.

My mum, dad, and best pal Sophie.

Finally, to Edinburgh, for being my home for 3 years, and re-igniting my love for Glasgow.

CHAPTER 1

Introduction

Chapter 1 Introduction

1.1 Haematopoiesis

Haematopoiesis describes the commitment and differentiation processes that lead to the production of all blood components required to sustain life. All blood cells are derived from a rare population of multipotent haematopoietic stem cells (HSCs), which reside at the top of the haematopoietic hierarchy, and undergo several discrete steps to produce mature, functional blood cells (Ema et al., 2014).

The discovery and biology of HSCs began in the 1950s, with two groups performing bone marrow (BM) transplantations on lethally irradiated mice and guinea pigs. After receiving the donor BM cells, the animals were rescued from lethality, and were seen to have developed functional myeloid and lymphoid differentiated cells, indicating the BM contained HSCs capable of repopulating the entire blood system (Jacobson et al., 1951; Lorenz et al., 1951). Further seminal research conducted by Till and McCulloch in 1961 utilised the *in vivo* colony-forming spleen (CFU-S) assay, to confirm the existence of clonogenic BM cells, and their ability to produce multilineage haematopoietic colonies in the spleens of lethally irradiated recipient mice. Moreover, it was discovered that a small fraction of these cells were able to reconstitute the entire haematopoietic system of secondary recipient mice, proving that HSCs can yield multilineage haematopoiesis, but also retain their stem-cell properties.

More recent studies have developed upon this notion, and have confirmed that HSCs reside at the top of a complex haematopoietic hierarchy, giving rise to progenitors which are progressively more restricted in their lineage, until unilineage terminal differentiation occurs, producing mature blood cells such as red blood cells (RBCs), megakaryocytes, myeloid and lymphoid cells. HSCs, as stem cells, are also capable of self-renewal, producing additional HSCs to sustain the haematopoietic demand of the organism (Morrison et al., 1994; Orkin and Zon, 2008).

HSCs are functionally defined by their unique capacity to reconstitute the entire haematopoietic system of an organism, and as such have been used extensively in the clinic as a treatment for BM failure or haematological malignancies (Orkin and Zon, 2008).

1.1.1 Early haematopoiesis

Since the process of hematopoiesis is conserved throughout all vertebrate species, animal models, such as mice, have been used to supplement and develop the study of human hematopoiesis (Orkin and Zon, 2008).

Early murine studies found that haematopoiesis occurs in multiple stages in specific anatomical sites (Johnson and Moore, 1975; Medvinsky and Dzierzak, 1996; Moore et al., 1972; Palis et al., 1999). As described in **Figure 1-1**, in mice, haematopoiesis originates in the yolk sac blood islands at embryonic day (E) 7.5, functioning to produce RBCs to oxygenate various tissues in the embryo as it develops. Megakaryocytes and macrophages are also produced in an aid to dispose of apoptotic cells and debris generated during the embryonic development process (Serrano et al., 2012). This initial wave of haematopoietic cell production is termed the "primitive wave", which is rapidly replaced by the "definitive wave" of haematopoiesis. The next stage in the development of the haematopoietic system occurs in the aorta-gonad mesonephros (AGM) region, in which definitive HSCs emerge at E 10.5 (Medvinsky and Dzierzak, 1996). Notably, at day E 10.5, there is limited HSC activity, whereas at E 11, the HSCs are functional, and thus capable of reconstituting lethally irradiated recipients. Notably, at this point in embryonic development, there are also HSCs present in the placenta (Alvarez-Silva et al., 2003). However, it is still debated if these cells arise from do novo generation, or blood circulation. Additionally, their contribution to the adult HSC population still remains largely contested (Gekas et al., 2005; Ottersbach and Dzierzak, 2005).

The definitive wave of haematopoiesis continues with the colonisation of the foetal liver (FL) at E 12.5, where active haematopoiesis occurs at E 14.5. As such, the FL is the main site of embryonic haematopoiesis, where HSCs will expand and differentiate, producing the hierarchical haematopoietic system (Kumaravelu et al., 2002; Morrison et al., 1995). Shortly before birth, the thymus, spleen and BM are colonised between E 16 and E 17, ready to support the adult hematopoietic system (Clapp et al., 1995; Zanjani et al., 1993).

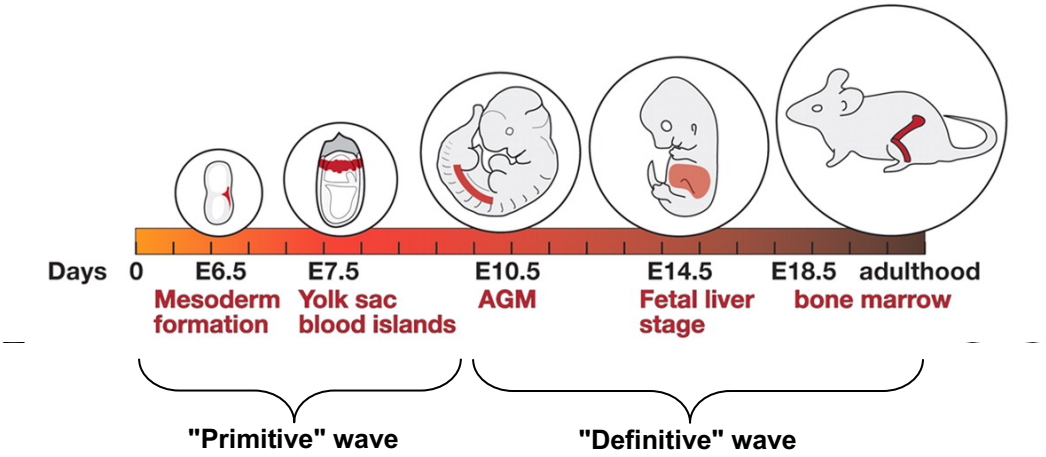

Figure 1-1 - Sites of HSC emergence during murine embryonic development. The mesoderm forms during gastrulation at embryonic (E) day 6.5, followed by the development of the yolk sac blood islands at E 7.5. The definitive wave of haematopoiesis begins with the emergence of HSCs in the aorta-gonad mesonephros (AGM) region at E 10.5. Active haematopoiesis occurs in the foetal liver (FL) at E 14.5 and is followed by colonisation of the bone marrow (BM) from E 18.5 into adulthood (Taken from Baron et al., 2012).

1.1.2 Properties of HSCs

HSCs are a relatively rare stem cell population at the apex of the haematopoietic differentiation hierarchy. These cells sustain adult haematopoiesis through their ability to self-renewal, maintaining the HSC pool, as well as differentiating into all mature blood lineages (Na Nakorn et al., 2002; Till and Mc, 1961).

HSCs, like other tissue stem cells, rely heavily on their microenvironment to regulate their biology (Ferraro et al., 2010). As such, changes in the stem cell microenvironment during embryogenesis impacts the intrinsic properties of HSCs. For example, due to the demanding requirements of the developing embryo, foetal liver HSCs are shown to actively cycle. Contrastingly, BM HSCs are largely quiescent, which protects them from genotoxic stress, while ensuring their long-term functionality in case of stress or injury (Arai and Suda, 2007; Essers et al., 2009; Orford et al., 2008). Notably, HSC quiescence can also have a detrimental effect, with nonhomologous end joining (NHEJ)-mediated DNA repair found to promote genetic mutation in these resting HSCs (Milyavsky et al., 2010; Mohrin et al., 2010)

When directed to exit quiescence, HSCs enter the cell cycle, typically dividing asymmetrically to produce one daughter cell resembling the parent, a process known as self-renewal, while the other will differentiate into a mature blood cell (Clevers, 2005; Doe and Bowerman, 2001) However, under conditions of stress, such as injury or transplantation, HSCs can also divide symmetrically, where daughter cells will share the same fate (Zhang et al.). HSCs can undergo other cellular fates such as apoptosis, which regulates the fitness and numbers of HSCs (Domen et al., 2000). Notably, dysregulation in these division processes can lead to serious pathological conditions such as BM failure or haematological malignancies (Blank and Karlsson, 2015).

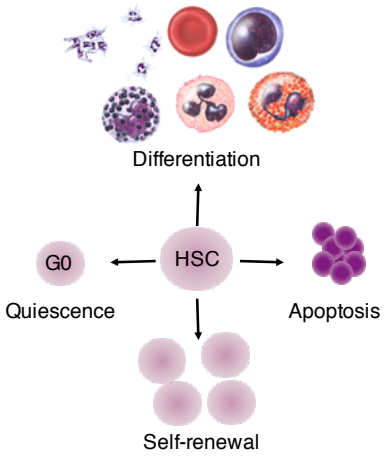

Figure 1-2 - HSC fates The tight regulation of adult HSCs protects the stem cell pool, whilst maintaining mature blood cell differentiation under steady state and stress conditions. Adult HSCs are primarily in a quiescent state, but upon entering the cell cycle, can self-renew, or differentiate, ultimately yielding mature functional haematopoietic cells. HSCs can also undergo apoptosis in an aid to regulate the fitness and quality of HSCs.

1.1.3 The haematopoietic hierarchy

Following seminal HSC transplantation experiments in the 1950s and 1960s (Jacobson et al., 1951; Lorenz et al., 1951; Till and Mc, 1961), haematologists in the 1970s and 1980s sought out to define the haematopoietic hierarchical process, ultimately proposing a tree-like roadmap, hypothesising haematopoiesis as a step-wise differentiation process, from multi-potent HSCs, to oligo- and unipotent progenitors (Abramson et al., 1977). Initial experiments using invasive stable clonal labelling, which were later replaced by the identification and use of cell-surface markers, allowed researchers to define the differentiation process in blood lineages (Lemischka et al., 1986). Following the successful and efficient isolation of pure HSCs using various combinations of cell-surface markers, the study of HSCs and their progeny evolved into a complex, and often controversial field (Adolfsson et al., 2001; Goodell et al., 1996; Oguro et al., 2013)

The original haematopoietic hierarchy, referred to as a the "classical" haematopoietic hierarchy roadmap, describes a distinct differentiation process from HSCs to their progeny. As shown in **Figure 1-3A**, this hierarchy divides HSCs, at the peak of hematopoiesis, into two distinct populations; long-term (LT)-HSCs, followed by short-term (ST) HSCs, placed further down the hierarchy (Ikuta and Weissman, 1992; Morrison et al., 1994; Spangrude et al., 1988). Notably, utilising *in vivo* limiting dilution assay (LDA) transplantation experiments, Morrison and Weissman in 1994 found that LT-HSCs were indeed able to provide successful long-term hematopoietic repopulation of irradiated recipient organisms, whereas ST-HSCs had a limited self-renewing capacity, able to sustain haematopoiesis in recipient organisms for 8 to 12 weeks. In 1997, Morrison and colleagues identified multipotent progenitor (MPP) cells, which were able to give rise to both myeloid and lymphoid lineages, but had no detectable self-renewal potential compared to HSCs.

Experiments by Konodo et al in 1997, and Na Nakorn et al in 2002, identified common lymphoid progenitors (CLPs), a progenitor cell population restricted to the lymphoid lineage, and common myeloid progenitors (CMPs), which give rise to mature myeloid cells. Both

populations are derived from MPPs, and together, in turn, differentiate into all functional blood cells.

In 2010, the "classical" haematopoietic hierarchy roadmap was updated to include a transitory HSC population referred to as intermediate-term (IT) HSCs, whose self-renewal ability falls between LT-HSCs and ST-HSCs (Benveniste et al., 2010; Yamamoto et al., 2013). Additionally, the MPP population was sub-divided into 4 distinct populations (MPP1, MPP2, MPP3 and MPP4), based on their immunophenotyped, BM abundance, cell-cycle status and differentiation ability. As shown in **Figure 1-3B**, the MPP1 population shares similar properties to that of the ST-HSCs, whereas MPP2 has a myeloid differentiation bias, and MPP4, a lymphoid differentiation bias (Cabezas-Wallscheid et al., 2014; Oguro et al., 2013; Pietras et al., 2015). Furthermore, Adolfsson and colleagues in 2005 discovered a sub-population of HSCs, with high expression of Flt3, ultimately defined as lymphoid-primed multipotent progenitors (LMPPs), sharing many characteristics with the MPP4 population (Forsberg et al., 2006).

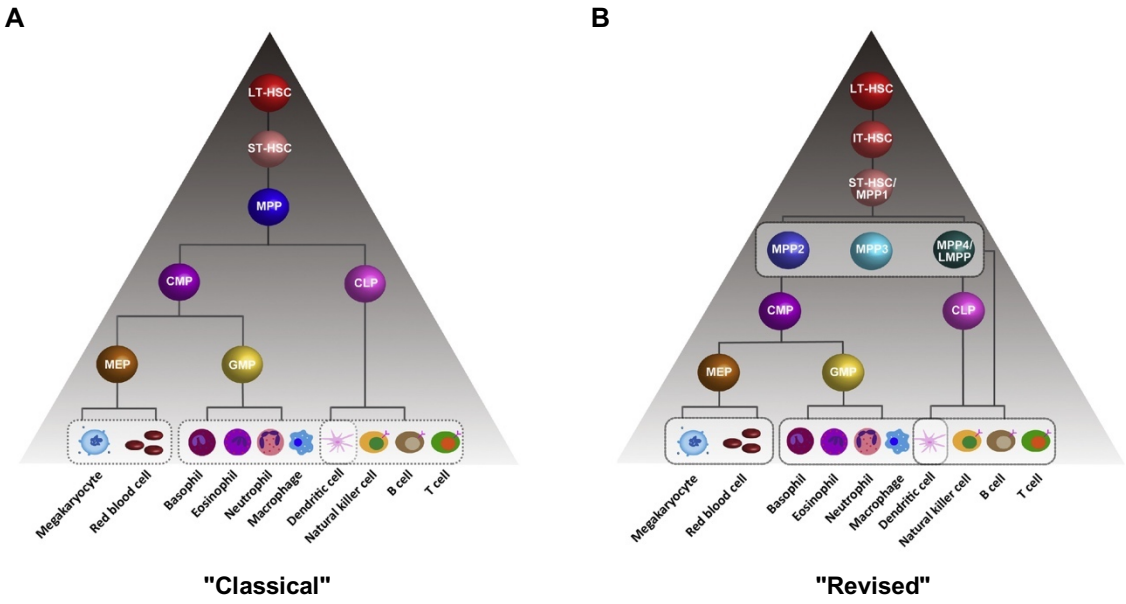

Figure 1-3 - Classical and revised haematopoietic hierarchy roadmaps (A) The "classical" model of the hematopoietic hierarchy describes long terms (LT) HSCs and short term (ST) HSCs, respectively, at the apex of the differentiation hierarchy. The HSCs give rise to multi-potent progenitor (MPP) cells, which, in turn, commit to either a committed lymphoid progenitor (CLP), which differentiate into lymphocytes, or committed myeloid progenitor (CMP). CMPs produce mature myeloid cells through the megakaryocyte/erythrocyte progenitor (MEP), or granulocyte/macrophage progenitor (GMP). **(B)** In the revised roadmap, LT-HSCs, IT-HSCs and ST-HSCs are all multipotent progenitors occupying the top of the hierarchy. HSCs then differentiate into MPP2, MPP3, and MPP4/LMPP cells. The MPP2 population gives rise to CMP cells, whereas MMP4/LMPP cells differentiate to yield cells of the lymphoid lineage. (Taken from Zhang et al., 2018).

1.1.3.1 Advances in the haematopoietic hierarchy

Until recently, dissection of the haematopoietic hierarchy relied upon functional transplantation assays, and well as cell-surface markers, identifying distinct, obvious hierarchical boundaries (Laurenti and Gottgens, 2018). Innovation in experimental design and techniques, such as single-cell RNA sequencing, gave rise to the study of individual HSCs, tracking their journey from the most primitive stem-cell status, to their differentiated cell fate (Zhang et al., 2018).

Computational analysis of high-throughput single-cell transcriptome data has been used to study the interaction dynamics between haematopoietic cells. Conducted in both zebrafish and murine models, these studies have unmasked the true nature of the haematopoietic process (Alemany et al., 2018; Briggs et al., 2018; Farrell et al., 2018). Using this strategy, multiple groups identified that instead of existing as a distinct, step-wise hierarchy, haematopoiesis occurs as a continuous process. In addition, lineage tracing experiments conducted by Sawai et al in 2016 verified that HSCs support endogenous steady-state haematopoiesis. Thus, the hierarchy is maintained by low-primed undifferentiated haematopoietic stem and progenitor (HSPC) cells, which gradually differentiate into mature functional blood cells (Plass et al., 2018; Velten et al., 2017).

Seminal work by Mansson and colleagues in 2007 further challenged the "classical" haematopoietic hierarchy by discovering that lineage segregation occurs during early haematopoiesis and does not rely upon linear hierarchical differentiation processes. In these studies, Sanjuan-Pla et al in 2013 found that some HSCs in their primitive state were found to have high expression of the von Willebrand factor (*Vwf),* a megakaryocyte-specific gene. Upon transplantation, these vWF^{+} HSCs had robust short- and long-term reconstitution ability for megakaryocytes. In concordance with this, more recent studies have found that the generation of megakaryocytes can bypass the stages of MPP, CMPs and MEPs, and can directly differentiate from HSCs (Notta et al., 2016). Moreover, it is now evident that within the immunophenotypically cell-surface marker defined HSC compartment, there is a population of HSCs which are not multipotent, but are instead pre-disposed to a lineage fate (Copley et al.,

2012; Muller-Sieburg et al., 2012). Tang et al in 2017, and Buenrostro et al in 2018 found that heterogenic HSCs retain their HSC-linked gene expression signature, but have altered chromatin architecture at lineage-specific gene loci, thus directing their lineage fate. Thus, these data present strong evidence of a continuous, unbalanced-lineage differentiation hierarchy, in direct contradiction to the "classical" or "revised" haematopoietic model.

1.1.4 Immunophenotypic characterisation of murine HSPCs

As previously mentioned, the study of hematopoiesis and its hierarchy was significantly propelled by the research into, and the success of, immunophenotypic characterisation of murine HSPCs (Goodell et al., 1996; Heimfeld and Weissman, 1991; Ikuta and Weissman, 1992; Weissman et al., 2001). Ikuta and Weissman in 1992 found that 5 to 10 % of all BM cells expressed the mast/stem cell growth factor receptor, CD117, also referred to as cKit. This marker of primitive haematopoiesis was combined with the stem cell antigen-1 (Sca-1$^+$), within the lineage negative population (Lin$^-$), to isolate Lin$^-$cKit$^+$Sca-1$^+$ (LSK) HSPC cells. This cell-surface marker combination successfully characterises LT-HSCs, ST- HSCs and MPPs, and still remains relevant in the haematopoietic field (Li and Johnson, 1995; Spangrude et al., 1988; Weissman et al., 2001).

Adolfsson and colleagues in 2001 and 2005 sought to further dissect the LSK compartment using CD34 and Flt3. It was discovered that there was no CD34 or Flt3 expression in the LT-HSCs at the top of the haematopoietic hierarchy, but cells acquire these markers as they become more progenitor-like in nature, with ST-HSCs expressing CD34 (LSKCD34$^+$Flt3$^-$), and LMPPs expressing both CD34 and Flt3 (LSKCD34$^+$Flt3$^+$). Notably, as an alternative to CD34 and Flt3, the HSPC compartment can be sub-categorised using the SLAM family of surface markers. These cell surface markers include CD48, CD150 and CD224 and can isolate LT-HSCs (LSK CD150$^+$CD224$^-$CD48$^-$), MPPs (LSK CD150$^-$CD224$^+$CD48$^-$) and the committed progenitors HPC1 (LSK CD150$^-$CD224$^-$CD48$^+$) and HPC-2 (LSK CD150$^+$CD224$^+$CD48$^+$) (Kiel et al., 2005; Kim et al., 2006; Oguro et al., 2013).

Currently, experiments requiring the isolation and purification of HSPCs rely on LSK analysis, in combination with either CD34 and Flt3, or CD150 and CD48 cell-surface markers (Guitart et al., 2017; Guitart et al., 2013; Kranc et al., 2009; Takubo et al., 2010; Vukovic et al., 2016). Notably, more committed progenitors such as CMP, CLP, MEP and GMP can also be studied using various cell surface markers including CD16/32, CD41, CD105, CD244.2, CD229, CD127 (**Fig. 1-4)** (Acar et al., 2015; Kiel et al., 2005; Morita et al., 2010; Pronk et al., 2007)

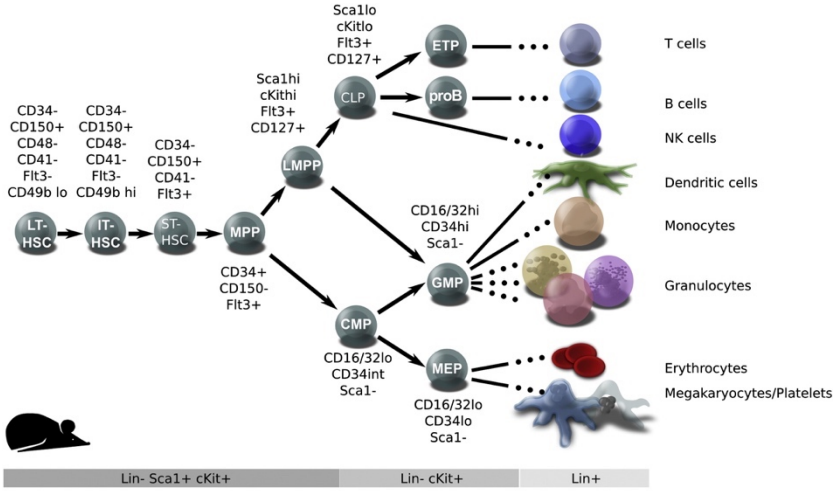

Figure 1-4 - Immunophenotypic characterisation of the murine haematopoietic hierarchy using cell-surface markers LT-HSCs ($CD34^{-}CD150^{+}CD48^{-}CD41^{-}Flt3^{-}CD49^{lo}$) reside at the top of the hierarchy giving rise to IT-HSCs ($CD34^{-}CD150^{+}CD48^{-}CD41^{-}Flt3^{-}CD49^{hi}$), ST-HSCs ($CD34^{-}CD150^{+}CD48^{-}Flt3^{+}$) and MPP cells ($CD34^{+}CD150^{+}Flt3^{+}$). MPPs then further differentiate into LMPPs ($Sca\text{-}1^{hi}cKit^{hi}Flt3^{+}CD127^{+}$) and which, in turn, commit either the CLP ($Sca1^{lo}cKit^{lo}Flt3^{+}CD127^{+}$) or GMP ($CD16/32^{hi}CD34^{hi}Sca\text{-}1^{-}$) fate. Concerning the myeloid lineage, the CMP ($CD16/32^{lo}CD34^{int}Sca\text{-}1^{-}$) can give rise to either GMP and MEP ($CD16/32^{lo}CD34^{lo}Sca\text{-}1^{-}$) populations (Taken from Doulatov et al., 2018).

1.1.5 Regulation of HSCs

The emergence, development and differentiation of HSCs is orchestrated by various intrinsic and extrinsic factors such as cytokines, growth factors, transcription factors, and the HSC niche. Understanding how these factors implicate the biology of HSCs is vital, as disruption of this fine balance of factors can result in pathological disorders such as BM failure or haematological malignancies (Krause., 2002).

1.1.5.1 Transcription factors

Intricate biological processes such as haematopoiesis rely on large transcriptional networks, with a high degree of connectivity between transcriptional factors (TFs) and transcriptional cofactors. By binding to specific DNA sequence motifs within gene regulatory regions, TF proteins are crucial in controlling gene expression, and thus control cellular phenotypes (Gottgens, 2015).Despite its complexity, multiple molecular techniques such as DNase1 mapping, whole genome sequencing and chromatin immunoprecipitation assays, have unveiled over 50 transcription factors (TF), which have all been shown to affect the functionality of HSCs (Wilson et al., 2008). Notably multiple TFs vital for HSC regulation such as Stem Cell Leukaemia (SCL), Runt-related transcription factor 1 (RUNX1), Mixed Lineage Leukaemia (MLL) and Lim Only domain 2 (LMO2) are also commonly present in chromosomal translocations in haematopoietic malignancies, demonstrating the vital importance in dissecting the role of these TFs in normal and malignant haematopoiesis (Chen et al., 2009; Okuda et al., 1996; Patterson et al., 2007; Robb et al., 1995). A summary of the main transcription factors implicated in haematopoiesis is shown below in **Table 1-1**.

In addition to roles in primitive haematopoiesis, there are multiple TFs that are essential to the lineage specification of HSCs and progenitor cells. Given the complexity of the haematopoietic hierarchy, there are various sets of TFs, which physically interact with one another, and play antagonising roles in lineage differentiation. For example, Purine-rich sequence 1 (PU.1), which activates genes involved in myelopoiesis, impacting the CMP, GMP and CLP populations, interacts with GATA-1, which is highly expressed in MEPs (Rhodes et al., 2005).

Table 1-1 Transcription factors controlling haematopoiesis

Transcription Factor (TF)	Role in haematopoiesis
Stem Cell Leukaemia (SCL)	A basic helix-loop-helix (bHLH) TF and a common translocation partner in T-ALL (Begley et al., 1989; Bernard et al., 1990). SCL dictates HSC fate towards the erythroid and megakaryocyte lineages (Kunisato et al., 2004; Zhang et al., 2005).
Runt-related transcription factor 1 (RUNX1)	A core binding factor (CBP) required for the emergence of HSCs in the yolk sac, and development of HSCs throughout adulthood (North et al., 2004; Teitell and Mikkola, 2006).
Mixed lineage leukaemia (MLL)	MLL has a critical role in HSCs in foetal and adult HSCs, as well as an involvement in AML and ALL (McMahon et al., 2007; Slany, 2009). It encodes a SET-domain containing a histone methyltransferase region, which is shown to be active in chromatin remodelling, activating *Hox* genes (Milne et al., 2002).
Lim only domain 2 (LMO2)	LMO2 belongs to the large zinc finger protein LMO family (Kadrmas and Beckerle, 2004), and is required for definitive haematopoiesis, and commitment to the erythroid lineage (Yamada et al., 1998).
Globin transcription factor 2 (GATA2)	GATA2 is essential for erythropoiesis and definitive haematopoiesis, with broad expression across all haematopoietic cells (Tsai et al., 1994; Weiss and Orkin, 1995). It is involved in the production and expansion of HSCs in the AGM, and the proliferation of HSCs in the BM (Ling et al., 2004).
Purine-rich sequence 1 (PU.1)	An ETS-family TF that functions in the early and late stages of both lymphoid and myeloid lineage differentiation and commitment (Gupta et al., 2009; Laslo et al., 2006).
Homeobox A9 (HOXA9)	HOXA9 is member of the class I homeobox genes and is highly expressed in both FL and BM primitive haematopoietic compartment (Ramos-Mejia et al., 2014; Sauvageau et al., 1994).
Myeloid ecotropic viral integration site 1 (MEIS1)	First discovered as a common viral integration site in the BXH-2 model of myeloid leukaemia (Moskow et al., 1995), MEIS1 is highly expressed in the primitive compartment, and is downregulated in differentiated cells (Argiropoulos et al., 2007; Pineault et al., 2002).

1.1.5.2 HSC niche

In adults, HSCs reside within the BM microenvironment, which helps protect and nourish HSCs through the secretion of soluble factors and instigating vital cell-cell interactions (Calvi et al., 2003; Kiel et al., 2005). First coined by Schofield in 1978, the "niche hypothesis" proposed that the BM niche prevented HSCs from entering the cell cycle, and so protected them from exhaustion and errors in DNA repair, thus ensuring efficient life-long haematopoiesis. Experiments by (Dexter et al., 1977)Dexter and colleagues in 1977 corroborated this hypothesis, discovering that BM stromal cells from the HSC niche promoted *ex vivo* proliferation and differentiation of HSPCs in long-term cultures.

Despite a greater understanding of the anatomy of the stem cell niches within the bone marrow, there is continued debate over the positioning of HSCs within this niche, and thus which cell-cell interactions directly implicate HSC biology. Initial studies aiming to locate the HSC niche within the BM microenvironment transplanted labelled HSPCs into recipient mice, and found that these primitive cells locate to the highly vascularised endosteal region near the bone surface (Nilsson et al., 2001; Xie et al., 2009). Further investigations by Kiel and colleagues in 2005, and Nombela-Arrieta and colleagues in 2013, found that the majority of HSCs are present in the perivascular region, and are enriched in the endosteal region.

Recent advances in imaging technology, in combination with simplified HSC isolation protocols, have greatly progressed the study and understanding of the HSC niche. Central to the biology of the BM microenvironment is the highly vascularised setting present in the long bones of adult mammals **(Figure 1-5).** In these bones, central arteries give rise to radial arteries, that ultimately branch into arterioles near the endosteum (Nombela-Arrieta et al., 2013). The vascular network includes venous sinusoids, which extend back toward the central cavity of the bone, where they form a large central sinus. Notably, despite the high vascular density of the tissue, the bone marrow microenvironment is hypoxic, with the lowest oxygen tensions found near sinusoids (Spencer et al., 2014).

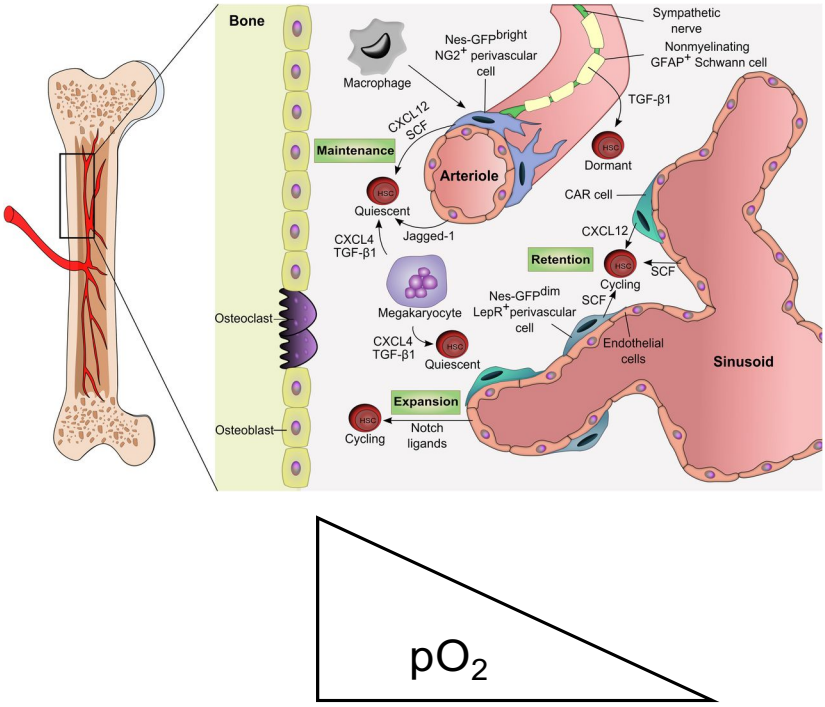

Figure 1-5 - Anatomy of the BM HSC niche The highly vascularised setting in the long bones of adult mammals dictates the biology of the HSC niche. Arterioles near the endosteum are hypothesised to support dormant HSCs, where factors such as CXCL12 and SCF secreted by perivascular, endothelial, Schwann, and sympathetic neuronal cells promote their maintenance. Venous sinusoids support quiescent or activated HSCs in the central BM. The revised model of oxygen tensions in the bone marrow revealed that the peri-sinusoidal region is more hypoxic than endosteal region, which is supplied with arterioles (Taken and adapted from Boulais et al., 2015; Spencer et al., 2014).

Interestingly, recent studies elucidate that the endosteal region itself can conceptually be split into two separate stem cell niches: the sinusoidal-megakaryocyte niche, which contains sinusoidal endothelial cells, megakaryocytes, and CAR cells; and the arteriolar-pericyte niche, which includes arteriolar endothelial cells, $NG2^+$ arteriolar pericytes, CAR cells, sympathetic nerves, and non-myelinating Schwann cells **(Figure 1-6)**. Advocates of the sinusoidal-megakaryocyte niche argue that approximately 20 % of phenotypic HSCs are localised adjacent to megakaryocyte cells, which in turn, are closely associated with BM sinusoidal epithelial tissue, showing close physical interaction between the niche and HSCs. Megakaryocytes are thought to suppress HSC proliferation, as ablation of megakaryocytes results in the increase of both HSC number and HSC cycling (Bruns et al., 2014; Zhao et al., 2014).

In support of the arteriolar-pericyte niche, Kunisaki and colleagues in 2013 demonstrated that the arteriolar niche, enclosed by a rare population of $NG2^+$ pericytes, helps maintain the quiescence of HSCs. Elements of this niche; the bone marrow endothelial cells and arteriolar pericytes, both produce multiple factors that contribute to HSC maintenance, including stem cell factor (SCF), CXCL12, and E-selectin (Ding et al., 2012; Greenbaum et al., 2013). Additionally, this niche is aided by cells of the nervous system, where sympathetic nerves regulate HSC egress from the bone marrow through controlling stromal cell CXCL12 expression (Katayama et al., 2003; Mendez-Ferrer et al., 2008), and non-myelinating Schwann cells support HSC quiescence through TGF- β (Yamazaki et al., 2009).

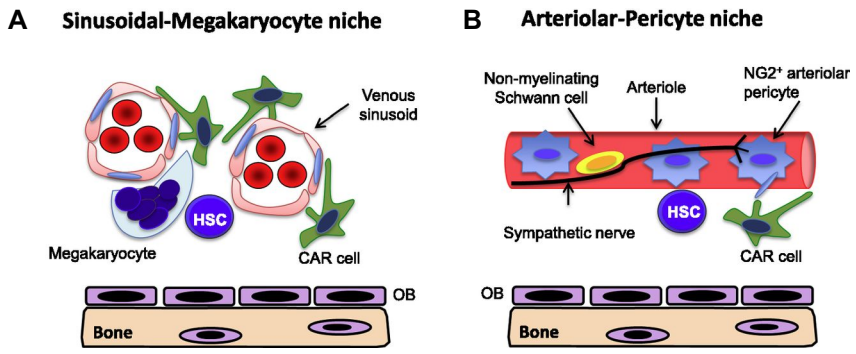

Figure 1-6 - Endosteal stem cell niches (A) The sinusoidal-megakaryocyte niche contains sinusoidal endothelial cells, megakaryocytes, and CAR cells. **(B)** The arteriolar niche includes arteriolar endothelial cells, $NG2^+$ arteriolar pericytes, CAR cells, sympathetic nerves, and non-myelinating Schwann cells. Notably, a subset of HSCs are known to localise near the endosteum, placing osteoblast lineage cells (OB) in these niches (Taken from Calvi et al., 2015).

The localisation of HSCs to endosteal sites supports the hypothesis that osteoblast lineage cells, also referred to as osteolineage cells, are a fundamental component of haematopoiesis. Osteolineage cells produce a number of cytokines implicated in HSC regulation, including granulocyte colony-stimulating factor (G-CSF), thrombopoietin, angiopoietin 1, and CXCL12, suggesting a supportive role in haematopoiesis (Jung et al., 2006; Qian et al., 2007; Taichman and Emerson, 1994; Yoshihara et al., 2007). Indeed, genetic studies using mice deficient in *Cbfa1*, a TF essential for osteogenesis, reported excessive extramedullary haematopoiesis in

the foetal liver and spleen of mutant embryos as a direct result of bone marrow failure (Deguchi et al., 1999). Zhang and colleagues in 2003 proposed that osteoblasts support HSC function, as they found a direct correlation between the number of spindle-shaped N-cadherin^{+}CD45^{-} osteoblastic (SNO) cells and HSCs. In addition, Calvi et al in 2003 found that an increase in osteoblastic cells resulted in an expansion of HSCs.

Opposing these data completely, Acar et al in 2015 reported that non-dividing HSCs were more abundant in the perisinusoidal region of the central marrow, not in the endosteal regions. This study used a novel GFP reporter mouse, under control of the *Ctnnal1* gene, which is expressed almost exclusively in HSCs, producing a very specific HSC reporter. It is evident, therefore, that there is still great contention surrounding the HSC niche and its role in HSC regulation.

1.1.6 Hypoxia and HSCs

HSCs reside within the BM microenvironment, which exhibits low pO_2 when compared to other tissues in the adult organism (Takubo et al., 2010). Seminal studies into the bone marrow microenvironment were conducted by Draenert and Draenert in 1980, who utilised a scanning electron microscope to generate three-dimensional images of the vascular organisation of the BM. These images revealed a unique vascularisation architecture, whereby arterioles gave rise to an enlarged canonical arrangement of arterial capillaries in the sinusoids, enabling easy movement of HSCs. The nature of this highly vascularised structure leaves it vulnerable to the limited perfusion and low pO_2. This is especially evident in the endosteal region of the BM, where HSCs are thought to reside (Nilsson et al., 2001; Wilson et al., 2008; Xie et al., 2009).

Oxygen measurements of BM aspirates of healthy individuals found a relatively high mean pO_2 value of 55 mmHg ± 0.95, and mean O_2 saturation of 87.5 % ± 1.1 % (Harrison et al., 2002). Simulation studies, however, predicted that close proximity (within 100 μm) to the BM vasculature resulted in a 90 % drop in the pO_2, consolidating the relationship between BM vasculature and low oxygen levels. Notably, due to abundance of haemopoietic cells in the BM, there is high O_2 consumption, lowering pO_2 overall (Chow et al., 2001).

The relationship between HSCs and their hypoxic bone marrow niche was dissected in a series of insightful experiments which injected mice with a perfusion dye, pimonidazole (Pimo), and the nucleic acid dye, Hoechst 33342 (Parmar et al., 2007; Simsek et al., 2010). Notably, Pimo is a 2-nitroimidazole-hypoxia probe, which is reduced in hypoxia, forming hydroxylamine, which covalently binds to thiol-containing proteins in hypoxic cells. The protein adducts can be detected using immunostaining techniques (Olive et al., 2000). These experiments found that cells isolated from areas of the BM with the highest concentration of HSCs and primitive progenitors, were at the lowest end of the Hoechst perfusion dye gradient. Furthermore, these cells with low Hoechst perfusion, highly retained the Pimo dye, suggesting the hypoxic nature of the HSCs (Parmar et al., 2007).

In concordance with this, to analyse the relationship between HSPCs and the cells of the BM niche, Lo Celso and colleagues in 2009 used a combination of high-resolution confocal microscopy and two-photon video imaging to study the calvarium BM of live adult mice. The authors found that transplanted HSPCs were found in close proximity (0 - 16 μm) to the vasculature, where there are low pO_2 levels. Interestingly, localisation of transplanted HSPCs closer to the highly vascularised endosteum region improved their engraftment potential, suggesting a role between hypoxia and HSC biology. Notably, employing live-imaging techniques in the calvarium, Spencer and colleagues in 2014 found that the perisinusoidal niche of the BM had lower pO_2 values when compared to the endosteal niche. The endosteal region (0-20 μm from the bone) was found to have pO_2 levels of 21.9 mm Hg (2.9 %) in the vessels, and 13.5 mm Hg (1.8 %) outside the vessels. Further from the bone (>40 μm), the perisinusoidal region had significantly lower pO_2 levels of 17.7 mm Hg (2.4 %) in the vessels, and 9.9 mm Hg (1.3%) outside the vessels. Notably, the authors also hypothesised this hypoxic sinusoidal region was the residence of non-diving HSCs. Despite their geographical differences, both Lo Celso and colleagues in 2009, and Spencer and colleagues in 2014 support the notion of a hypoxic HSC niche.

Interestingly, HSCs that are localised in a low-oxygenated niche remain quiescent, expressing high levels of *Notch1, N-cadherin*, and the cell cycle inhibitor *p21,* compared to cells residing near well-oxygenated vasculature (Jang and Sharkis, 2007). In agreement with this, Hermitte and colleagues in 2006 found that under extreme hypoxic conditions (0.1 %), human $CD34^+$ cells acquired a quiescent state. Moreover, human $CD34^+CD38^-$ cord blood cells cultured in 1% O_2, re- acquired this hypoxic induction of quiescence, and exhibited improved reconstitution potential with enhanced expression of *p21* when transplanted into immunodeficient mice (Danet et al., 2003; Shima et al., 2009). This suggests hypoxia protects the immature, quiescent state of HSCs, and so, in turn, safeguards lifelong haematopoiesis.

Unwin and colleagues in 2006 compared the proteome of primitive LSK cells, with the proteome of haematopoietic cells lacking cKit expression ($Lin^-Sca\text{-}1^+cKit^-$). The authors found

145 dysregulated proteins, a large percentage of which were involved in metabolic adaption, with LSK cells favouring anaerobic glycolysis over mitochondrial oxidative phosphorylation. Simsek et al in 2010 corroborated this result, and stated that LT-HSCs switch to glycolysis to help meet their energy demands.

1.2 Hypoxia signaling pathways

Cellular responses to low oxygen levels are predominantly orchestrated by the hypoxia-inducible factors (HIFs), Hif-1, Hif-2, and Hif-3. These factors regulate gene expression of important cellular processes such as cell cycle and cell growth, metabolism, oxygen homeostasis, apoptosis and autophagy (Greijer et al., 2005). Experiments utilising genomic chromatin immunoprecipitation (ChIP) assay techniques, found that HIF binds to more than 100 genomic loci, suggesting it is actively involved in the transcription of hundreds of genes (Mole et al., 2009; Schodel et al., 2011).

HIFs exist as heterodimeric transcription factors, comprising of a cytoplasmic oxygen-regulated α subunit (HIF-α) and a stable constitutive nuclear β subunit (HIF-β) (Kaelin and Ratcliffe, 2008; Wang et al., 1995). Under normoxic conditions, the HIF-α subunit is hydroxylated by the HIF-prolyl hydroxylases (HPHs), also referred to as prolyl hydroxylase domain (PHDs) proteins (Masson and Ratcliffe, 2003). PHDs recognise a specific LXXLAP motif in the oxygen-dependent degradation domain (ODDD) of the HIF-α subunits, and hydroxylate two conserved proline residues, Pro402 and Pro564. Notably, PHDs belong to a subfamily of dioxygenases that use 2-oxoglutarate (2-OG) and O_2 as co-factors, and are thus oxygen-dependent. This process is highly efficient, as HIF is almost undetectable when oxygen is available. Following hydroxylation by PHDs, the hydroxylated HIF-α subunits are recognised by VHL (von Hippel-Lindau), which fittingly has a 1000-fold increase in affinity for hydroxylated HIF, compared to its non-hydroxylated form (Masson et al., 2001). VHL then acts as an E3 ubiquitin ligase, and HIF-α is rapidly destroyed via the polyubiquitination/proteasomal degradation pathway (Ivan et al., 2001; Jaakkola et al., 2001; Maxwell et al., 1999). In hypoxic, or low oxygen conditions, there is a decrease in the activity of PHDs, yielding a significant reduction in the hydroxylation of HIF-α subunits, resulting in their accumulation. As such, HIF-α translocates to the nucleus, where it binds with its HIF-β partner and recruits p300/CBP co-activator to form a transcriptionally active complex (Wang et al., 1995) **(Figure 1-6)**. Downstream, the HIF complex binds to the hypoxia response elements (HREs) of hypoxia-responsive genes, such as EPO (erythropoietin) and VEGF (vascular endothelial growth

factor), promoting their transcription (Elvidge et al., 2006; Ruas et al., 2005; Schodel et al., 2011).

Notably, in addition the PHD proteins, HIF regulation, and thus the hypoxia response, is controlled by another member of the 2OG dependent oxygenase family, FIH-1 (factor inhibiting HIF-1). FIH-1 hydroxylates an asparagine residue (Asn 803) in the C terminus of HIF-α, preventing its binding to the transcriptional co-activator p300/CBP (Elvidge et al., 2006). While PHDs are highly dependent on oxygen and have significant affinity to HIF, FIH on the other hand is known to be active under severe hypoxia and has alternative substrates, namely members of the ankyrin repeat domain (ARD) family, for which it has a higher affinity to than HIF (Hancock et al., 2015; Markolovic et al., 2015).

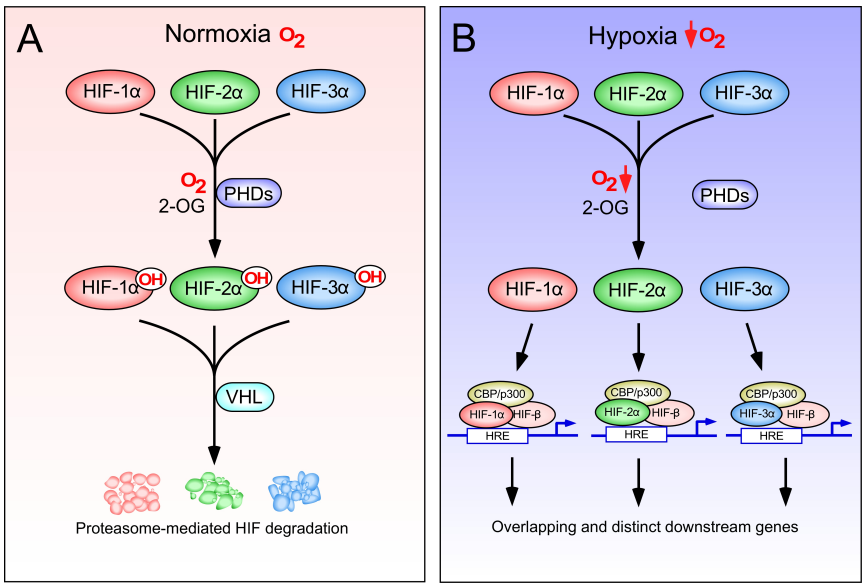

Figure 1-7 - Hypoxia signalling pathway (A) Under normoxic conditions, PHD enzymes hydroxylate the Hif-α subunits, targeting them degradation in the proteasome. **(B)** In low oxygen conditions, the PHD enzymes are less active, and so the Hif-α subunits are able to translocate to the nucleus, bind to their Hif-β partners, and activate expression of multiple genes vital for the hypoxia response (Taken from Gezer et al., 2014).

1.2.1 HIF in haematopoiesis

Given the intricate relationship between the hypoxic bone marrow niche and haematopoiesis, there have been significant research efforts to understand the role of the HIF in normal and malignant haematopoiesis. Early experiments in this field found that both Hif-1α and Hif-2α are highly expressed in HSCs, and that Hif-1 is upregulated at both a transcriptional and protein level in primitive LSK cells (Takubo et al., 2010; Simsek et al., 2010).

Following this, multiple research papers, including those published by the Kranc laboratory, have dissected the role of HIF in haematopoiesis using transgenic mouse models (Gezer et al., 2014; Guitart et al., 2013; Vukovic et al., 2015; Vukovic et al., 2016). Published in 2013, Guitart and colleagues generated a transgenic mouse model which deleted *Hif-2α* specifically within the haematopoietic system (*Hif-2α*^{CKO}). These conditional knockout mice were used to study the effect of *Hif-2α* deletion on steady-state and stressed haematopoiesis. Analysis of these mice found that deletion of *Hif-2α* had no effect on the number of HSCs, or their self-renewal capacity under transplantation assay. Additionally, co-deletion of *Hif-1α* and *Hif-2α* had no effect on the HSC compartment. Further studies by the Kranc laboratory unveiled that, analogous to results shown in the *Hif-*2α^{CKO} mice, *Hif-1α* deletion proved to be dispensable for cell-autonomous HSC survival, even in stress-induced conditions (Vukovic et al., 2016). Altogether, these results present significant evidence that both *Hif-1α* and *Hif-2α* are not essential regulators of HSC function.

Conversely, work published by Takubo et al in 2010 reported that *Hif-1α* had a vital role in HSC regulation, with *Hif-1α*^{CKO} mice displaying decreased HSC numbers, as well as a reduction in HSC fitness upon transplantation. Notably, these experiments were conducted using the same *Hif-1α*^{CKO} (*Hif1*$^{fl/fl}$*;Mx-Cre*$^{+}$), mice and were carried out with only minor experimental differences. As such, it is evident that there is still significant controversy in the field.

After comprehensively investigating the effect of HIF deletion in haematopoiesis, and discovering that deletion of *Hif-1α* and *Hif-2α* has no effect of normal hematopoiesis, this manuscript focuses on the role of the HIF prolyl hydroxylase domain (PHDs) proteins, the negative regulators of the HIF proteins, in normal and malignant haematopoiesis.

1.3 Prolyl hydroxylase domain proteins (PHDs)

Prolyl hydroxylase domain proteins (PHDs) belong to a superfamily of iron- and 2-oxoglutarate-dependent dioxygenases, referred to as 2-oxoglutarate (2-OG) dioxygenases. In mammals there are 4 PHD isoforms; PHD1, PHD2, PHD3, and the recently discovered PDH-TM (Koivunen et al., 2007). Overall the PHDs show a 42 – 59% sequence similarity, with PHD2 most closely related to the ancestral HIF-PHDs found in *Drosophila melanogaster* and Caenorhabditis elegans (Appelhoff et al., 2004). Notably, there is significant literature on PHD1, PHD2 and PHD3, but little is known about the function of PHD-4 (also referred to as P4H-TM) (Fan et al., 2014).

The full-length structures of PHD1 and PHD2 have over 400 amino acid residues (407 and 426 in humans, respectively), and share approximately 55 % identity within the well-conserved hydroxylase domain at their C-terminus. The N-terminal halves, however, are more variable, and have not been extensively characterised (Epstein et al., 2001). Notably, the PHD3 protein is significantly shorter than PHD1 or PHD2, composed of only 293 amino-acid residues in humans. It contains the shared hydroxylase domain, but only a short stretch of divergent N-terminal sequence (Jokilehto and Jaakkola, 2010) **(Figure 1-7)**.

All PHD isoforms hydroxylate proline residues on HIF-α but differ in their substrate specificity. Interestingly, it was found that PHD2 has a greater affinity to HIF-1α than HIF-2α, whereas PHD1 and PHD3 hydroxylate HIF-2α more efficiently (Appelhoff et al., 2004).

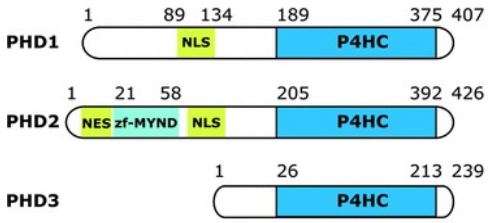

Figure 1-8 – Structure of PHDs PHD1, PHD2 and PHD2 all have a conserved hydroxylase domain (P4HC) at the C-terminal ends. Additionally, PHD2 contains a zf-MYND (zinc-finger domain) that may interact with regulatory proteins. Both PHD1 and PHD2 contain potential subcellular localization signal sequences, nuclear localization signal or nuclear export signal (NLS). Taken from Jokilehto and Jaakkola., 2010.

1.3.1 PHD activity

Post-translation protein hydroxylation has been well studied and characterised in structural biology, however, the hydroxylation of HIF-α by the PHD proteins is the first identified example of a hydroxylation reaction being used in cell signalling (Schofield and Ratcliffe, 2005). Therefore, the activity of PHDs is of great biochemical and physiological interest.

Hirsila et al in 2005 found that, similarly to protein hydroxylases which orchestrate structural modifications, PHDs have a high enzymatic turnover rate, measuring at approximately 50 mol/mol/min. Despite this high rate of turnover, and the low abundance of the enzymatic substrate HIF, the hypoxia response is limited by the hydroxylation activity of PHDs. In all situations, except a blockade in VHL activity, accumulation of HIF is in a non-hydroxylated form, elucidating that the hydroxylation step is rate limiting. Additionally, genetic or pharmacological inactivation of PHDs leads to consistent constitutive activation of the HIF pathway, regardless of the oxygen status (Joharapurkar et al., 2018).

Given the evident importance of PHD activity within the hypoxia response, it is vital to understand the regulation of PHDs *in vivo.* For PHDs to function as hydroxylases, they require molecular oxygen, the citric acid cycle 2-oxoglutarate (2-OG), iron (Fe^{2+}), and ascorbic acid (vitamin C) (Bruick and McKnight, 2001; Epstein et al., 2001; Schofield and Ratcliffe, 2005). As such, each of these factors can limit the activity of the PHDs, thus the hypoxia response. Moreover, as shown in **Figure 1-8**, there are also multiple intracellular factors that can impact the activity of PHDs.

Following on from their previous research into the enzymatic activity of PHDs, Hirsila and colleagues in 2005 found that all PHDs have K_m values for oxygen between 230 and 250 μm, which is above the concentration of atmospheric O_2 at approximately 200 μm. Intracellular oxygen concentrations are typically below this, thus high K_m values ensure facilitation of oxygen-dependent hydroxylase activity, given sufficient levels of all other substrates and cofactors. Supporting this, human and murine cell lines cultured under very low oxygen

conditions (0.5 - 2 % O_2) accumulate HIF-1α. Notably, Pan et al in 2007, and Hagen et al in 2013 found that this HIF-α accumulation is dependent on functional mitochondria.

Mitochondria have a significant role in the activity of PHDs as they produce 2-OG, an essential co-substrate in the hydroxylation reaction due to its role in the Fe^{2+} coordination in the catalytic centre (Epstein et al., 2001). Moreover, mitochondria produce other TCA cycle intermediates such as succinate and fumarate, which have an inhibitory role in the enzymatic activity of the PHDs, by competing for the 2-OG active site (Selak et al., 2005). Under normal physiological circumstances, the cytosolic concentrations of succinate and fumarate are very low, and so do not pose a threat to PHD activity. However, mitochondrial defects, or experimental overexpression of these factors does lead to a significant accumulation of HIF-1α levels (Hewitson et al., 2007).

Reactive oxygen species (ROS), which can also be produced by the mitochondria, are also thought to inhibit PHDs by chelating Fe^{2+} and oxidising PHD bound Fe^{2+} to Fe^{3+}, essentially disrupting the interaction between oxygen and PHDs (Ozer and Bruick, 2005; Pan et al., 2007). Notably, other heavy metals including Co^{2+}, Ni^{2+} and Mn^{2+} are also chelators of Fe^{2+}, inhibiting PHD enzymatic activity (Goldberg et al., 1988).

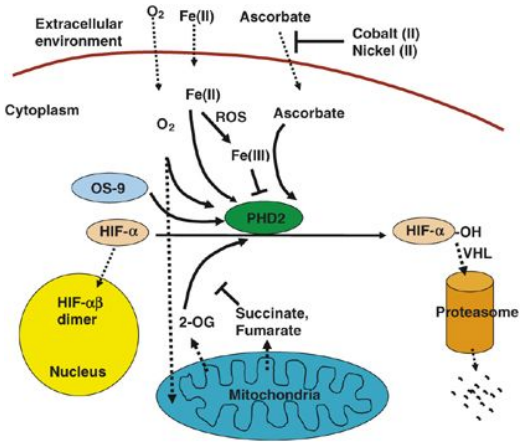

Figure 1-9 – Factors regulating the function of PHDs PHDs require 2-OG, O_2 and Fe^{2+} to hydroxylate HIF-α. Inhibitory factors of PHD function include the metabolic intermediates succinate and fumarate; divalent metal ions such as Co^{2+} or Ni^{2+}, which compete with Fe^{2+} binding to PHDs; and reactive oxygen species (ROS), which can disrupt oxygen interaction with PHDs (Fong and Takeda, 2008).

1.3.2 HIF-independent functions of PHDs

Despite the strong affinity to HIF, and an intimate relationship with molecular oxygen, PHDs are also known to function in a HIF-independent manner, where they are able to regulate the expression of target proteins, with or without hydroxylation (Hiwatashi et al., 2011). Notably, this is an emerging area of research, with further HIF-independent PHD functions likely to emerge.

Studies by Koditz et al in 2007 sought to identify novel PHD protein interactions through a yeast-2-hybrid experimental system. Results from these experiments revealed an interaction between ATF-4 and both PHD1 and PHD3. ATF-4 is a member of the ATF/CREB family of transcription factors, which are activated following cellular stress (B'Chir et al., 2013). Koditz et al also reported that HeLa cells treated with the PHD inhibitor dimethyloxalylglycine (DMOG), had an increase in ATF-4 activity, suggesting that PHD negatively regulates ATF-4. In concordance with this, co-immunoprecipitation assays confirmed the direct interaction between PHD1 and ATF04, and PHD3 and ATF-4, entirely independent from HIF (Hiwatashi et al., 2011).

Additionally, multiple papers have unveiled an association between the PHD family and the NF-κβ pathway, which is known to play a role in many biological processes such as apoptosis, differentiation, proliferation and immune responses (Liu et al., 2005). Studies by Fu and Taubman in 2007 found that cells treated with DMOG had an enhanced activation of the NF-κβ signalling pathway. Downstream, PHD inhibition also induced expression of NF-κβ target genes such as YY1 and Cyclin D1. Notably, PHD1 has also been reported to bind and inhibit Iκκβ, which is known to regulate NF-κβ activity (Cummins et al., 2006).

Furthermore, a fascinating study by Duran et al in 2013 found that amino acid starvation results in depletion of 2-OG, resulting in a reduction in PHD activity, but not HIF stabilisation. Inhibition of PHDs with DMOG and short-hairpin constructs targeting the PHD family, resulted in increased autophagy, and prevented mammalian target of rapamycin complex 1 (mTORC1)

activation by amino acids. These PHD dependent phenotypes were also found to function in a HIF-independent manner. This paper suggests that in addition to their oxygen sensing role, PHDs are also involved in the amino-acid sensing process, possibly unveiling a role for PHDs in a broader, nutrient-sensing network.

1.3.3 Biological function of PHDs

The hypoxia dependent, and newly discovered hypoxia-independent roles of the PHD family, translate into various biological functions *in vivo*. First discovered in the model organism Caenorhabditis elegans, loss of EGL-9, the prototype of PHDs, was found to significantly elevate levels of HIF-*α* and reduce egg-laying function (Epstein et al., 2001). In *Drosophila melanogaster* its single PHD protein was found to be essential for cell growth in fat bodies and wing imaginal discs (Frei and Edgar, 2004; Frei et al., 2005).

In humans, the hypoxia pathway is implicated in multiple biological processes including angiogenesis, energy metabolism and erythropoiesis (Pugh and Ratcliffe, 2017). As such, the PHD enzymes have a number of important developmental and physiological functions. For example, during normal development, PHD3 orchestrates the apoptosis of sympathetic neuronal precursor cells. Deletion of PHD3 in this setting results in a failure of apoptosis and development of neuroendocrine tumours known as pheochromocytomas (Lee et al., 2005). However, PHDs have also been reported to have an anti-apoptotic role, with deletion of PHDs in maturing chondrocytes, promoting cell survival rather than apoptosis (Bohensky et al., 2007).

Takeda and colleagues in 2007 investigated the role of PHDs *in vivo* using *Phd2* conditional knockout mice and found that deletion of *Phd2* resulted in an increase in angiogenic factors such as VEGF-A and erythropoietin (EPO). Increase in circulating levels of VEGF and EPO resulted in an increase in vascular growth observed in the density and lumen sizes of vasculature tissues. Given that cells deficient in PHD2 have increased erythropoiesis and vascular growth, there is now substantial interest in the pharmacological value of PHD inhibitors, with multiple compounds showing positive therapeutic results in kidney disease and ischemia (Haase, 2017; Nangaku et al., 2007; Ogle et al., 2012).

1.3.4 The role of PHDs in cancer

The vast growth and colonisation of solid tumours results in abnormal vasculature and rapid proliferation of cancer cells. As a result, this environment is very low in oxygen, and so relies upon the hypoxia signaling pathway response (Harris, 2002). Multiple laboratories have worked to dissect the role of PHDs in cancer, with great debate over their tumour suppressor or oncogenic status.

The PHD2 isoform is frequently associated with cancer and is often associated with a tumour suppressor function. Kato et in in 2006 reported that around 60% of endometrial cancers studied had an increased incidence of PHD2 mutations. Introduction of the wild-type PHD2 gene (EGLN1) into endometrial cancer cell lines that carried a mutant EGLN1 induced senescence, reducing their growth. Studies into colorectal tumours found that PHD2 expression was decreased in carcinogenic tissue compared to the surrounding healthy colon tissue, suggesting that PHD2 may regulate tumour development. Transplantation of colorectal carcinoma cells with silenced PHD2 levels into severe combined immunodeficient (SCID) mice, found that recipient mice had increased tumour growth in absence of PHD2. These tumours lacking PHD2 exhibited increased blood vessel formation, suggesting that PHD2 functions as a tumour suppressor by negatively regulating angiogenesis (Chan et al., 2009).

Contradicting the tumour suppressor function of PHD2, overexpression of all PHD isoforms have been recorded in multiple other tumour types and are associated with a negative outcome in patients. Overexpression of PHD1, PHD2 and PHD3 have all been recorded in non-small cell lung cancer (NSCLC) and are associated with poor survival rates (Andersen et al., 2011). In human hepatocellular carcinoma (HCC), high PHD2 expression is associated with larger tumour size and limited tumour differentiation, resulting in shorter disease-free survival and overall survival in patients (Zhen et al., 2014).

In addition to solid tumours, PHDs isoforms have been recently implicated in haematological malignancies. Recent research by Bur and colleagues in 2018 found that overexpression of PHD1 predicts a poor outcome in patients with classic Hodgkin's lymphoma (cHL).

1.4 Acute Myeloid Leukaemia

Acute myeloid leukaemia (AML) is a heterogenous clonal disorder, resulting from the expansion of primitive, undifferentiated myeloid progenitors (myeloblasts) within the BM microenvironment (Khwaja et al., 2016; Metzeler et al., 2016). Replacement of healthy BM cells with these malignant, dysfunctional myeloblasts results in anaemia, haemorrhage and an inability to fight infection. These myeloblasts then infiltrate other tissues in the body including the liver, spleen, lymph nodes and the central nervous system (Lowenberg et al., 1999).

Strikingly, the standard therapy for AML has not been significantly altered in over 30 years (Dohner et al., 2010). AML therapy typically involves induction chemotherapy, followed by further cycles of consolidation and maintenance chemotherapy. Patients may also receive an HSC transplant, which can result in a high rate of curability (Wunderlich et al., 2013; Zuber et al., 2009). The induction phase of treatment is referred to as the "7 + 3" method and commonly combines 7 to 10 days of continuous infusion of cytarabine (Ara-C), with 3 days of an anthracycline (typically daunorubicin or idarubicin). Due to a higher tolerance, this treatment schedule is repeated 3 - 4 times in younger people, whereas older patients (> 70 years) typically receive 2 -3 round due to the toxic effects of chemotherapy. As such, AML is particularly difficult to eradicate in older patients and, in addition, many older adults are ineligible for stem cell transplantation due to the risks associated with high-dose chemotherapy (Guinn et al., 2007).

Notably, AML has a very poor long-term survival outcome, even in patients who achieve disease remission. This is due to the fact that a large proportion of AML patients will suffer a disease relapse, which is often fatal (Sarkozy et al., 2013). Historically, this was thought to be a result of mutation-based drug resistance, with mutations arising from toxic chemotherapeutic drugs (Goldie and Coldman, 1984). Recent evidence, however, suggests that this disease relapse is in fact caused by re-emergence of a rare cancer stem cell population, that is not eliminated by conventional chemotherapy, and can give rise to further AML disease.

1.4.1 Leukaemic Stem Cells (LSCs)

Following investigations into the cell of origin in AML, John Dick in 2003 coined the "cancer stem cell hypothesis", which describes a rare population of cancer cells, stem-like in nature, which through their self-renewal ability, can initiate and sustain the bulk cancer population (Krivtsov et al., 2006). In the context of AML, these cancer stem cells are referred to as leukaemic stem cells (LSCs), and mirror the HSC hierarchy, with the LSCs at the apex, and AML blast cells at the base **(Figure 1-9).**

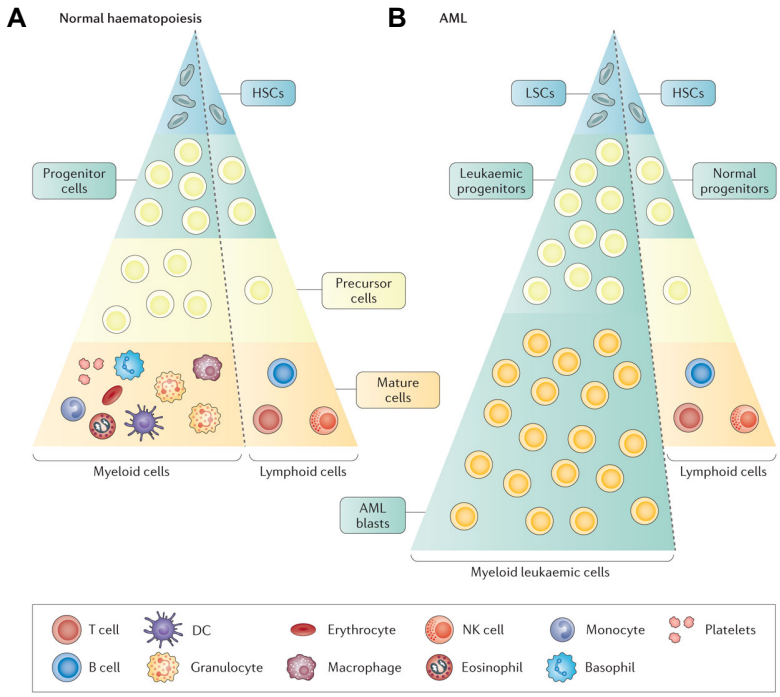

Figure 1-10 – HSC and LSC hierarchies (A) Normal haematopoiesis is a hierarchical process in which HSCs sit at the apex, and give rises to progenitor precursor cells, ultimately resulting in mature differentiated cells. **(B)** In AML, the HSC hierarchy is paralleled, will LSCs at the apex. LSCs generate leukaemic progenitor cells, which give rise to immature, dysfunctional AML blast cells. (Taken from Khwaja et al., 2016).

In concordance with the HSC field, LSCs are characterised by their ability to initiate and serially propagate AML disease upon transplantation (Schepers et al., 2015). Parallels between the phenotypes and functions of HSCs and LSCs, pointed to a stem-cell cell of origin in AML (Wang and Dick, 2005). Recent research, however, suggests that in an aggressive leukaemia such as AML, LSCs may not be confined to the HSC compartment, but instead can also derive from progenitor cells (Eppert et al., 2011; Goardon et al., 2011).

In an aid to dissect the cell of origin in AML, Wang and Dick in 2005 transplanted LSCs into secondary and tertiary recipient mice and found significant variations in their repopulation ability. This indicated that there may be distinct subsets of LSCs with differing self-renewal abilities. Experiments by Krivtsov and colleagues in 2006, transformed granulocyte macrophage progenitor (GMP) cells with an MLL-AF9 fusion protein and transplanted them into irradiated syngeneic recipient mice. LSCs isolated from these mice were able to give rise to leukaemic disease in secondary recipients. These cells were found to retain the gene expression profile of GMPs, but also expressed a subset of genes highly expressed in HSCs. This suggests that both HSCs and committed progenitors, through the acquisition of an HSC gene expression pattern, can give rise to LSCs (Cozzio et al., 2003; Krivtsov et al., 2006; Wong et al., 2007).

Given that LSCs have different repopulation capacities, multiple clinical and scientific papers were published investigating the link between LSC activity and the clinical outcome of AML disease. In this vein, van Rhenen and colleagues in 2005 found that an increased stem cell frequency in patients at diagnosis predicts a high minimal residual disease and poor survival outcome. Moreover, Pearce et al in 2005 used *in vivo* transplantation assays to further dissect the relationship between LSC status and patient survival. The authors discovered that patient samples which were able to engraft in immunocompromised NOD/SCID recipient mice were derived from patients with a significantly shorter overall survival when compared to samples which did not engraft. This shows a direct link between functional LSC activity and prognostic outcome. Importantly, Krivstov and colleagues in 2013 found that murine LSCs deriving from

an HSC source were more resistant to the chemotherapeutic drugs cytarabine and doxorubicin, when compared to LSCs derived from a GMP progenitor source.

All together, these experiments suggest that an increase in primitive LSC frequency decreases patient survival through both an increase in disease maintenance, as well as chemotherapy resistance. Given the current failures in AML treatment, it is vital to identify therapeutic targets that can eliminate LSCs. Using these, in conjunction with current chemotherapies, could lead to efficient relapse-free treatment of AML.

1.5 Hypothesis and Aims

Given that deletion of *Hif1* and *Hif2* was found to accelerate the development of AML, this thesis aims to investigate the therapeutic potential of targeting LSCs using the HIF-pathway through inhibition of the Prolyl Hydroxylases Domain (PHD) enzymes. To further validate PHDs as therapeutic targets in AML, this thesis explores the impact of developmental and systemic deletion of *Phd1* and *Phd2 in vivo*. As a potential therapeutic target, it is vital to ensure that inhibition of PHDs has no detrimental effect on steady-state or stressed hematopoiesis.

This thesis hypothesises that inhibition of the Prolyl Hydroxylase Domain enzymes will target and eradicate leukaemic stem cells, but will not be detrimental to normal haematopoiesis. As such, this thesis is an investigation into the role of Prolyl Hydroxylase Domain enzymes in normal and malignant haematopoiesis. Experiments were designed to address the following specific aims:

1) To examine the effect of genetic deletion of *Phd1, Phd2* or both *Phd1* and *Phd2* specifically within the haematopoietic system **(Chapter 3)**

2) To investigate the effect of systemic *Phd2* deletion on the haematopoietic system **(Chapter 4)**

3) To evaluate if genetic deletion or knockdown of *Phd1, Phd2* or both *Phd1* and *Phd2* inhibits AML development and maintenance **(Chapter 5)**

CHAPTER 2

Materials and Methods

Chapter 2 Materials and methods

2.1 Mouse strains

Vav-iCre mice were purchased from Jackson Laboratory (Stock no. 008610). *Vav1-Cre* mice, also known as *Vav-iCre*, were originally developed by de Boer et al in 2003, and are a well-established transgenic line utilised for tissue-specific deletion within the haematopoietic system (Ogilvy et al., 1998; Ogilvy et al., 1999; Shimshek et al., 2002). Although originally discovered as proto-oncogene in oesophageal cancers, expression of the normal *Vav* allele is only found in haematopoietic tissues, resulting in the synthesis of a 95 kDa protein (Bonnefoy-Berard et al., 1996; Katzav et al., 1989). Murine *Vav* expression begins at embryonic day (E) 11, and increases at E 14, shortly after the emergence of definitive haematopoiesis (de Boer et al., 2003).

Phd1fl/fl, *Phd2fl/fl* mice were donated by Sir Peter J Ratcliffe (Mazzone et al., 2009). *Phd1fl/fl; Vav-iCre* and *Phd2fl/fl; Vav-iCre* mice were generated by crossing *Phd1fl/fl* and *Phd2fl/fl* males to *Vav-iCre* females. Littermates from these crosses were then bred to generate *Phd1fl/fl; Phd2fl/fl; Vav-iCre* mice.

Double heterozygous, double transgenic *CAG-rtTA+/-;TRE-shPhd2+/-* (referred to in this thesis as *rtTA/shPhd2)* and *CAG-rtTA+/-;TRE-/-* (referred to as Control *rtTA*) mice were donated by Chris W Pugh and Sir Peter J Ratcliffe and were bred to generate *CAG-rtTA+/-;TRE-shPhd2+/-* and *CAG-rtTA+/-; TRE-shPhd2-/-* mice used in all experiments. The reverse tetracycline trans-activator (*rtTA)*, under the cytomegalovirus early enhancer element and chicken β-actin *(CAG)* promoter allows strong ubiquitous expression. Upon doxycycline (Dox) treatment, there is activation of the tetracycline response element (*TRE*) controlled *GFP-shPhd2* cassette (*TRE-shPhd2*), which is downstream of the collagen type I gene (*Col1a1).* This results in transcription of both GFP and *shPHD2* in the *rtTA/shPhd2* mice, and not the control (*rtTA*) mice (**Fig 2-1)**.

All mice were on the C57BL/6 genetic background. All transgenic and knockout mice were CD45.2^{+}. Congenic recipient mice were CD45.1^{+} /CD45.2^{+}. Animal experiments were authorized by the UK Home Office. All mice were mixed sex, and tissues analysed at 8 - 12 weeks of age, unless otherwise stated.

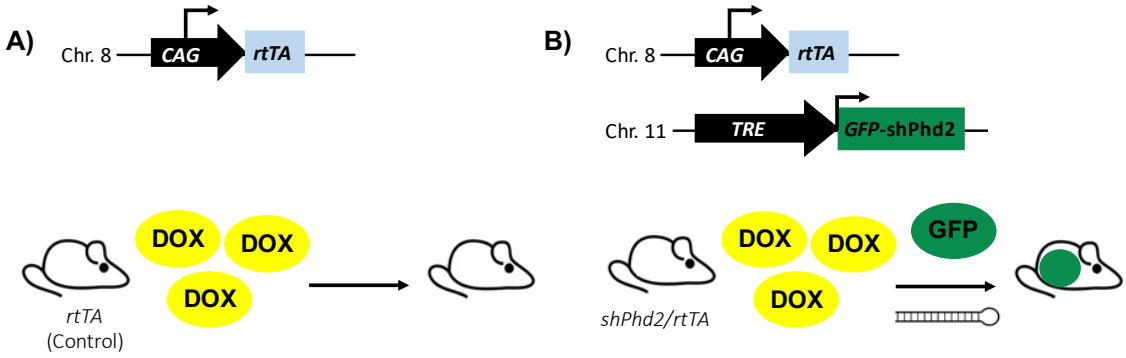

Figure 2-1 - Inducible sh*Phd2* knockdown mouse model Schematic of Phd2-targeted shRNA transgenic strains: *CAG-rtTA+/-;TRE-/-* (Control) and *CAG-rtTA+/-;TRE-shPhd2+/-* (*shPhd2/rtTA).* **(A)** Both mouse strains express a *CAG*-promoted tetracycline reverse trans-activator (*rtTA*). **(B)** In the presence of doxycycline (Dox) there is transcription of an mRNA encoding GFP and a silencing shRNA directed against *Phd2*.

2.2 Doxycycline administration

2.2.1 *Doxycycline treatment in vivo*

Control (*rtTA*) and experimental (*rtTA/shPhd2)* mice received 2 mg/ml of Dox (Doxycycline hyclate, Alfa Aesar) in drinking water, with 3.5 % sucrose to improve palatability. For transplantation experiments, CD45.1^{+}/CD45.2^{+} recipient mice were treated with 2 mg/ml Dox, with 3.5 % sucrose in their drinking water 4 weeks post-transplantation. For *Meis1/Hoxa9* pre-LSC transplantation experiments, mice were treated with 2 mg/ml Dox; 3.5 % sucrose in their drinking water 60 days post-transplantation. The water bottle containing Dox and sucrose was changed twice per week.

2.2.2 Doxycycline treatment *in vitro*

Initial Dox titration experiments *in vitro* with *Meis1/Hoxa9*-transformed pre-LSCs used an incremental scale of 0 - 1000 ng/ml of Dox dissolved in dH_2O. Based on these experiments, a 250 ng/ml Dox was added in all future experiments.

2.3 DNA extraction

Genomic DNA from animal tissue (mouse ear notch, foetal liver (FL) or bone marrow (BM)) or cultured cells was extracted and prepared for PCR using Mouse Direct PCR Kit (B40013-BIT, Stratech). Tissue or cells were resuspended in 100 μL of Buffer L, with 2 μL of Protease Plus added to each sample. Samples were then incubated for 25 - 30 min at 55 °C, followed by 5 min at 95 °C. Extracted DNA was stored at -20 °C.

2.4 Genotyping and PCR primers

The PCR Mix for *Vav-iCre*, and *Phd1, Phd2, Cag (rtTA)* and *Col1a1 (TRE-shPhd2)* was prepared using Mouse Direct PCR Kit (B40013-BIT, Stratech). Each reaction used 2 μL of genomic DNA. All primers were at a concentration of 100 μM. The sequence of the primers and the PCR programs are listed in **Table 2-1**.

2.5 Gel Electrophoresis

PCR product, along with a DNA ladder and H_2O loading control was loaded into an agarose gel (1.5 % to 2.5 %) (Thermo Fisher Scientific, 17852) stained with SYBR™ SAFE™ DNA Gel Stain (Invitrogen S33102). Following electrophoresis, images of the agarose gel where taken using UV excitation. A representative image of an agarose gel from *Vavi-Cre* genotyping is shown below in **Figure 2-2.**

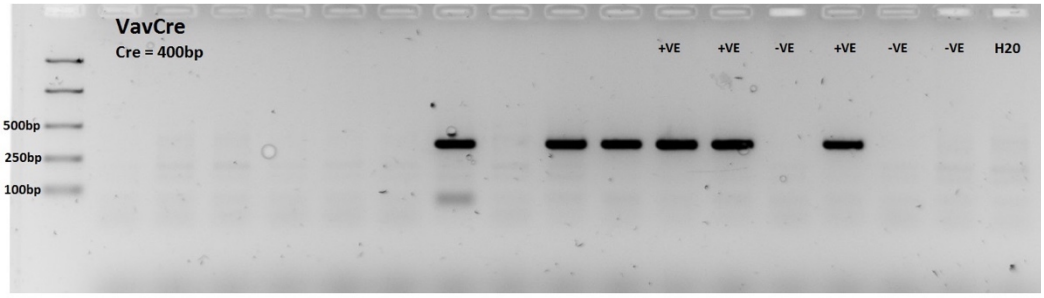

Figure 2-2 - Representative gel electrophoresis image *Vav-iCre* PCR product, DNA ladder and an H_2O loading control were loaded into a 2.5 % agarose gel, stained with SYBR™ SAFE™ DNA stain. Following electrophoresis, an image was taken using UV excitation. Positive and negative genotyping results, as well as the H_2O control are shown (Image by Lewis Allen).

Table 2-1 PCR programs and primer sequences

	Vav-iCre		
PCR Program	95°C	5 mn	
	94°C	40 sec	
	64°C	40 sec	x30
	72°C	30 sec	
	72°C	5 min	
	10°C	forever	
Primer Sequence	*Vav-iCre* Fw 5' CCGAGGGGCCAAGTGAGAGG 3'		
	Vav-iCre Rev 5' GGAGGGCAGGCAGGTTTTGGTG 3'		

	Cag			*ColA1*		
PCR Program	94°C	5 mn		94°C	5 mn	
	94°C	30 sec		94°C	30 sec	
	57°C	45 sec	x35	57°C	45 sec	x35
	72°C	60 sec		72°C	60 sec	
	72°C	5 min		72°C	5 min	
	10°C	forever		10°C	forever	
Primer Sequence	*Cag* Com: 5' CGAAACTCGGTTGACATG 3'			*ColA1* Fw: 5' AATCATCCCAGGTGCACAGCATTGCGG *3'*		
	Cag TG: 5' ATGCCCTGGCTCACAAATAC 3'			*ColA1* Rev: 5' CTTTGAGGGCTCATGAACCTCCCAGG *3'*		
	Cag WT: 5' TGCCTATCATGTTGTCAAA 3'			Tandem Rev: 5' GAAAGACCGCGAAGAGTTTG 3'		

	Phd1			*Phd2*		
PCR Program	95°C	5 mn		95°C	5 mn	
	95°C	30 sec		95°C	30 sec	
	56°C-60°C	40 sec	x12	55°C	45 sec	x32
	(-0.5°C/cycle)					
	72°C	60 sec		72°C	45 sec	
	72°C	5 min		72°C	5 min	
	10°C	forever		10°C	forever	
Primer Sequence	*Phd1* Flox Fw : 5' GAGGCTCCTTGAGTCTG 3'			*Phd2 WT* Flox Fw : 5' TTGCAGTGTGCAACAGTCAG 3'		
	Phd1 Flox Rev : 5' ATTTAGTTCAGTTCTCAG 3'			*Phd2* WT Flox Rev : 5' CACGGGGAACTCTGATTCAT 3'		
				Phd2 Flox Excised Rev : 5' CCAAAATCACCAATCTAGAATAACTTC 3'		

2.6 Maxiprep of plasmids

Maxiprep of all plasmids was conducted using the HiSpeed Plasmid Maxi Kit (12662, Qiagen), according to the manufacturer's instructions. Briefly, a starter culture was incubated ON at 37 °C in 500 mL of LB media with 100 mg/mL ampicillin. The bacteria were harvested by centrifugation at 6,000 x g for 15 min at 4 °C. The bacterial pellet was resuspended in 10 mL of Buffer P1, followed by 10 m L of Buffer P2, and incubated for 5 min at room temperature. Following this, 10 mL of chilled Buffer P3 was added and the cell lysate was filtered through an equilibrated HiSpeed Tip. Following this, 60 mL of Buffer QC was added to wash the HiSpeed Tip, and the DNA was eluted with 15 mL of Buffer QF Concentration of eluted DNA was measured by a nanodrop spectrometer (Nanodrop ND1000 Spectrophotometer; Labtech International Ltd, East Sussex, UK), recording absorbance at wavelength 260 nm. The DNA purity was assessed through the ratio of absorbance at 260 nm and 280 nm.

2.7 RNA extraction

RNA was extracted and purified using RNeasy micro Kit (74004, Qiagen) according to the manufacturer's instructions. Briefly, cells were harvested, and 350 μL RLT buffer was added to cell pellets, followed by 350 μL 70 % ethanol. The mixture was centrifuged in RNeasy MiniElute spin columns for 15 sec at 8,000 x g. Following this, 350 μL RWI buffer was added and the columns were centrifuged for 15 sec at 8,000 x g. 80 μL of DNase I incubation mix was added and incubated for 15 min at room temperature. 350 μL RWI buffer was added and columns were centrifuged for 15 sec at 8,000 x g. 500 μL RPE buffer was then added and samples were centrifuged again for 15 sec at 8,000 x g. Subsequently, 500 μL 80 % ethanol was added and columns were centrifuged for 2 min at 8,000 x g to wash the spin column membrane. The spin column was centrifuged at full speed for 5 min to dry the membrane. Finally, 15 μL RNAse free water was added and centrifuged for 1 min at 8,000 x g to elute RNA. The concentration of RNA was measure by NanoDrop 1000 Spectrophotometer.

2.8 RT-PCR

RT-PCR was performed in order to transcribe the RNA into cDNA using the reverse transcriptase enzyme. The High-Capacity cDNA Reverse Transcription Kit was used for all RT-PCR reactions (Applied BiosystemsTM - 4368813). The mix consisted of 2 μL 10X RT buffer, 0.8 μL dNTP mix (100 mm), 2.0 μL 10X RT random primers, 1.0 μL reverse transcriptase, 0.5 μL RNase inhibitor, and 3.7 μL distilled water (DNase and RNase free; Gibco®, ThermoFisher Scientific - 10977-035). The samples were processed using Professional Basic Thermocycler, using the cDNA synthesis program that ran at 25 °C for 10 min, 37 °C for 120 min, and 85 °C for 5 min. 1 μg of RNA was used in each reaction, diluted 1x after cDNA synthesis.

2.9 qPCR

Equal concentrations of RNA were reverse transcribed as indicated in 2.6. mRNA levels were quantified for *Phd2* in BM samples of Dox-treated *shPhd2/rtTA* and control mice. Technical triplicates of each sample were analysed and reactions were performed in a 5 μL volume. Each well was filled with 2.5 μL TaqMan® Universal PCR Master Mix (Applied Biosystems™, ThermoFisher Scientific, Cat. 4304437), 0.25 μL of the TaqMan ® probe/primer set for each gene (see **Table 2-2** below), 1.25 μL distilled water, and 1 μL of the cDNA sample. The samples were analysed using LightCycler® 480 (Roche), using the following program: 50 °C for 2 min, 95 °C for 10 min, followed by 40 cycles of 95 °C for 15 sec and 60 °C for 1 min. Finally, 60 °C for 5 min and 40 °C for 5 min. All signals were quantified using the ΔΔCt method using β-actin as the housekeeping gene (as optimised in the Kranc laboratory).

Table 2-2 TaqMan probes for *Phd2* expression

Gene	TaqMan Probe
β-actin	Mm00607939_s1
Phd2	Mm00459770_m1

2.10 Preparation of haematopoietic tissues

Tibias and femurs of both hind legs were taken from adult mice and crushed using a pestle and mortar until a homogenous cell suspension was achieved. Cells were collected in cold phosphate-buffered saline, supplemented with 2% heat-inactivated foetal calf serum and 2 mM ethylenediaminetetraacetic acid (PBS, 2 % FCS, 2 mM Ethylenediaminetetraacetic acid (EDTA)), and filtered through a 70 μm nylon strainer (BD Falcon, 352340). Spleen, thymus and lymph node tissue were dissected from adult mice and crushed with a syringe plunger to produce a single cell suspension in PBS (2 % FBS, 2 mM EDTA). Foetal liver (FL) cells were retrieved from 14.5 dpc embryos and mashed through a 70 μm nylon strainer.

2.11 Immunophenotypic characterisation of haematopoietic cells

SLAM staining: $12x10^6$ bone marrow (BM) cells were incubated in CD16/32 (Fc Block) antibody in 50 μL of cold PBS (2% FCS, 2 mM EDTA) for 5 min on ice. 50 μL of 2X SLAM antibody mix containing a biotin-conjugated lineage cocktail (CD3, CD4, CD5, CD8a, Gr-1, CD19, B220, Ter119) and Sca-1, CD117 (cKit), CD48 and CD150 was added and cells were incubated at 4 °C (protected from light) for 30 - 45 min. Cells were then washed in cold PBS (2% FCS, 2 mM EDTA) and pelleted by centrifugation at 500 x g for 5 min. The pellet was then re-suspended in 100 μL of Streptavidin and incubated for 15 min at 4 °C. Cells were then washed, pelleted by centrifugation and prepared for flow cytometry analysis.

Lineage staining: $2x10^5$ of BM, spleen or thymus cells were incubated with antibody mix: myeloid (CD11b, Gr-1); B-lymphoid (CD19, B220), T-lymphoid (CD4, CD8a), erythroid (Ter119, CD71) and incubated for 20 min at 4 °C (protected from light). Cells were then washed in cold PBS (2% FCS, 2 mM EDTA) and pelleted by centrifugation at 500 x g for 5 min.

Transplantation analysis staining: To evaluate the engraftment of transplantation experiments, BM, spleen, thymus, lymph node and foetal liver cells were additionally stained by anti-CD45.1 and CD45.2 antibodies.

For all experiments, cells were acquired on FACSFortessaV (BD). Cell sorting was performed on a FACSAria Fusion cell sorter (BD). Data were acquired through BD FACSDiva (BD Biosciences) and analysed by Flowjo software (Tree Star Inc., USA). The gating strategy for subsequent cell sorting and analysis was performed based on single stains, as no isotype controls were used. The antibodies used in these experiments are listed in **Table 2-3**. Representative gating strategies for all flow cytometry experiments are shown in **Figure 2-3, 2-4** and **2-5.**

Table 2-3 Flow cytometry antibodies

	Antibody	Concentration	Conjugate	Cat. No.	Clone	Manufacturer
Lineage Cocktail	CD4	0.3125 µg/mL	biotin	553649	H129.19	BD Biosciences
	CD5	0.625 µg/mL	biotin	553019	53-7.3	BD Biosciences
	CD8a	0.625 µg/mL	biotin	553029	53 -6.7	BD Biosciences
	CD11b	2.5 µg/mL	biotin	553009	M1/70	BD Biosciences
	CD45R/B220	2.5 µg/mL	biotin	553086	RA3-6B2	BD Biosciences
	Ter119	10 µg/mL	biotin	553672	TER-119	BD Biosciences
	Gr-1/Ly-6G/C	5 µg/mL	biotin	553125	RB6-8C5	BD Biosciences
HSPCs and Committed Progenitors	CD117/cKit	1 µg/mL	APC	105812	2B8	Biolegend
	Sca-1/Ly-	1 µg/mL	APC-Cy7	122513	E13-161.7	Biolegend
	Sca-1/Ly-	2.5 µg/mL	FITC	122506	E13-161.7	Biolegend
	CD48	0.4 µg/mL	PE	103406	HM48-1	Biolegend
	CD150	1 µg/mL	PE-Cy7	115914	12F12.2	Biolegend
Erythroid	Ter119	0.2 µg/mL	APC-Cy7	116223	TER119	Biolegend
	CD71	0.2 µg/mL	PE	113807	RI7217	Biolegend
B Cells	CD19	0.2 µg/mL	APC-Cy7	115530	6D5	Biolegend
	CD45R/B220	0.2 µg/mL	PerCP	103236	RA3-6B2	Biolegend
Myeloid Cells	CD11b	0.5 µg/mL	APC	101224	M170	Biolegend
	Gr-1/Ly-6G/C	0.2 µg/mL	PE-Cy7	108416	RB6-8C5	Biolegend
T Cells	CD4	0.2 µg/mL	PE	130310	H129.19	Biolegend
	CD8a	0.08 µg/mL	PE	100708	53-6.7	Biolegend
	CD8a	0.2 µg/mL	APC	100712	53-6.7	Biolegend
Transplantation Assays	CD45.1	0.5 µg/mL	FITC	110706	A20	Biolegend
	CD45.1	0.2 µg/mL	BV711	110739	A20	Biolegend
	CD45.2	0.5 µg/mL	Pacific Blue	109820	104	Biolegend
Strepavidin	Strepavidin	0.5 µg/mL	Pacific Blue	405225	-	Biolegend
	Strepavidin	1 µg/mL	PerCp	405213	-	Biolegend
Fc Block	CD16/32	10 µg/mL	none	553142	2.4G2	BD Pharmingen

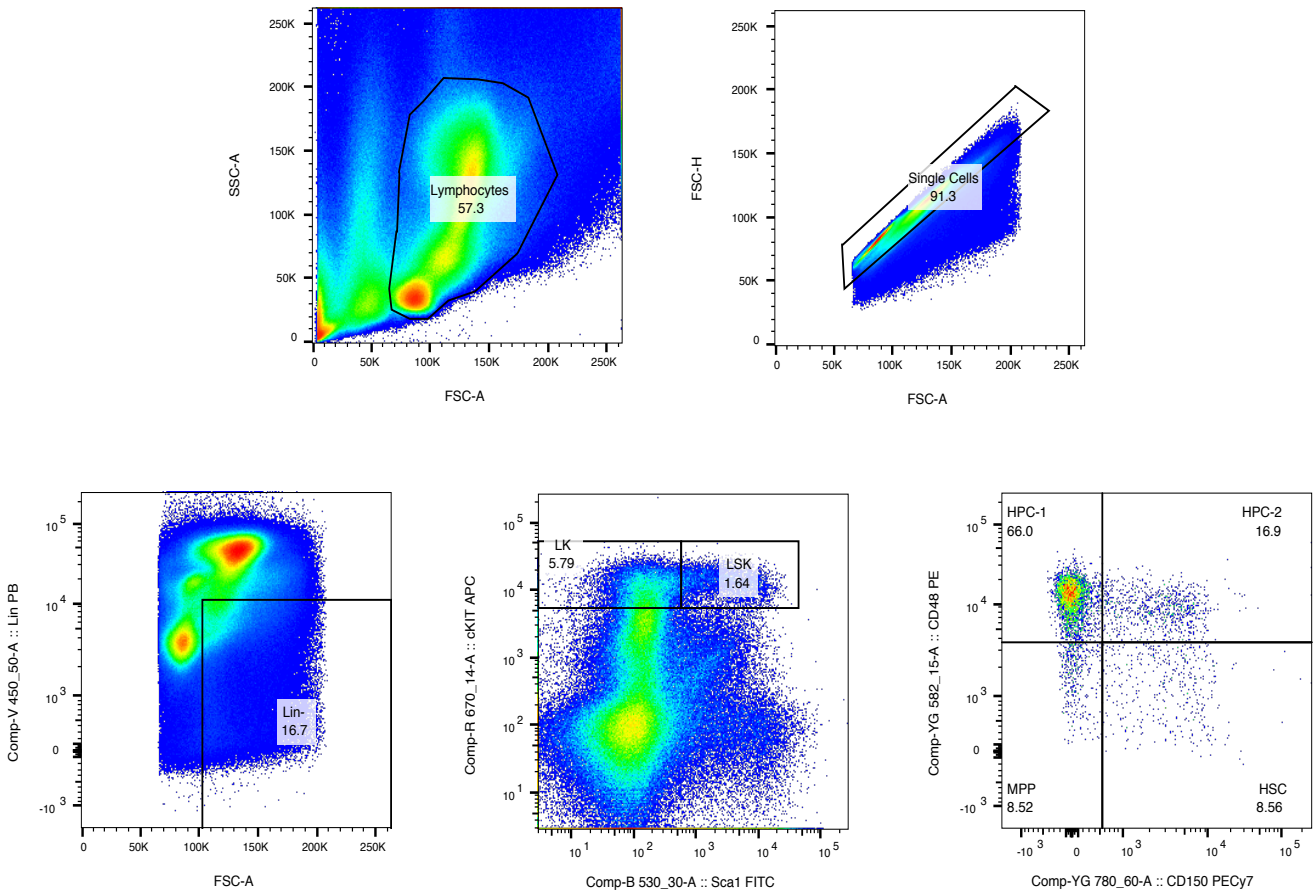

Figure 2-3 - Representative flow cytometry gating strategy for HSPC SLAM analysis Total BM cells were first live and size gated using forward scatter area (FSC-A) and side scatter area (SSC-A). Doublets were excluded using FSC-A versus FSC height (FSC-H). Lineage positive cells were excluded by gating on the lineage negative (Lin^-) population which contains the LK (Lin^-cKit^+) and LSK ($Lin^-cKit^+Sca\text{-}1^+$) cells. LSK cells were further sub-gated on haematopoietic stem cells (HSCs: LSK $CD48^-CD150^+$), multipotent progenitors (MPPs: LSK $CD48^-CD150^-$), haematopoietic progenitor cells-1 (HPC-1: LSK $CD48^+CD150^-$) and haematopoietic progenitor cells-2 (HPC-2: LSK $CD48^+CD150^+$) (Oguro et al., 2013).

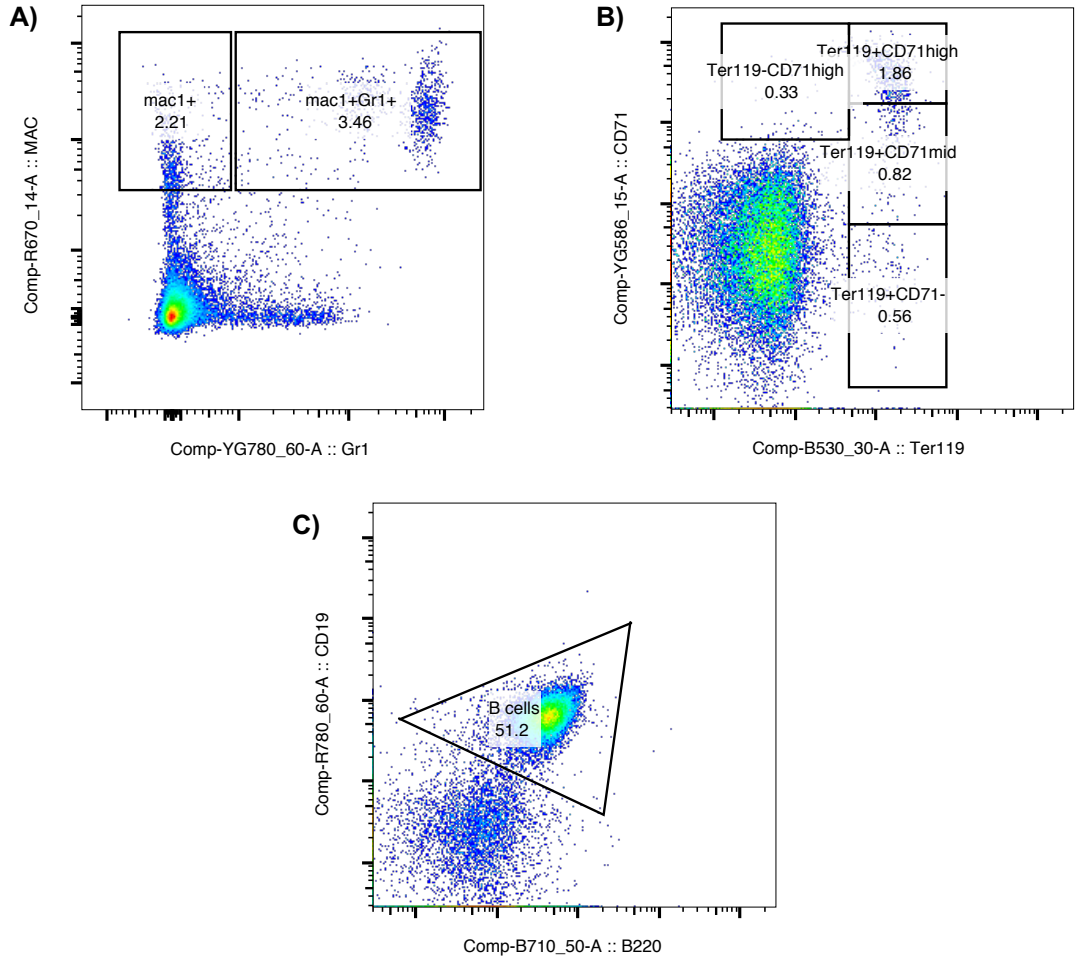

Figure 2-4 - Representative flow cytometry gating strategy for lineage staining analysis Total BM cells were first live and size gated using forward scatter area (FSC-A) and side scatter area (SSC-A). Doublets were excluded using FSC-A versus FSC height (FSC-H). Differentiated haematopoietic population were then gated as shown. **(A)** Gating of monocyte ($Mac1^+$) and granulocyte ($Mac1^+Gr1^+$) populations. **(B)** Erythrocyte populations were analysed using Ter119 and CD71 staining ($Ter119^-CD71^{high}$), ($Ter119^+CD71^{high}$), ($Ter119^+CD71^{mid}$) and ($Ter119^+CD71^-$) (Rasmussen et al., 2010). **(C)** Representative B cell (CD19+B220+) gating.

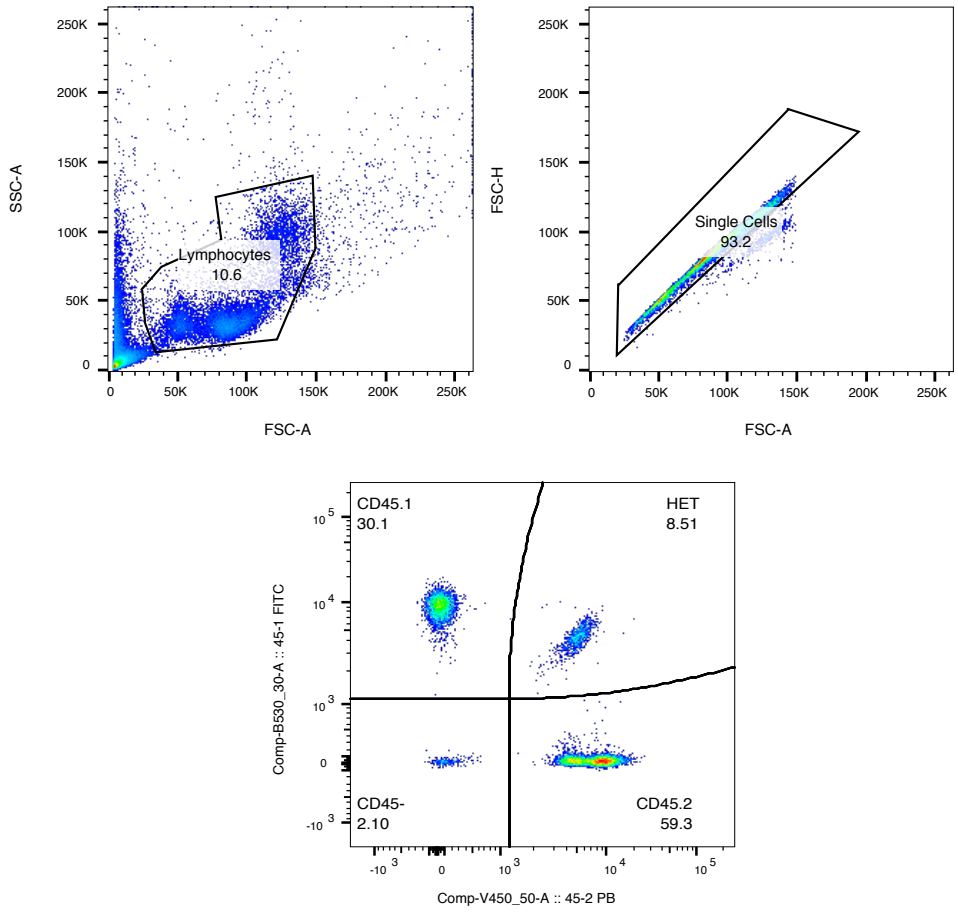

Figure 2-5 - Representative flow cytometry gating strategy for transplantation analysis Total peripheral blood cells were lysed with NH_4Cl and live and size gated using forward scatter area (FSC-A) and side scatter area (SSC-A). Doublets were excluded using FSC-A versus FSC height (FSC-H). Anti-CD45.1 and anti-CD45.2 antibodies were used to evaluate the engraftment of transplanted cells in $CD45.1^+$ /$CD45.2^+$ congenic recipient mice. Representative gating strategy of $CD45.1^+$ (support), $CD45.2^+$ (donor) and recipient $CD45.1^+$/$CD45.2^+$ (HET) populations are shown.

2.12 Transplantation assays

Irradiation Details: 8 to 12 weeks old mice were subjected to whole body *gamma* irradiation (Gammacell 40 Executor unit, Serial number 59R (Best Theratronics); source: Caesium 137) using a 33% attenuator. Lethal irradiation of $CD45.1^+$ /$CD45.2^+$ recipient mice was achieved using a split dose of 11 Gy (two doses of 5.5 Gy administered at least 4 h apart) at an average rate of 0.58 Gy/min.

Primary transplantations: For total BM transplantations, 500 000 unfractionated $CD45.2^+$ BM cells from transgenic mice were mixed with 500 000 unfractionated WT support cells expressing $CD45.1^+$ (or Ly5.1) and injected via the tail vein into healthy lethally irradiated $CD45.1^+$ /$CD45.2^+$ syngeneic recipient mice (11Gy). For HSC transplantations, 200 Lin^- cKit+Sca-1+ (LSK) CD48-CD150+ (HSCs) were sorted from donor BM ($CD45.2^+$) and transplanted together with 200 000 unfractionated $CD45.1^+$ WT BM wild-type cells. All donor mice were 8 to12 weeks old.

***Meis1/Hoxa9*-driven AML transplantation assays:** 100 000 $cKit^+$ Pre-Leukaemic Stem Cells (Pre-LSCs) from Colony Forming Assay (CFC) 3 were harvested and mixed with 200 000 unfractionated $CD45.1^+$ WT BM wild-type cells. These cells were then injected via the tail vein into healthy lethally irradiated $CD45.1^+$ /$CD45.2^+$ syngeneic recipient mice (11Gy). For secondary transplantation assays 50,000 LSCs ($CD45.2^+$ $cKit^+$) from the BM of primary recipients were transplanted into secondary lethally irradiated $CD45.1^+$ /$CD45.2^+$ syngeneic recipient mice (11Gy).

2.13 Blood sampling

To assess transplantation engraftment, peripheral blood (PB) samples were taken from the tail vein every 4 weeks. Blood was collected using capillary blood collection tubes coated with EDTA (Microvette CB300 K2E - 16.444, Sarstedt).

2.14 Isolation of HSPCs from 14.5 dpc FL cells

Embryos were aseptically removed and a homogenous cell suspension was achieved as previously described **(Section 2.10)**. Red blood cells (RBCs) were lysed by incubation with ammonium chloride (NH_4Cl) (Stem Cell Technologies - 07850) for 1 min. Cells were washed in cold PBS (2% FCS, 2 mM EDTA) to stop the reaction, and pelleted by centrifugation at 500 x g for 5 min. Cells were re-suspended in 100 μL of PBS (2% FCS, 2 mM EDTA) and incubated with immunomagnetic microbeads, conjugated to monoclonal anti-mouse CD117 (cKit) antibody (isotype: rat IgG2b) (Miltenyi Biotec – 130091224) for 25 min at 4 °C. Cells were added to a MACS LS column (Miltenyi Biotec - 130042401) attached to a QuadroMACS (Miltenyi Biotec) magnetic separator, and washed four times with PBS (2% FCS, 2 mM EDTA). To collect the cKit enriched cells, PBS (2% FCS, 2 mM EDTA) was added, the column was removed from the magnet, and the cKit enriched fraction was flushed out.

2.15 Retroviral production

Meis1/Hoxa9 retroviral production was conducted using a packaging cell line (Platinum E), allowing for retroviral packaging with a single plasmid transfection (Vukovic et al., 2015). The Platinum E (Plat-E) cell line, based on the 293T cell line, ensures high and stable expression of *gag, pol* and *env* (packaging viral proteins) through the *EF1α* promoter (Cell biolabs, Inc; https://www.cellbiolabs.com/platinum-e-plat-e-retroviral-packaging-cell-line).

2.15.1 Transfer vectors and components

MSCV-Meis1-puro: cDNA encoding murine *Meis1* was cloned into the MSCV (murine stem cell virus) vector, MSCVPGK. PGK (phosphoglycerate kinase internal promoter) controls the expression of the puromycin resistance cassette and the long terminal repeat (LTR) region drives the expression of *Meis1* gene (Kroon et al., 1998).

MSCV-HoxA9-neo: cDNA encoding murine HoxA9 fragment was inserted at BamHI-XhoI site of a pMSCVneoEB (neomycin (G418) resistance) (Kroon et al., 1998). The LTR region controls

the expression of HoxA9 gene and PGK promoter drives the expression of the neomycin resistance cassette.

PGK: the phosphoglycerate kinase (PGK) promoter drives the expression of antibiotic resistance genes, and therefore enables the selection of infected cells on the basis of antibiotic resistance.

MSCV: The Murine Stem Cell Virus (MSCV) retroviral vector is optimized for introducing and expressing target genes in pluripotent cells, including murine haematopoietic cells.

LTR: the retroviral long terminal repeat (LTR) contains promoters that drive gene expression in many infected cell types, including multiple haematopoietic lineages.

Subcomponents of LTR: U3-R-U5- element. U3 and U5 are found at the end of the viral genomic RNA and contain sequences necessary for activation of viral genomic RNA transcription.

2.15.2 Packaging vectors

VSV-G: Vesicular stomatitis virus G glycoprotein is the envelope vector that determines the tropism of the virus (broad tropism envelope protein).

2.15.3 Preparing the retrovirus

Plat-E cells were transfected by the Calcium Phosphate method, a method that involves the formation of calcium phosphate-DNA precipitates that facilitate the binding of condensed DNA to the cell surface, allowing the DNA to enter the cell by endocytosis (Kingston et al., 2003). The supernatant (containing viral particles) was collected 24 h after transfection, filtered through a 0.45 mm non-protein binding filter (Merck Millipore Corporation, SLHVM33RS) and snap frozen in dry ice and stored at -80 °C.

2.16 Retroviral transduction of HSPC cells

cKit$^+$ FL cells were incubated overnight in Iscove's Modified Dulbecco's Medium (IMDM) with 10 % FCS, 40 ng/mL of mouse recombinant stem cell factor (SCF) (carrier-free) (Biolegend, Cat. 579702), 20 ng/mL of recombinant mouse IL-3 (carrier-free) (Biolegend, Cat. 575502) and IL-6 (Biolegend, Cat. 575702) to promote cell cycle entry and proliferation of cells. Non-tissue culture treated 24 well plates (Nunc, 144530) were coated with RetroNectin® (Takara, T100A) and left overnight at 4 °C. RetroNectin® is a recombinant human fibronectin fragment which was used to enhance retroviral mediated gene transduction. The next day, RetroNectin® was removed from each well and 1 mL (500 μL of *Meis1*, 500 μL Hoxa9) of retroviral supernatant was added to the wells. The plate was centrifuged at 2000 x g for 2 h at 32 °C in order for the viral particles to bind to the plate. After centrifugation, the viral supernatant was removed and 250 000 cKit$^+$ cells in IMDM with 10 % FCS, and 40 ng/mL SCF, 20 ng/mL IL-3 and 20 ng/mL IL-6, were seeded onto the virus-coated plate and left overnight at 37 °C, 5 % CO_2. 12 h later, a second RetroNectin®-coated plate was similarly prepared with virus. The cKit$^+$ cells were then washed off the first plate and transferred onto the new viral plate. This sequence was repeated 12 h later, after which the cKit$^+$ cells were transferred onto a non-coated plate to recover and start expressing antibiotic resistance genes. 24 h later, cells were seeded in media (IMDM with 10 % FCS, and 40 ng/mL SCF, 20 ng/mL IL-3 and 20 ng/mL IL-6) containing 1.5 μg/mL puromycin and 1 mg/mL neomycin. Antibiotic selection lasted for 3 days.

2.17 Colony-Forming Cell (CFC) assay

2500 *Meis1/Hoxa9* transduced cKit$^+$ cells were plated in MethoCult^{TM} M3231 (Stem Cell Technologies, 03231) supplemented with 20 mL IMDM; 20 ng/mL of SCF; 10 ng/mL of IL-3; 10 ng/mL of IL-6 and 10 ng/mL of GM-CSF (granulocyte-macrophage colony stimulating factor; Biolegend - 576302), 100 Units/mL penicillin and 100 mg/mL streptomycin. 1.5 μg/mL puromycin and 1 mg/mL neomycin were added for continued antibiotic selection. Empty wells were filled with PBS in order to avoid evaporation of the semi-solid medium. After 6 days in

culture (CFC1), colonies were counted and re-plated at the same concentration with the same culture conditions (CFC2, CFC3). After CFC3, these cells are referred to as pre-LSCs.

2.18 Colony size assessment

1250 cells/well were seeded into MethoCult™ M3231 (Stem Cell Technologies, 03231) on a 6-well plate. Images were acquired at 37°C 5% CO_2 after 6 days in culture on an Operetta high content microscope (Perkin Elmer). Image analysis was performed in Columbus 2.7.1 (Perkin Elmer) by manual training as described in O'Duibhir et al, 2018. Colony data were analysed in Spotfire HCP 7.5.0 Perkin Elmer informatics.

2.19 Proliferation assay

Cells were adjusted to 50 000 cells/well in Iscove's Modified Dulbecco's Medium (IMDM) with 10 % FCS, 40 ng/mL of mouse recombinant stem cell factor (SCF) (carrier-free) (Biolegend - 579702), 20 ng/mL of recombinant mouse IL-3 (carrier-free) (Biolegend - 575502) and IL-6 (Biolegend - 575702), and plated in a 24-well plate in triplicate. Counting of cells was performed by trypan blue exclusion.

2.20 Cell death assay

Cells were counted to a concentration of 5000 cells/well in Iscove's Modified Dulbecco's Medium (IMDM) with 10 % FCS, 40 ng/mL of mouse recombinant stem cell factor (SCF) (carrier-free) (Biolegend - 579702), 20 ng/mL of recombinant mouse IL-3 (carrier-free) (Biolegend - 575502) and IL-6 (Biolegend - 575702), and plated in a 96-well plate in triplicate. 48 hrs later cells were washed and stained with TO-PRO™-3 Iodide (Molecular Probes, T3605) as a marker of dead cells. TO-PRO-3+ cells were measured using a BD Accuri flow cytometer.

2.21 Statistical analysis

All statistical analyses and graphing were performed with GraphPad Prism Software (v6.0h). Data represent mean ± standard error mean, except when data are presented as fold-change values. **** for P < 0.0001, *** for P < 0.001, ** for P 0.01, and * < for P 0.05 were considered statistically significant and were indicated in related figure legends and graphs.

The number of experiments noted in figure legends indicate independent experiments that were performed on different days, with 2-6 biological replicates. For transplantation experiments, 5-6 technical recipients were used. The sample size used in each experiment was not predetermined or formally justified for statistical power.

To assess the statistical significance of a difference between two treatments a two-tailed Student's *t*-test or a Mann–Whitney *U*-test was used. In **Chapter 3** and **Chapter 5**, Control (*Vav-iCre^{-})* samples were compared separately against *Phd1^{CKO}* (*Phd1$^{fl/fl}$;Vav-iCre^{+})* samples, *Phd2^{CKO} (Phd2$^{fl/fl}$;Vav-iCre^{+})* samples or *Phd1/2^{CKO} (Phd1$^{fl/fl}$;Phd2$^{fl/fl}$;Vav-iCre^{+})* samples. In **Chapter 4** and **Chapter 5**, Control (*rtTA)* samples were compared against *shPhd2/rtTA* samples. To assess the statistical difference between two treatments at multiple time points, a Multiple t-test was used, with statistical significance determined using the Holm-Sidak method. The statistical significance of differences in survival was assessed using the Mantel–Cox log-rank test.

CHAPTER 3

The role of Prolyl Hydroxylase Domain enzymes in steady state haematopoiesis

Chapter 3 The role of Prolyl Hydroxylase Domain enzymes in steady state haematopoiesis

3.1 Introduction

HSCs reside at the top of the hematopoietic differentiation hierarchy and function to sustain life-long production of all blood lineages. The pivotal balance between the quiescence, self-renewal and multi-lineage differentiation of HSCs is orchestrated by the bone-marrow microenvironment in which they reside (Mendelson and Frenette, 2014). These so-called bone marrow "niches" expose HSCs to numerous cues to regulate their biology, including TGFβ, CXCL12, angiopoietin-1, and environmental hypoxia (Arai et al., 2004; Sugiyama et al., 2006; Yamazaki et al., 2009).

Cellular responses to low-oxygen conditions are predominantly orchestrated by the heterodimeric hypoxia-inducible factors Hif-1 and Hif-2, which consist of the ubiquitously expressed HIF-α subunit and a constitutively expressed HIF- β subunit (Wang et al., 1995). The activity of the HIF-α subunit is regulated by the HIF prolyl hydroxylase domain enzymes, which in the presence of oxygen hydroxylate proline sites on HIF-α, targetting the protein for degradation (Epstein et al., 2001). As such the PHD family is integral to the hypoxia response, regulating the downstream transcription of hypoxia-related genes. Given that hypoxia is a key feature of HSC biology, and therefore downstream haematopoiesis, it is vital to dissect the role of the PHD family in this fundamental process.

3.1.1 PHDs

The PHD proteins are part of an evolutionary conserved family of dioxygenases that use oxygen and 2-OG as substrates, and iron and ascorbate as cofactors. Although there is only one HIF-specific prolyl hydroxylase in lower model organisms such as *Caenorhabditis elegans* (known as EGL-9) and *Drosophila melanogaster* (dHPH), humans and mammals have three PHD isoforms (PHD1, PHD2, PHD3) (Bruick and McKnight, 2001; Schofield and Ratcliffe, 2005). At an RNA level, all three PHD isoforms are widely distributed across various tissues, with PHD1 highest in the testes, and PHD3 highest in the heart. Notably, at a protein level, there is greater disparity between the PHD isoforms, with PHD2 the most abundant, and PHD3 only present at very low levels in normoxia (Berra et al., 2003; Stiehl et al., 2006). As such, Berra and colleagues in 2003 found that when various cell lines are cultured in normoxic conditions, PHD2 is the main isoform causing HIF-α degradation, quite possibly due to its plentiful expression. In addition to the differing affinities to HIF-α, and differential regulation, PHDs also have different sub-cellular location profiles, and so often function in distinct roles (Appelhoff et al., 2004; Lieb et al., 2002).

3.1.2 The role of PHDs in *in vivo* physiology

Given the importance of the hypoxia response in various tissues and biological processes, there have been significant research efforts to identify the role of each PHD isoform *in vivo.* Seminal studies by Takeda et al in 2006 generated transgenic *Phd* knock-out mice: *Phd1*$^{-/-}$, *Phd2*$^{-/-}$ and *Phd3*$^{-/-}$, excising the exons required for Fe^{++} binding, and therefore removing prolyl hydroxylase activity. The authors found that the *Phd2*$^{-/-}$ embryos were not viable, with embryonic lethality occurring between E 12.5 and E 14.5, with 70 % of the embryos dead at E 13.5. Notably, the *Phd2*$^{-/-}$ mice suffered severe placental and heart defects preceding embryonic death. As expected there were increased levels of HIF-1α and HIF-2α in the embryo overall, but not within the heart, suggesting the lethal heart defects were a systemic effect of PHD2 deletion, or a HIF-independent phenomenon. While the *Phd2*$^{-/-}$ embryos did not survive, *Phd1*$^{-/-}$and *Phd3*$^{-/-}$ mice were born healthy and in normal Mendelian ratios. This identified a unique role of PHD2 in embryogenesis, and provided further evidence that PHD2 remains the critical PHD isoform.

Unable to produce viable offspring using *Phd2* knockout mice, Takeda and colleagues in 2007 endeavoured to construct a *Phd2* conditional knockout transgenic model using tamoxifen-induced *Cre*, to study the role of PHD2 in adult mice. *Phd2* conditional knockout mice (*Phd2*^{CKO}*)* treated with tamoxifen had a significant increase in vasculature *in vivo*, thus concluding that PHD2 is a negative regulator for vascular growth. In addition, these PHD2-deficient adult mice had an approximately 230-fold increase in EPO expression and developed severe polycythaemia (Takeda et al., 2007). In concordance with this, in humans, there are 2 separate point mutations identified in the *PHD2* gene, both of which cause red blood cell defects (congenital erythrocytosis and polycythaemia) (Barradas et al., 2018; Percy et al., 2006).

3.1.3 The role of PHDs in haematopoiesis

Findings from early *in vivo* studies into the hypoxia pathway, as well as human clinical evidence, suggests an important role for PHDs in haematopoiesis. In addition, given that haematopoiesis occurs within the hypoxic environment of the BM, there has been notable research efforts to dissect the role of PHDs in this process in transgenic murine models.

Since there were no adverse phenotypes observed in the *Phd1*$^{-/-}$ or *Phd3*$^{-/-}$ single knockout mice, Takeda et al in 2008 generated *Phd1*$^{-/-}$;*Phd3*$^{-/-}$ double knockout (DKO) mice, analysing the apparent haematopoietic phenotypes observed in the tamoxifen-treated *Phd2*^{CKO} mice. These mice presented with morphological phenotypes consistent with increased erythropoietic activity such as enlarged haematopoietic organs (liver and spleen), and significant elevation in red blood cell (RBC) number, haemoglobin levels and haematocrit values in the peripheral blood (PB). As expected, flow cytometry analysis of the BM, spleen and liver of these mice showed a significant increase in erythroid progenitors (Ter119^{+} expression). Interestingly, analysis of the haematopoietic stem and progenitor cell (HSPC) compartment using Lin^{-} Sca1^{+} cKit^{+} cell surface markers (known as LSK cells) unveiled a significant increase in this compartment within the BM, spleen and liver. Methylcellulose colony formation cell (CFC) assay, however, showed no increase in the self-renewal capacity of these cells. Given that this transgenic model drives deletion of *Phd1* and *Phd3* in all tissues, it is possible these phenotypes are not a haematopoietic-specific effect. Nonetheless, there is evidence that *Phd1* and *Phd3* alter the biological processes surrounding haematopoiesis. In addition, as there are significant phenotypes in the DKO model, but none present in the *Phd1*$^{-/-}$ or *Phd3*$^{-/-}$ single knockout mice alone, there is an evident redundancy between *Phd1* and *Phd3*.

Further haematological analysis of tamoxifen-treated *Phd2*^{CKO} mice revealed that RBC, haemoglobin, haematocrit and white blood cell (WBC) levels were increased in the PB of mice with a deficiency of *Phd2*. As observed in the *Phd1*$^{-/-}$;*Phd3*$^{-/-}$ DKO mice, *Phd2*^{CKO} mice showed increased erythroid expression (Ter119^{+}) by flow cytometry, and an increase in LSK cells. Notably, in CFC assay there was no difference in colony formation in cells lacking *Phd2* versus

the WT. This data provides strong evidence that PHDs are vital in the process of haematopoiesis, but given the systemic deletion of *Phd2* in this tamoxifen-inducible model, it cannot be determined if this is a cell-autonomous or non-cell-autonomous phenotype within the haematopoietic system.

Following on from these seminal studies by Takeda, Singh and colleagues in 2013 explored the effect of deletion of *Phd2* within the haemopoietic system using a CD68 *Cre* mouse line. Using the CD68 promoter, this *Phd2*^{CKO} strain was found to have reduced *Phd2* levels in entire BM, as well as epithelial cells, and erythropoietin-producing cells in the kidney and brain. To verify that the CD68 *Cre* transgenic model promoted excision of *Phd2* in primitive haematopoietic compartments, as well as the total BM, the authors isolated LSK cells from tamoxifen-treated *Phd2*^{CKO} mice and performed RT-qPCR analysis. As hoped, *Phd2* ^{CKO} cells showed reduced expression of *Phd2*, and a subsequent increase in *Phd1* expression versus the WT, suggesting a compensatory mechanism between *Phd1* and *Phd2* in these cells. BM analysis of mice with conditional deletion of *Phd2* showed an increase in the absolute number of LSK cells, but no difference in the number of HSCs (LSK CD48^{-} CD150^{+}). Interestingly, in a non-competitive whole BM transplantation experiment, PHD2-deficient cells were able to successfully repopulate an irradiated recipient mouse. However, competitive transplantation of the LSK cells found that PHD2-deficient cells were outcompeted by their WT counterparts. This suggests that, although functional, haematopoietic progenitor cells lacking PHD2 are outcompeted under severe stress.

Importantly, the authors in this study employed a conditional PHD2 mouse line using *Cre*-recombinase under the control of the human CD68 promoter (Franke et al., 2013). This *Cre* was originally developed as a macrophage-specific *Cre*, deleting in monocytes and macrophages, and so does not delete in a large number of haematopoietic cells (Gough et al., 2001). In addition, this promoter also results in deletion in other tissues such as epithelial cells. Although significantly more specific than the tamoxifen-treated *Phd2*^{CKO} mice engineered by

Takeda et al, the CD68 *Cre* conditional knockout system still does not answer the fundamental question: what is the role of PHDs specifically within the haematopoietic system.

3.2 Aims and objectives of Chapter 3

Evidence from multiple studies in the field suggest significant roles for the PHD family in haematopoiesis. Previous *in vivo* studies have either employed a haematopoietic-specific *Cre*, with off-target deletions in non-haematopoietic tissues, or an inducible *Cre-lox* system driven by Tamoxifen or antibiotics such as Tetracycline, or its synthetic derivative Doxycycline (Dox). As such, to fully explore to the role of PHDs in haematopoiesis, this thesis utilises both models; the haematopoietic-specific *Vav-iCre*, and a Dox-inducible model, which generates a short-hairpin targeting *Phd2.* These models are described in **Chapter 3**, and **Chapter 4** respectively.

Previous studies published by the Kranc laboratory investigating the effect of haematopoietic-specific deletion of *Hif1-α* and *Hif2-α* found no significant or deleterious effect on steady-state haematopoiesis (Guitart et al., 2013; Vukovic et al., 2015; Vukovic et al., 2016). As such, this study hypothesises that haematopoietic-specific deletion of *Phd1, Phd2,* or both *Phd1* and *Phd2*, therefore stabilising *Hif1-α* and *Hif2-α,* will have no effect on steady-state haematopoiesis. To address this, the aim of this chapter is to investigate the role of *Phd1* and *Phd2* in steady-state haematopoiesis of adult mice using the *Vav-iCre* system. Flow cytometric analysis of the haematopoietic stem and progenitor cell compartment, as well as mature blood cells in the BM, will unveil if deletion of *Phd1, Phd2,* or both *Phd1* and *Phd2* have a cell-autonomous effect on the adult blood system.

3.3 Loss of *Phd1,* or both *Phd1* and *Phd2* results in an altered stem cell compartment

In order to determine the role of the PHD family within steady-state haematopoiesis, I analysed the HSPC and differentiated haematopoietic compartment of young adult mice (8-12 weeks old) with conditional deletions of *Phd1* (*Phd1$^{fl/fl}$;Vav-iCre^{+}*), *Phd2* (*Phd2$^{fl/fl}$;Vav-iCre^{+}*), or both (*Phd1$^{fl/fl}$; Phd2$^{fl/fl}$;Vav-iCre^{+}*), as well their *Vav-iCre^{-}* littermate controls .

Phd1$^{fl/fl}$ and *Phd2$^{fl/fl}$* mice were kindly provided by our collaborator Prof. Sir Peter Ratcliffe, and crossed with *Vav-iCre* mice (Mazzone et al., 2009, Boer et al., 2003). Notably, the *Phd1$^{fl/fl}$* and *Phd2$^{fl/fl}$* mice are engineered to have *loxP* sites flanking exon 3 of *Phd1* and exon 2 of *Phd2,* which both encode the sequences required for prolyl hydroxylase activity. Thus, upon *Cre-loxP*-mediated recombination with *Vav-iCre,* PHDs are unable to function to hydroxylate HIF-α (Epstein et al., 2001). Conditional knockout mice of *Phd1* (*Phd1$^{fl/fl}$;Vav-iCre^{+}*), *Phd2* (*Phd2$^{fl/fl}$;Vav-iCre^{+}*), or both (*Phd1$^{fl/fl}$; Phd2$^{fl/fl}$;Vav-iCre^{+}*), referred to as *Phd1^{CKO}, Phd2^{CKO}, Phd1/2^{CKO}* respectively were born in normal Mendelian ratios, and had no apparent health issues before analysis at 8-12 weeks.

Analysis of the BM of *Phd1^{CKO}, Phd2^{CKO}* and *Phd1/2^{CKO}* mice revealed a significant decrease in the BM cellularity of *Phd1^{CKO}* and *Phd1/2^{CKO}* mice versus the control **(Fig. 3-1B, 3-2B)**. The frequency and total number of Lin^{-} cells was also significantly reduced in *Phd1^{CKO}* and *Phd1/2^{CKO}* mice **(Fig. 3-1C, 3-2C)**. Importantly the percentage of both primitive progenitor Lin^{-} cKit^{+} (LK) cells and Lin^{-} cKit^{+} Sca-1^{+} cells is significantly higher in the *Phd1^{CKO}* and *Phd1/2^{CKO}* mice, suggesting a shift in haematopoiesis towards the progenitor populations **(Fig. 3-1D)**. However, due to the decrease in total BM cellularity, this phenotype is not reflected in the total LK and LSK numbers **(Fig. 3-2D)**.

Further flow cytometric analysis of the LSK compartment was conducted using the SLAM family marker CD150, alongside the CD48. This experiment allows for more in depth analysis of the stem and progenitor cell compartment, with the identification of haematopoietic stem

cells (HSCs: LSK CD48-CD150+), multipotent progenitors (MPPs: LSK CD48-CD150-), haematopoietic progenitor cells-1 (HPC-1: LSK CD48+CD150-) and haematopoietic progenitor cells-2 (HPC-2: LSK CD48+CD150) (Oguro et al., 2013). Focusing on the distribution of the LSK compartment, as shown in **Figures 3-1E-H**, there are no significant differences between the conditional knockout and control mice. Notably, however, there is an increase in total HSC number in the mice lacking both *Phd1*^{CKO} and *Phd2*^{CKO} versus the control **(Fig. 3-2E)**.

Notably, contrary to published research in the field, there is no apparent phenotype in the *Phd2*^{CKO} mice. This is likely due to the use of the haematopoietic-specific *Vav-iCre* opposed to other non-haematopoietic specific *Cres,* or the systemic ablation of *Phd2* in adult mice using tamoxifen. Unlike other models, *Vav-iCre* deletes only within the haematopoietic system, thus this study unveils the cell-autonomous effect of PHD deletion. Notably, however, there is strong evidence of an altered stem-cell compartment in *Phd1/2*^{CKO} mice, suggesting there is a redundancy between *Phd1* and *Phd2* within these primitive haemopoietic cells.

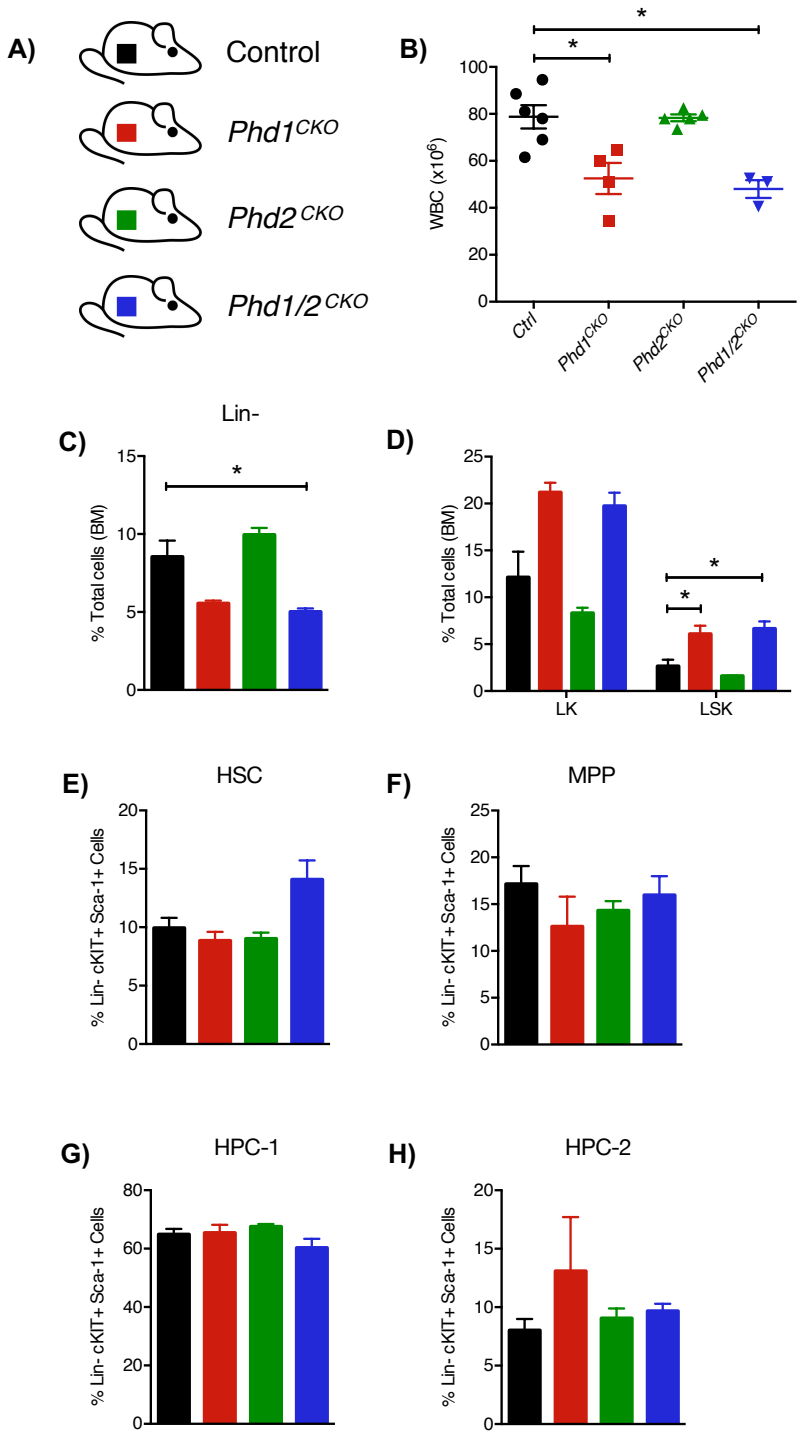

Figure 3-1 - Mice lacking *Phd1* or both *Phd1* and *Phd2* show an increased percentage of LSK cells
(A) Schematic representation of the control, *Phd1*^{CKO}, *Phd2*^{CKO} and *Phd1/2*^{CKO} transgenic mice **(B)** Total numbers (per 2 femurs and 2 tibias) of white blood cells (WBC). Percentage of Lin$^-$ **(C)**, and Lin$^-$ cKit$^+$ and Lin$^-$ cKit$^+$ Sca-1$^+$ cells **(D)** in the total bone marrow (BM). Percentage of haematopoietic stem and progenitor cells within the LSK compartment. Characterisation was based on expression of SLAM markers**:** haematopoietic stem cells (HSCs: LSK CD48$^-$CD150$^+$) **(E)** multipotent progenitors (MPPs: LSK CD48$^-$CD150$^-$) **(F)** haematopoietic progenitor cells-1 (HPC-1: LSK CD48$^+$CD150$^-$) **(G)**; haematopoietic progenitor cells-2 (HPC-2: LSK CD48$^+$CD150$^+$) **(H)**. n=3-8 biological replicates per genotype. Data are mean ± SEM. *, P < 0.05 (Mann-Whitney U test).

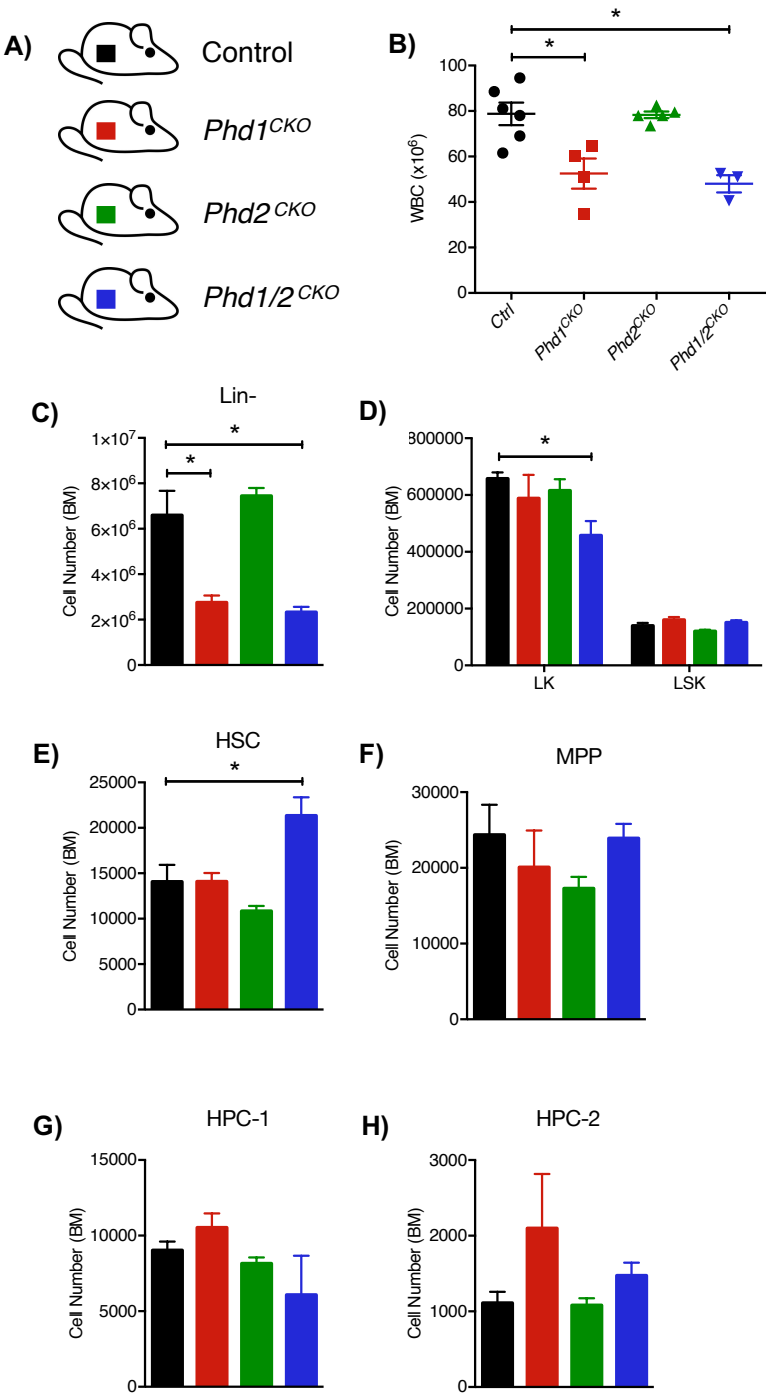

Figure 3-2 - Mice deficient in *Phd1* or both *Phd1* and *Phd2* have lower BM cellularity and an altered HSPC compartment (A) Schematic representation of the control, *Phd1*^{CKO}, *Phd2*^{CKO} and *Phd1/2*^{CKO} transgenic mice **(B)** Total numbers (per 2 femurs and 2 tibias) of white blood cells (WBC), Lin$^-$ **(C)**, and Lin$^-$ cKit$^+$ and Lin$^-$ cKit$^+$ Sca-1$^+$ cells **(D)**. Characterisation of haematopoietic stem and progenitor cells was based on expression of SLAM markers**:** haematopoietic stem cells (HSCs: LSK CD48$^-$CD150$^+$) **(E)** multipotent progenitors (MPPs: LSK CD48$^-$CD150$^-$) **(F)** haematopoietic progenitor cells-1 (HPC-1: LSK CD48$^+$CD150$^-$) **(G)**; haematopoietic progenitor cells-2 (HPC-2: LSK CD48$^+$CD150$^+$) **(H)**. n=3-8 biological replicates per genotype. Data are mean ± SEM. *, P < 0.05 (Mann-Whitney U test).

3.4 PHD1 and PHD2 are not required for mature haematopoietic cell differentiation

To investigate the role of PHD1 and PHD2 in differentiated haematopoietic cells, I analysed the BM of 8-12-week-old *Phd1*^{CKO}, *Phd2*^{CKO} and *Phd1/2*^{CKO} mice using B cell (CD19, B220), T cell (CD4, CD8) and myeloid (Mac1 and Gr1) cell surface markers. Flow cytometric analysis revealed there are no significant differences in the frequency of B cell, T cell or myeloid cells in the *Phd* conditional knockout mice versus the control **(Fig. 3-3)**. Notably, there is a decrease in the percentage of myeloid cells in both *Phd1*^{CKO} and *Phd1/2*^{CKO} mice, but this is not significant.

There is a significant decrease in the number of B cells and myeloid cells in mice lacking *Phd1,* and both *Phd1* and *Phd2* **(Fig. 3-4E)**. Notably, this reduction is in concordance with a decrease in the total BM cellularity, as shown in **Figure 3-4E**. As such, the significant decrease in B cells and myeloid cells, along with further decreases in other differentiated compartments that were not analysed, are likely to have contributed to the overall decrease in BM cellularity.

Overall, it is evident that PHD1 and PHD2 do not play a significant role in differentiated blood cells, but deletion of both *Phd1* and *Phd2* may lead to a decrease in B cell and myeloid cell populations.

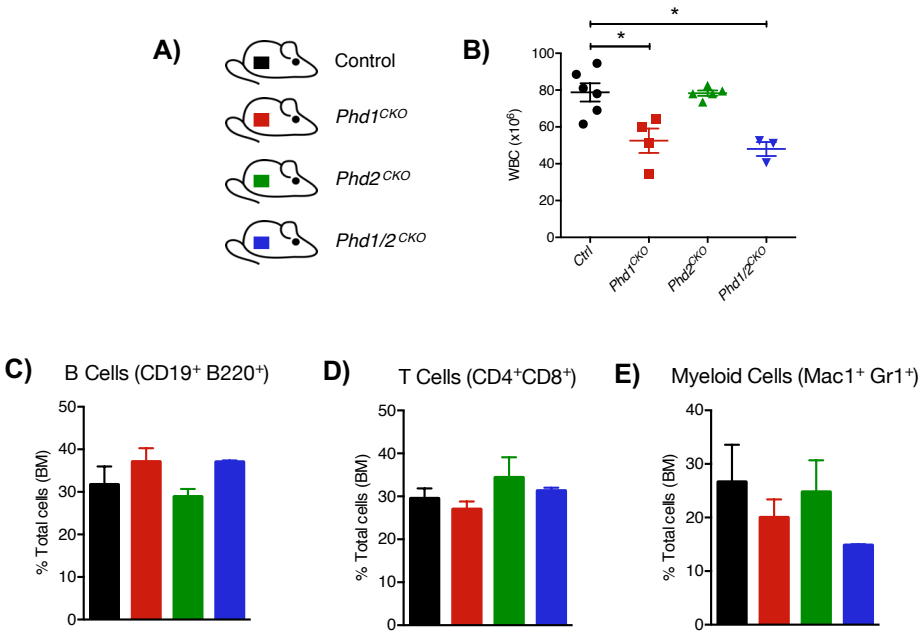

Figure 3-3 - Deletion of *Phd1, Phd2* or both *Phd1* and *Phd2* has no effect on mature haematopoietic cells (A) Schematic representation of the control, *Phd1*^{CKO}, *Phd2*^{CKO} and *Phd1/2*^{CKO} transgenic mice **(B)** Total numbers (per 2 femurs and 2 tibias) of white blood cells (WBC). Percentage of B cells (CD19^{+}B220^{+}) **(C)**, T cells (CD4^{+}CD8^{+}) **(D)**, and myeloid cells (Mac1^{+}Gr1^{+}) **(E).** n=3-8 biological replicates per genotype. Data are mean ± SEM. *, P < 0.05; **, P < 0.01 (Mann-Whitney U test).

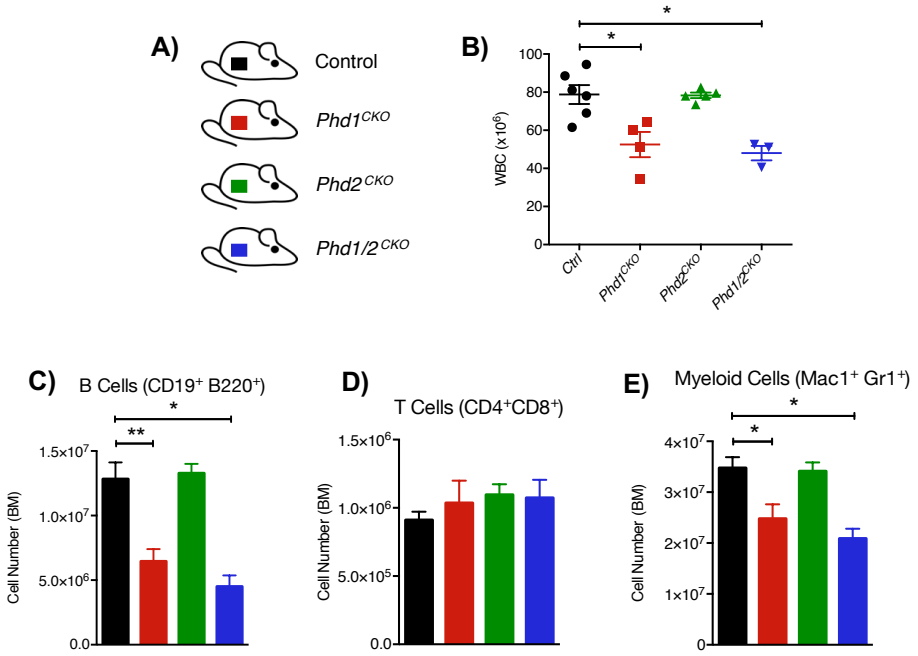

Figure 3-4 - Ablation of *Phd1,* or both *Phd1* and *Phd2* reduces total numbers of B cells and myeloid cells (A) Schematic representation of the control, *Phd1*^{CKO}, *Phd2*^{CKO} and *Phd1/2*^{CKO} transgenic mice **(B)** Total numbers (per 2 femurs and 2 tibias) of white blood cells (WBC). Total numbers in the BM of B cells (CD19^{+}B220^{+}) **(C)**, T cells (CD4^{+}CD8^{+}) **(D)**, and myeloid cells (Mac1^{+}Gr1^{+}) **(E).** n=3-8 biological replicates per genotype. Data are mean ± SEM.

3.5 Discussion

In conclusion, work in this chapter unveils new roles for *Phd1* and *Phd2* in steady state haematopoiesis, with ablation of *Phd1,* or both *Phd1* and *Phd2* resulting in a decrease in BM cellularity and an altered stem cell compartment. Although phenotypes presented in this chapter are somewhat less significant than other research published in this field, especially with regards to the effect of deletion of *Phd2* (Takeda et al., 2007; Takeda et al., 2008; Singh et al., 2013), my research focused on dissecting the role of PHDs specifically within the haematopoietic system. As such, utilising *Vav-iCre* gave specific deletion with blood and immune cells, with significant accuracy over other haematopoietic *Cres*. In fact, a study by Abram et al in 2014 analysed various hematopoietic deleting strains, and found *Vav1-cre:*ROSA-EYFP mice had the largest percentage of expression with a 98-100 % deletion in all hematopoietic cells. As such, using *Vav-iCre* in this study ensures near-complete deletion of *Phd1* and *Phd2* within the cell compartments studied.

Most notably, Singh et al in 2013 generated a $Phd2^{CKO}$ mouse model utilising the CD68 *Cre*, with BM analysis of these mice showing an increase in LSK cell number, a phenotype not observed in results in this chapter. This result was also recorded in tamoxifen-treated $Phd2^{CKO}$ mice, where *Phd2* is deleted in all tissues upon tamoxifen induction (Takeda et al., 2008). In comparison to *CD68-Cre*, *Vav-iCre* is often regarded as the gold standard for hematopoietic-specific *Cre* strains and is restricted to only cells of the haematopoietic system, apart from some low-level expression in the testis and ovaries (de Boer et al., 2003). CD68, on the other hand, is known to be expressed in multiple other cell types, including epithelial tissue (Gough et al., 2001). This suggests that *Phd2* is not essential for cell-autonomous LSK function, but does have a wider, systemic role in the biology and maintenance of the LSK compartment.

This chapter unveiled a new role for *Phd1* specifically within the haematopoietic system. Previous work focused solely on $Phd1^{-/-}$ knockout mice, or $Phd1^{-/-};Phd3^{-/-}$ double knockout mice, with deletion of *Phd1* or *Phd1* and *Phd3* in all tissues. Notably, the haematopoietic system in $Phd1^{-/-}$ knockout mice has not been analysed, but $Phd1^{-/-};Phd3^{-/-}$ double knockout

mice presented with an increased LSK compartment. Opposing data published by Takeda et al in 2008 revealed that ablation of *Phd1* within the haematopoietic system resulted in a significant decrease in BM cellularity **(Fig. 3-1B)**. Ablation of both *Phd1* and *Phd2* also yields a decrease in BM cellularity, but deletion of *Phd2* does not reduce this further **(Fig. 3-1B)**. Thus, *Phd1* has an important cell-autonomous effect on BM cellularity.

Notably, as a consequence of the reduced BM cellularity, there are also decreases in the Lin^- and LK populations in the $Phd1^{CKO}$ and $Phd1/2^{CKO}$ mice **(Fig. 3-2C, 3-2D)**. Interestingly, however there is a significant increase in the percentage of LSK cells in the BM of $Phd1^{CKO}$ and $Phd1/2^{CKO}$ mice, perhaps mirroring the results of Takeda and colleagues in 2008. However, when adjusted to total cell number using the BM cellularity, there is no decrease in the total number of LSK cells **(Fig. 3-1D, 3-2D)**.

The most striking phenotype from the steady-state analysis is the significant increase in the frequency and total number of HSCs in mice lacking both *Phd1* and *Phd2* versus the control **(Fig. 3-1E, 3-2E)**. This is especially remarkable given the noted decrease in BM cellularity of these mice. Given the lack of phenotype in $Phd1^{CKO}$ and $Phd2^{CKO}$ mice, it can be concluded that there is a cell-autonomous synergistic role between *Phd1* and *Phd2* in the HSC compartment. As deletion of both *Phd1* and *Phd2* increases HSC number, further analysis of $Phd1/2^{CKO}$ cells, including cell-cycle and transplantation assays, would unveil the fitness of these cells versus the WT. Notably, it is possible that these cells have expanded, but are no longer fit, to the detriment of the haematopoietic system. Given that HSCs are dispensable for steady-state haematopoiesis (Busch et al., 2015), putting these cells under stress inducing conditions such as IFNα or serial HSC transplantation would test their functionality (Essers et al., 2009). If HSCs lacking *Phd1* and *Phd2* were indeed functional, it is possible that *Phd1* and *Phd2* could be targets in the *in vitro* expansion of HSCs.

Notably, this chapter did not focus on the role of *Phd3* in steady-state haematopoiesis, as the isoform is expressed at very low levels in the blood system (Stiehl et al., 2006). However,

given the significant phenotypes observed in the *Phd1/2*^{CKO} mice, especially within the primitive and HSC compartments, the generation of *Phd1/2/3*^{CKO} mice (*Phd1*$^{fl/fl}$*; Phd2*$^{fl/fl}$*; ; Phd3*$^{fl/fl}$ *Vav-iCre*$^{+}$), would give interesting further insight into the role of the PHD family in haematopoiesis.

In conclusion, this chapter has contributed significantly to the field, demonstrating that *Phd2* is dispensable in cell-autonomous steady-state haematopoiesis. In addition, the expansion of HSCs in *Phd1/2*^{CKO} mice merits further investigation as the PHD family may unveil themselves as fundamental regulators in HSC biology.

CHAPTER 4

The role of Prolyl Hydroxylase Domain enzymes in steady state haematopoiesis

Chapter 4 The role of systemic *Phd2* knockdown in haematopoiesis

4.1 Introduction

As described in **Chapter 3**, several studies have attempted to the define the physiological or pathological activities of the PHD proteins using genetic inactivation. PHD2 is the most abundantly expressed of the PHD isoforms, and thus has been studied extensively (Berra et al., 2003; Stiehl et al., 2006). At the whole animal level, knockout of *Phd2* results in developmental defects and embryonic lethality (Takeda et al., 2006). Conditional knockout of *Phd2* using a tamoxifen-inducible *Cre*, systemically deleting *Phd2* in all adult tissues, lead to an increase in angiogenesis, erythrocytosis and changes in energy metabolism, with ultimately lethal consequences (Minamishima et al., 2008; Takeda et al., 2008; Takeda et al., 2007). Additionally, recent research success of PHD2 inhibitors for the treatment of diseases such as ischemia and chronic kidney disease, and their subsequent use in multiple clinical trials, gives further weight for precise analysis of the effect of *Phd2* depletion *in vivo* (Haase, 2017).

Data presented in **Chapter 3**, utilising the *Vav-iCre* system to delete *Phd2* specifically within the haematopoietic system concluded that *Phd2* was not required for steady state haematopoiesis. Given that this data is at odds with that published within the field (Takeda et al., 2008; Singh et al., 2013). I chose to further investigate the role of *Phd2* in haematopoiesis using an inducible RNA interference gene knockdown *in vivo*. This offers the advantages of timed, reversible and specific gene silencing in mature cells, producing effects potentially more analogous to those which might occur physiologically, pathologically or in response to pharmacological inhibition.

4.1.1 Inducible *shPhd2*-mediated knockdown model

As outlined in **Chapter 2** and **Figure 2-1**, *rtTA/shPhd2* and Control *rtTA* mice were donated by Chris W Pugh and Sir Peter J Ratcliffe and are described in Yamamoto et al, 2019 (in submission, JCI). Notably, the reverse tetracycline trans-activator (*rtTA)* is placed under control of the *CAG* promoter which gives a stronger and greater ubiquitous expression than under the *R26-rtTA* promoter (Dow et al., 2012). Upon doxycycline (Dox) treatment, there is activation of the tetracycline response element (*TRE*) controlled *GFP-shPhd2* cassette (*TRE-shPhd2*), which results in transcription of both GFP and *shPHD2* in the *rtTA/shPhd2* mice. Control *rtTA* mice do not have the *GFP-shPhd2* cassette, and so upon Dox treatment, there is no transcription of GFP or *shPHD2.* Notably, the GFP reporter was utilised in flow cytometry and fluorescence activated cell sorting (FACS) to identify cells lacking *Phd2* under this transgenic system.

4.2 Aims and objectives of Chapter 4

Given that results described in this thesis **(Chapter 3)** contradict those already published in the field, the aim of this chapter is to determine the effect of *Phd2* knockdown in the haematopoietic system of adult mice using immunophenotypic and transplantation assay analysis. *shPhd2/rtTA* mice, which upon Dox treatment transcribe a short-hairpin targeting *Phd2,* as well as *GFP*, were utilised to perform acute *Phd2* depletion in both steady-state haematopoiesis and transplantation experiments. In concordance with published research in the field (Singh et al., 2013; Takeda et al., 2008; Takeda et al., 2007; Takeda et al., 2006), this chapter hypothesises that systemic deletion of *Phd2* will impact haematopoiesis under steady and stressed conditions.

Analyses of the primitive and differentiated hematopoietic compartments were performed in both experiments to fully dissect the role of *Phd2* in all stages of haematopoiesis. Notably, following the exposure of myeloid-specific phenotypes in **Chapter 3**, this chapter sub-divides the myeloid compartment ($Mac1^+Gr1^+$) into monocytes ($Mac1^+$), which can develop into dendritic cells or macrophages, and granulocytes ($Mac1^+Gr1^+$), which are either neutrophils, eosinophils or basophils (Yam et al., 1971). Results from these experiments will determine if there is, indeed, a significant role for *Phd2* in haematopoiesis, under both normal and stressed conditions.

4.3 Validation of the *shPhd2/rtTA* transgenic model

Upon receiving *shPhd2/rtTA* and *rtTA* (Control) mice from Chris W Pugh and Sir Peter J Ratcliffe from the University of Oxford, I first set out to validate this novel and unpublished transgenic *in vivo* model. Notably, qPCR analysis conducted at the University of Oxford found than upon Dox treatment, *shPhd2/rtTA* mice displayed significant reduction in *Phd2* levels in multiple tissue types including liver, kidney, thymus, spleen, heart, skin and BM. As expected, as a consequence of reduced *Phd2* levels, there was an increase in *Phd3* and *Bnip3* (a HIF target gene) in these tissues measured by qPCR. This suggests that the tissues are able to compensate for the reduction of *Phd2* and HIF activity is increased, respectively (Yamamoto et al., in submission).

To validate this mouse strain for further haematopoietic analysis, *shPhd2/rtTA* and *rtTA* (Control) mice were treated with Dox for 5 weeks (as advised by Chris W Pugh and colleagues). Following this, BM cells were extracted and GFP expression was measured by flow cytometry analysis. As shown in **Figure 4-1C** and **Figure 4-1D**, there is strong GFP expression in the BM of *shPhd2/rtTA* mice, but no GFP expression in the BM of control mice. To ensure that GFP expression was correlated with a reduction in *Phd2* levels, RNA was extracted from control, as well as the GFP^-, and GFP^+ fraction of *shPhd2/rtTA* BM cells, and qRT-PCR was performed. Notably the GFP^- and GFP^+ *shPhd2/rtTA* BM cells were isolated by FACS. **Figure 4-1B** shows that, as expected, there is a significant reduction in *Phd2* mRNA levels in the GFP^+ *shPhd2/rtTA* cells when compared to the control. There is a slight reduction in *Phd2* expression in the GFP^- *shPhd2/rtTA* cells, this, however, is likely an artefact of FACS gating strategy, including a small number of cells, with low GFP-expression in the GFP^- gate.

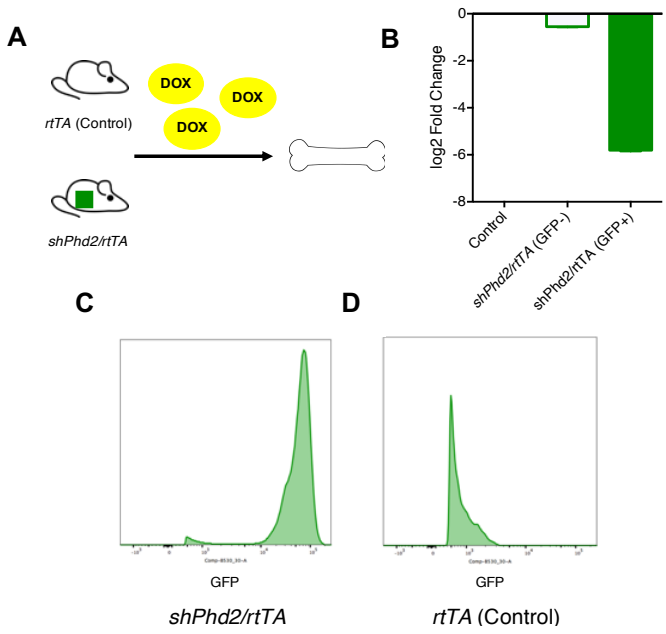

Figure 4-1 - Upon Dox treatment, *shPhd2/rtTA* mice show a decrease in *Phd2* levels and expression of GFP (A) Schematic representation of the *rtTA (*Control) and *shPhd2/rtTA* transgenic mice. Control and *shPhd2/rtTA* mice were treated with 2 mg/ml Dox in their drinking water for 5 weeks and BM cells were isolated. GFP^+ and GFP^- cells were collected by FACS, and RNA extracted **(B)** qRT-PCR analysis of control, GFP^- *shPhd2/rtTA* and GFP^+ *shPhd2/rtTA* cells. Data are represented as fold change over control after normalising to β-actin levels using the ΔΔCT method. Representative flow cytometry histogram plots of GFP expression in *shPhd2/rtTA* **(C)** and control BM cells **(D)**.

4.4 Knockdown of *Phd2* results in a reduction of mature blood cells in the PB

To investigate the effect of systemic knockdown of *Phd2* in steady state haematopoiesis, 5-week old control and *shPhd2/rtTA* mice were treated with Dox for 8 weeks, with subsequent final BM analysis at 12 weeks of age. Notably, analysis of these young adult mice ensured exclusion of any aged phenotypes, and allowed for valid comparisons with the *Phd2*^{CKO} mice, investigated in **Chapter 3**, which were analysed at 8 - 12 weeks of age. Although there is no evidence of Doxycycline affecting steady-state or stressed haematopoiesis, treating both *shPhd2/rtTA* and control mice with Dox ensures any phenotypes observed in *shPhd2/rtTA* mice are independent of Dox, thus a direct consequence of knockdown of *Phd2*.

In addition to final BM analysis, peripheral blood (PB) samples from control and *shPhd2/rtTA* mice were taken at 4 weeks and 8 weeks during Dox treatment to evaluate the effect of *Phd2* depletion on the peripheral blood. As shown in **Figure 4-1B** and **4-1E**, at both 4 and 8 weeks of Dox treatment there is significant GFP expression in the PB of *shPhd2/rtTA* mice, with an average GFP expression of 68.75 %. Notably there is no GFP expression in the control mice treated with Dox. This suggests there is a significant reduction of *Phd2* levels in the peripheral blood of *shPhd2/rtTA* mice.

After 4 weeks of Dox treatment, there is a significant decrease in the percentage of T cells ($CD4^+$ $CD8^+$), and an increase in granulocytes ($Mac\text{-}1^+$ $Gr1^+$). 4 weeks later, there is no difference in the percentage of T cells in the PB when comparing the control and *shPhd2/rtTA* mice, but there is instead a significant decrease in B Cells ($CD19^+$ $B220^+$). Notably, the increase in the granulocyte population shown at week 4 is still present, and has increased further at week 8 **(Fig. 4-1C, 4-1F)**.

Haematological parameters of the PB samples were measured at week 4 and week 8 of Dox treatment using a HEMAVET® 950 analyser, and it was discovered that at week 8 the WBC, RBC, haemoglobin (HGB) and haematocrit (HCT) values were decreased in the *shPhd2/rtTA*

mice versus the control. Notably, these phenotypes were also observed in parallel experiments at the University of Oxford (Yamamoto et al., in submission). As these changes only became apparent after 8 weeks of Dox treatment, it is evident that the long-term reduction of *Phd2* levels has a significant effect on the PB.

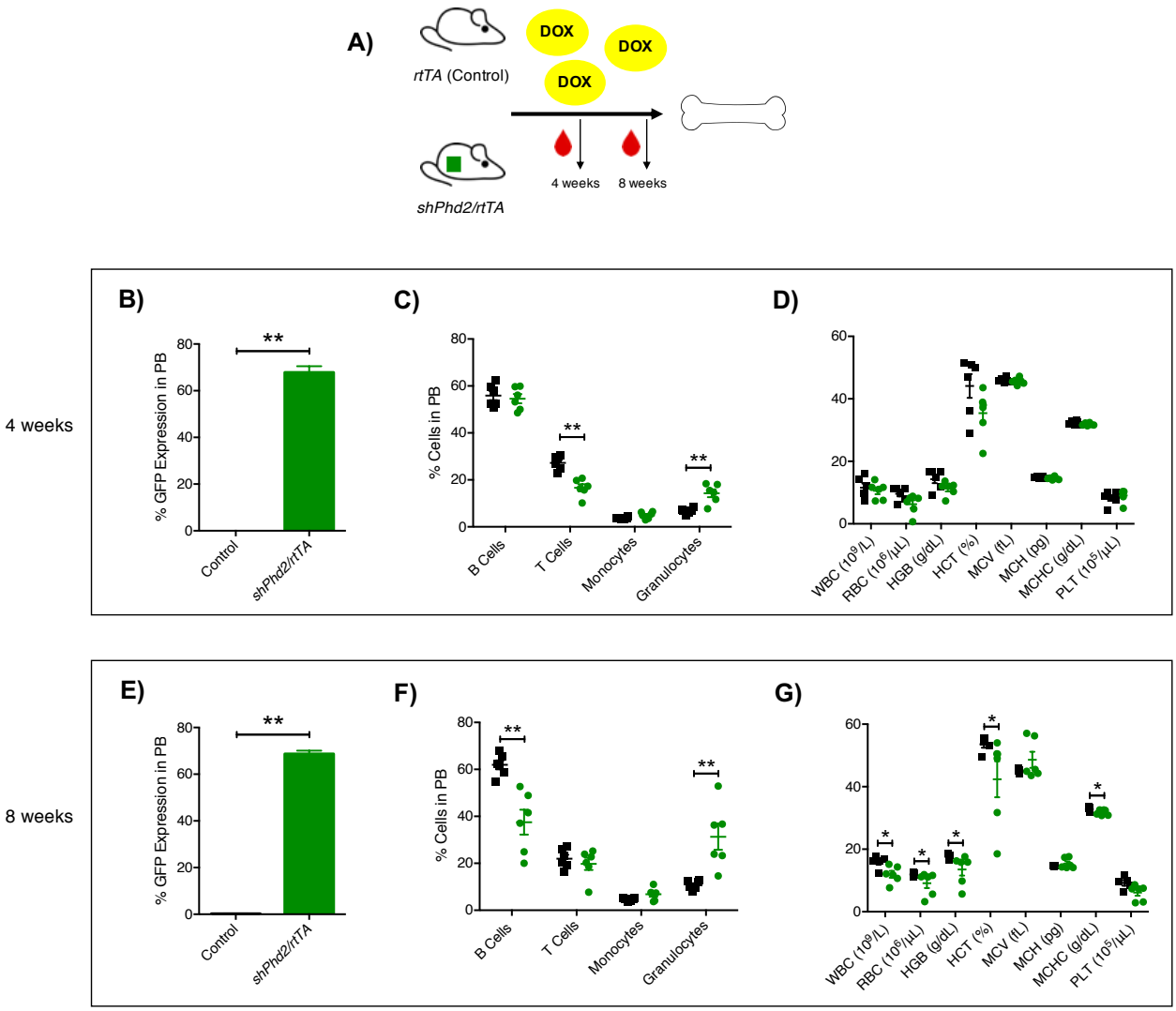

Figure 4-2 - Systemic reduction of *Phd2* levels results in abnormal haematological parameters **(A)** Schematic representation of the *rtTA (*Control) and *shPhd2/rtTA* transgenic mice. Control and *shPhd2/rtTA* mice were treated with 2 mg/ml Dox in their drinking water for 8 weeks. PB blood samples were taken at 4 and 8 weeks of Dox treatment. At week 4, the percentage of GFP **(B)** and mature blood cells (B cells ($CD19^+B220^+$), T cells ($CD4^+CD8^+$), monocytes ($Mac1^+$) and granulocytes ($Mac1^+Gr1^+$)) were analysed by flow cytometry **(C)** Haematological parameters; White Blood Cell (WBC), Red Blood Cell (RBC), haemoglobin (HGB), haematocrit (HCT), Mean Cellular Volume (MCV), Mean Cellular Height (MCH), Mean Corpuscular Haemoglobin Concentration (MCHC) and Platelets (PLT) were measured using a HEMAVET® 950 analyser **(D)**. Flow cytometry analysis was conducted **(E)(F)**, and haematological parameters **(G)** were measured again at week 8. n=6 biological replicates per genotype. Data are mean ± SEM. **, $P < 0.01$ (Mann-Whitney U test).

4.5 *Phd2* is not required for mature haematopoietic cells in the BM

In order to investigate the role of *Phd2* in differentiated haematopoietic cells, I analysed the BM of control and *shPhd2/rtTA* mice described in **Section 4.1.1**. As shown in **Figure 4-3**, there was no difference in the BM cellularity or the number of RBCs in the mice with knockdown of *Phd2* versus control.

In concordance with data presented in **Figure 4-1C** and **Figure 4-1D**, flow cytometry analysis of the BM found significant GFP expression in the *shPhd2/rtTA* mice, when compared to the control, with mean percentage GFP expressions of 82.37 % and 0.23 % respectively **(Fig. 4-4B)**. Further immunophenotypic analysis of the BM using B cell (CD19, B220), T cell (CD4, CD8) and myeloid (Mac1 and Gr1) cell surface markers found there was no difference in the mature haematopoietic compartment following acute reduction of *Phd2* levels **(Fig. 4-4D)**.

Additionally, given that tissue hypoxia is known to regulate the process of erythropoiesis, I decided to study the role of systemic *Phd2* knockdown in the differentiation of erythroid progenitors using the cell-surface markers CD71 and Ter119 (Koulnis et al., 2011). The co-staining of Ter119, which specifically marks maturing erythrocytes, and CD71, a transferrin receptor expressed on all proliferating cells, is widely used in erythropoiesis research (Levy et al., 199) (Fraser et al., 2007). Zhang and colleagues in 2003 dissected this novel flow cytometry-based staining, comparing it to the morphological phenotypes of the analysed cells, and found that the $TER119^-$ $CD71^-$population corresponded to the most primitive erythropoietic cells; the proerythroblasts and early basophilic erythroblasts. In the $TER119^-$ $CD71^+$ they found early and late basophilic erythroblasts, in the $TER119^+$ $CD71^+$ population chromatophilic and orthochromatophilic erythroblasts, and finally the most differentiated cells (late orthochromatophilic erythroblasts and reticulocytes) in the $TER119^+$ $CD71^-$ population. Analysis of the BM of *shPhd2/rtTA* and control mice showed no difference in any of the stages of erythropoiesis. This, in addition to the RBC counts shown in **Figure 4-3C**, suggest that, despite the role of the hypoxia pathway in erythropoiesis, there is no effect of systemic knockdown of *Phd2* in the BM of adult mice **(Fig. 4-4F)**.

Notably, GFP expression in the B cell, monocyte and granulocyte compartments suggest there is a significant knockdown of *Phd2* in these differentiated haematopoietic cells **(Fig. 4-4C)**. In the Ter119/CD71 staining, however, there is disparate GFP expression between the most primitive erythroid compartments (with high GFP expression), and the more differentiated stages of erythropoiesis (with low GFP expression) **(Fig. 4-4E)**. Notably, low GFP expression may correlate with a less significant knockdown of *Phd2,* and may explain the lack of phenotype shown in these mature erythropoietic cells.

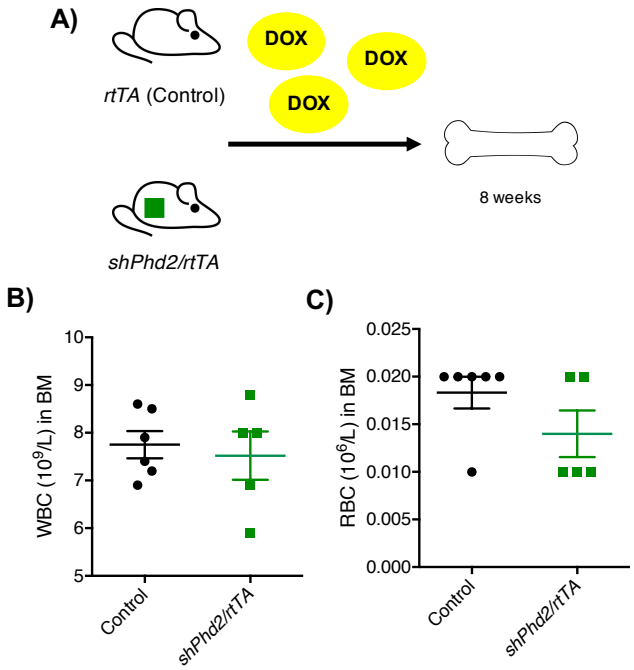

Figure 4-3 - Systemic ablation of *Phd2* has no effect on WBC and RBC numbers (A) Schematic representation of the *rtTA (*Control) and *shPhd2/rtTA* transgenic mice. Control and *shPhd2/rtTA* mice were treated with 2 mg/ml Dox in their drinking water for 8 weeks. **(B)** The number of White Blood Cells (WBC) and Red Blood Cells (RBC) **(C)** were measured using a HEMAVET® 950 analyser n=5-6 biological replicates per genotype. Data are mean ± SEM.

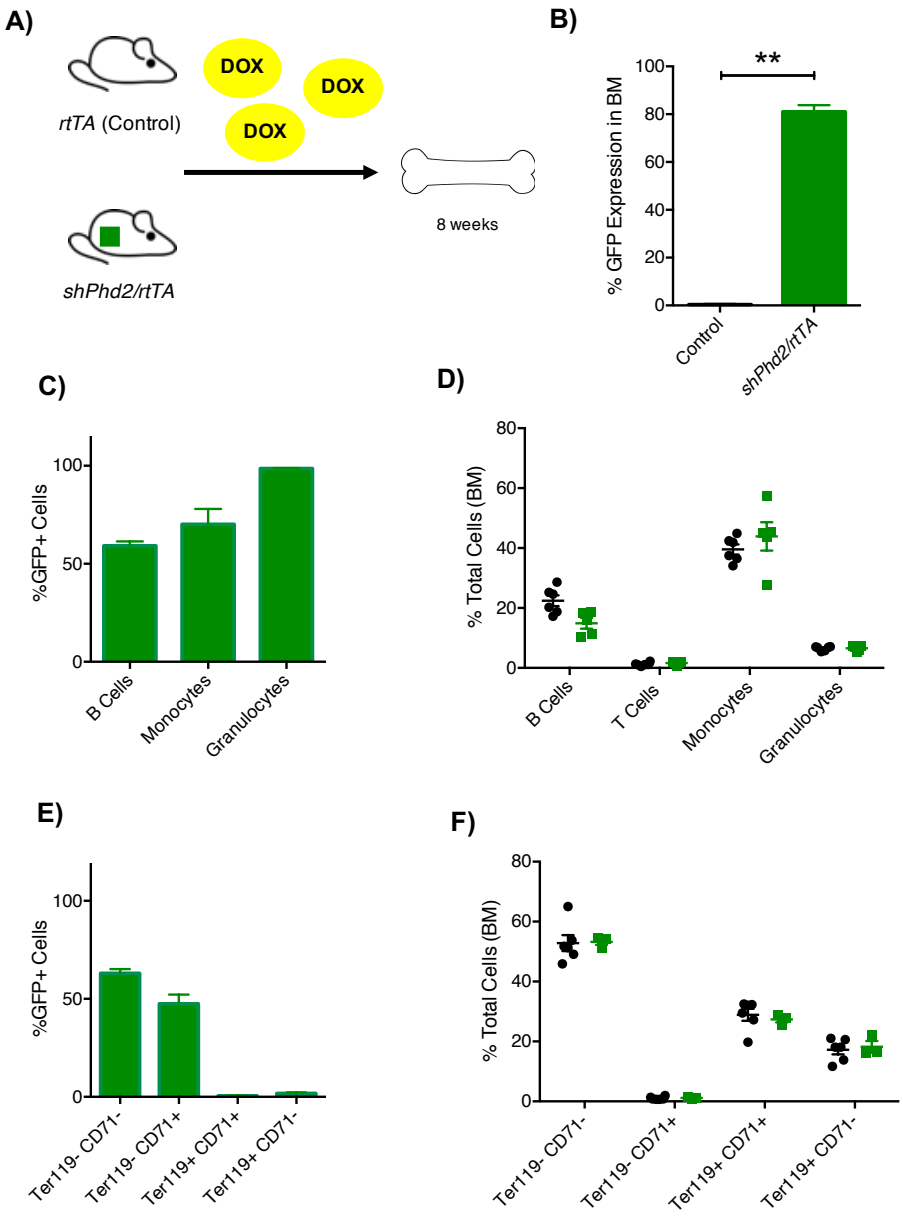

Figure 4-4 - *Phd2* has no role in the differentiated haematopoietic compartment of the BM
(A) Schematic representation of the *rtTA (*Control) and *shPhd2/rtTA* transgenic mice. Control and *shPhd2/rtTA* mice were treated with 2 mg/ml Dox in their drinking water for 8 weeks. **(B)** GFP expression in the total BM. GFP expression **(C),** and percentage of mature blood cells (B cells ($CD19^+B220^+$), monocytes ($Mac1^+$) and granulocytes ($Mac1^+Gr1^+$) **(D)** were analysed by flow cytometry. GFP expression **(E),** and percentage of $TER119^-$ $CD71^-$, $TER119^-$ $CD71^+$, $TER119^+$ $CD71^+$ and $TER119^-$ $CD71^-$ cells. n=5-6 biological replicates per genotype. Data are mean ± SEM. **, $P < 0.01$ (Mann-Whitney U test).

4.6 Systemic knockdown of *Phd2* alters the HSPC compartment

Given the contentious debate surrounding to role of *Phd2* in the HSPC compartment, I utilised the Dox-inducible *shPhd2* transgenic model to analyse the effect of systemic *Phd2* knockdown on the stem and progenitor compartments of the haematopoietic system within steady state conditions. Control and *shPhd2/rtTA* mice were treated with Dox for 8 weeks, and immunophenotypically analysed by flow cytometry.

In concordance with studies by Takeda et al in 2008, there is an increase in the frequency of the LSK compartment in the *shPhd2/rtTA* mice versus the control **(Figure 4-5C)**. Further analysis of the LSK compartment using CD48 and CD150 cell-surface markers, displayed an altered stem cell compartment, with a significant decrease in the most primitive compartments; HSC and MPP, and an increase in the least primitive compartment; HPC-2 cells. This result overall shows a global increase in CD48 expression within the LSK compartment, suggesting a trend towards the progenitor populations HPC-1 and HPC-2. Thus, a systemic decrease in *Phd2* levels decreases the HSC pool in the BM, and in turn, increases the frequency of haematopoietic progenitors further down the differentiation hierarchy **(Fig. 4-5D)**.

Notably, GFP expression is highest in the HSC compartment at the top of the haematopoietic hierarchy, and decreases in expression through the LK and Lin^- populations. This is very interesting, and confirms there is substantial knockdown of *Phd2* in the primitive compartments, which is especially important, given the compelling phenotype **(Fig. 4-5B)**.

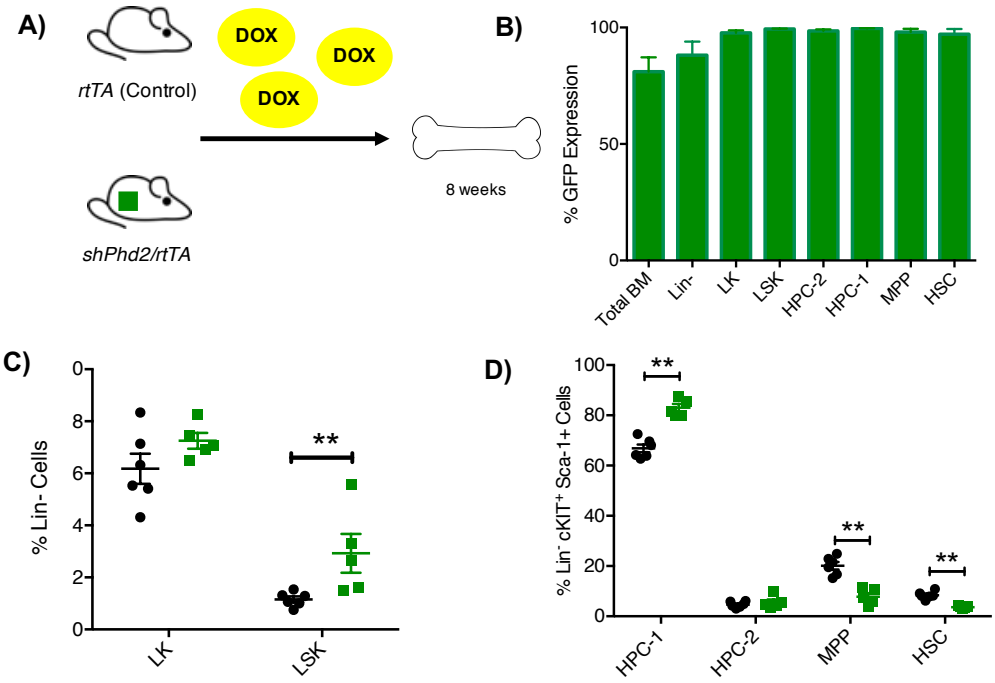

Figure 4-5 - Mice lacking *Phd2* show a decrease in the most primitive HSPC compartments (A) Schematic representation of the *rtTA (*Control) and *shPhd2/rtTA* transgenic mice. Control and *shPhd2/rtTA* mice were treated with 2 mg/ml Dox in their drinking water for 8 weeks. **(B)** GFP expression in total BM, Lin^-, LK (Lin^- $cKit^+$), LSK (Lin^- $cKit^+$ $Sca\text{-}1^+$), HSCs (LSK $CD48^-CD150^+$), MPPs (LSK $CD48^-$ $CD150^-$), HPC-1s (LSK $CD48^+CD150^-$) and HPC-2s (LSK $CD48^+CD150^+$). **(C)** LK and LSK cells as a frequency of the Lin^- compartment. **(D)** Percentage of haematopoietic stem and progenitor cells within the LSK compartment. n=5-6 biological replicates per genotype. Data are mean ± SEM. **, $P < 0.01$ (Mann-Whitney U test).

4.7 Reduction of *Phd2* levels results in an expansion of haematopoietic cells in the spleen

Previous published work has shown that, in addition to changes with the BM, knockdown of *Phd2* can have effects on sites of extramedullary haematopoiesis, including the spleen (Takeda et al., 2008). Notably, extramedullary haematopoiesis can often be a readout of the fitness of the BM or BM niche, with multiple factors including infection, bone marrow failure or malignancy increasing extramedullary haematopoiesis in peripheral organs such as the liver or spleen (Kim., 2010). As such, it may be possible that *Phd2* is essential to the BM microenvironment, and its loss results in an active extramedullary haematopoiesis response in the spleen. To investigate this hypothesis further, I treated control and *shPhd2/rtTA* mice with Dox for 8 weeks, and analysed the spleen for mature and primitive haematopoiesis.

Haematopoietic parameter analysis of the spleen using the HEMAVET® 950 analyser, revealed that the number of WBCs and RBCs in mice with reduced levels of *Phd2* was substantially higher than the control **(Fig. 4-6B, 4-6C)**. In accordance with this, there is a significant increase in spleen weight in *shPhd2/rtTA* mice when compared to the control, with mean spleen weights of 308.63 mg and 69.8 mg respectively **(Fig. 4-6D)**. This confirms a significant expansion of extramedullary haematopoiesis in the spleen following knockdown of *Phd2* levels.

Notably, one *shPhd2/rtTA* mouse recorded a significantly higher spleen weight of 759.8 mg versus others in the cohort, and is responsible for the outlining data point present in **Figures 4-6, 4-7, 4-8** and **4-9.**

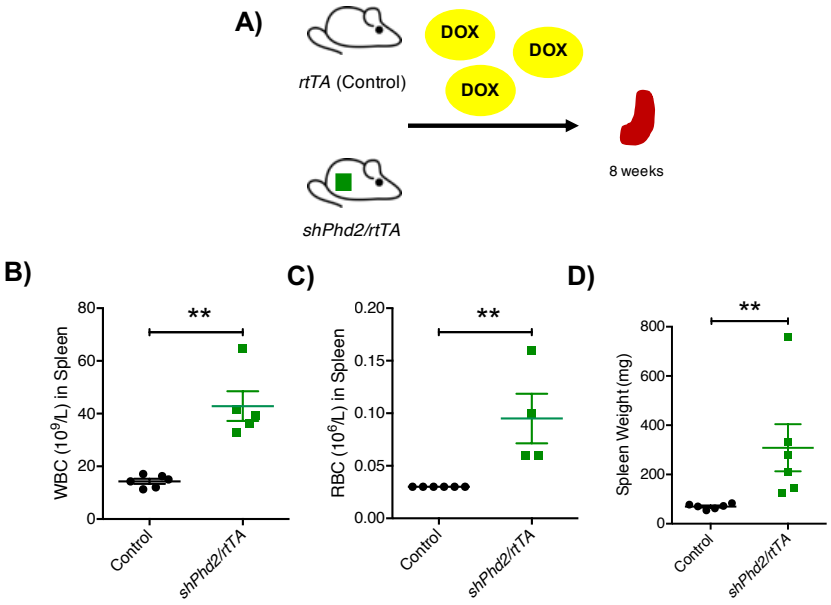

Figure 4-6 - Systemic ablation of *Phd2* increase WBC and RBC numbers in the spleen (A) Schematic representation of the *rtTA (*Control) and *shPhd2/rtTA* transgenic mice. Control and *shPhd2/rtTA* mice were treated with 2 mg/ml Dox in their drinking water for 8 weeks before analysis of the spleen. **(B)** The number of White Blood Cells (WBC) and Red Blood Cells (RBC) **(C)** were measured using a HEMAVET® 950 analyser. **(D)** Spleen weights of Dox-treated control and *shPhd2/rtTA* animals. n=5-6 biological replicates per genotype. Data are mean ± SEM. **, P < 0.01 (Mann-Whitney U test).

4.8 Systemic knockdown of *Phd2* does not affect the distribution of mature blood cell lineages

Given there was a significant increase in the WBC and RBC numbers in the spleen of *shPhd2/rtTA* mice when compared to the control, I sought to analyse the differentiated haematopoietic compartment to investigate if there was any difference of the lineage distribution in these mature blood cells.

Despite dramatic expansion of haematopoiesis in the spleen of mice with reduced *Phd2* expression, and therefore a global increase in the number of differentiated cells **(Fig. 4-8)**, there is no strong evidence of lineage bias in the differentiated compartment. There was no difference in the percentage of B cells, T cells, or granulocytes in the *shPhd2/rtTA* mice versus the control **(Fig. 4-7C)**. However, there was a significant increase in the percentage of the monocyte population, a trend also shown in the BM, although not significant **(Fig. 4-4D).** Notably, as shown in the BM in **Figure 4-4C**, there is evidence of GFP expression in the B cell, T cell, monocyte and granulocyte compartments. Additionally, as found in the BM experiments, there is an increased GFP expression in myeloid cells (monocytes and granulocytes), versus lymphoid cells (B cells and T cells). As such, it cannot be ruled out that *Phd2* may have a significant role in lymphopoieses, but the levels of *Phd2* are not as reduced as in the myeloid compartment, so the phenotype is concealed. qRT-PCR analysis of the separate differentiated haematopoietic compartments would verify this hypothesis.

Surprisingly, despite the strong link between hypoxia and increased ectopic erythropoiesis in the spleen, there were no evident differences in the Ter119/CD71 staining between the control mice, and mice with the knockdown of *Phd2* **(Fig. 4-7E)** (Adamson., 1988). Notably, as shown in the BM experiments in **Figure 4-4E**, there is increased GFP expression in the primitive erythroid cells ($Ter119^{-}CD71^{-}$, $Ter119^{-}CD71^{+}$) versus the more mature erythroid cells ($Ter119^{+}CD71^{+}$, $Ter119^{+}CD71^{-}$).

Overall, these results conclude that there is no lineage bias in the extramedullary haematopoiesis shown in the spleen, in reaction to reduction of *Phd2.*

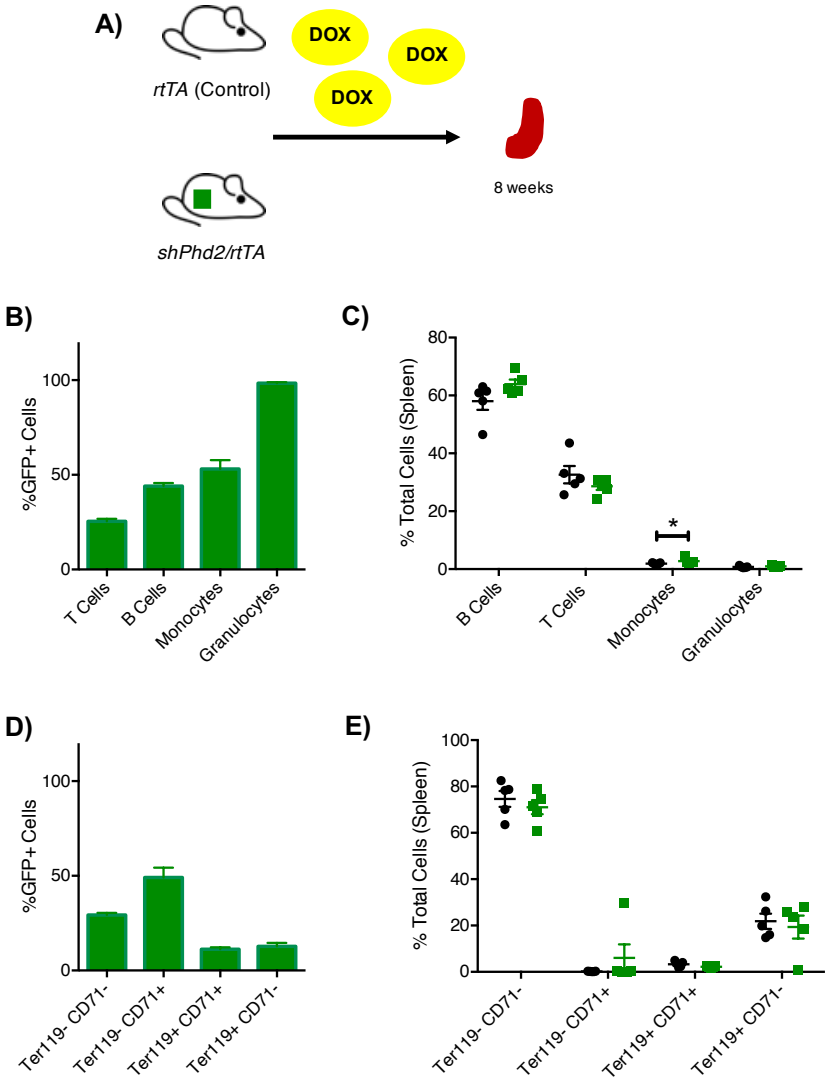

Figure 4-7 - Reduction of *Phd2* has no effect on the lineage bias of differentiated cells (A) Schematic representation of the *rtTA (*Control) and *shPhd2/rtTA* transgenic mice. Control and *shPhd2/rtTA* mice were treated with 2 mg/ml Dox in their drinking water for 8 weeks before analysis of the spleen. **(B)** GFP expression and the percentage of total cells **(C)** of B cells ($CD19^+B220^+$), T cells ($CD4^+CD8^+$), monocytes ($Mac1^+$) and granulocytes ($Mac1^+Gr1^+$). GFP expression **(D),** and percentage of $TER119^-$ $CD71^-$, $TER119^-$ $CD71^+$, $TER119^+$ $CD71^+$ and $TER119^-$ $CD71^-$ cells in the spleen **(E)**. n=5-6 biological replicates per genotype. Data are mean ± SEM. *, $P < 0.05$ (Mann-Whitney U test).

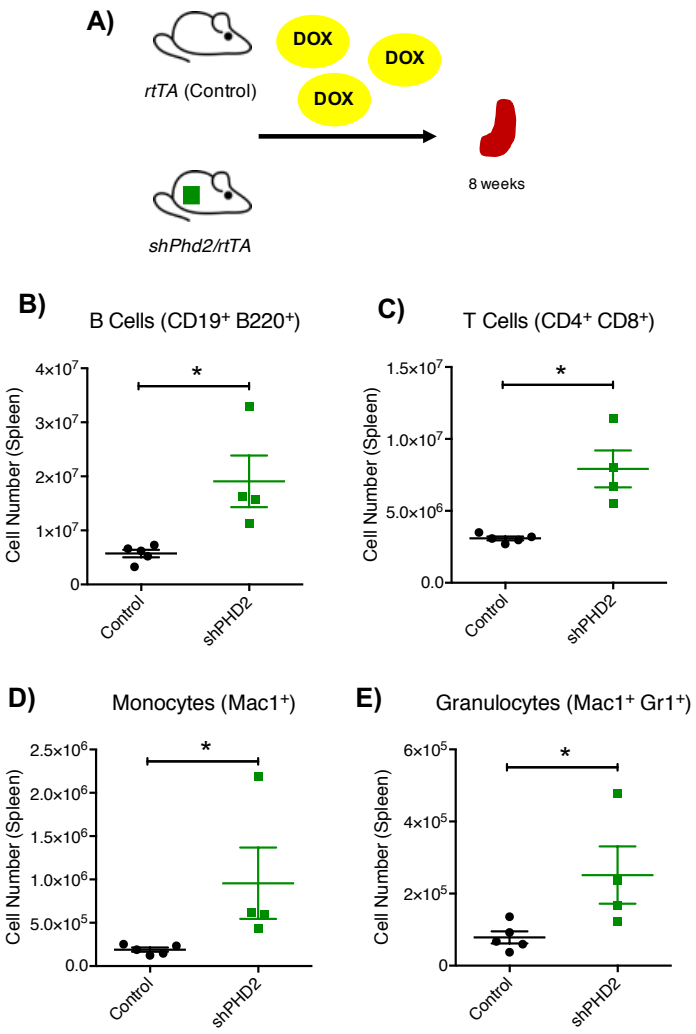

Figure 4-8 - Reduction of *Phd2* increases the number of mature blood cells in the spleen (A) Schematic representation of the *rtTA (*Control) and *shPhd2/rtTA* transgenic mice. Control and *shPhd2/rtTA* mice were treated with 2 mg/ml Dox in their drinking water for 8 weeks before analysis of the spleen. **(B)** Total numbers in the spleen of B cells ($CD19^+B220^+$) **(C)**, T cells ($CD4^+$ or $CD8^+$) **(D)**, monocytes ($Mac1^+$) and granulocytes ($Mac1^+Gr1^+$) **(E).** n=4-5 biological replicates per genotype. Data are mean ± SEM. *, $P < 0.05$ (Mann-Whitney U test.

4.9 Increased extramedullary haematopoiesis results in an increased cell numbers within the LK compartment in mice with *Phd2* depletion

In order to further investigate the effect of *Phd2* knockdown on the spleen, and the effect of the significant increase in extramedullary haematopoiesis observed in **Figure 4-6**, I analysed the LK progenitor cell compartment in *shPh2/rtTA* and control mice.

Initial analysis by flow cytometry showed, as expected, significant GFP expression in the mice expressing the knockdown of *Phd2*, versus the control **(Fig. 4-9B)**. *shPh2/rtTA* mice had a mean GFP expression of 41.2 %, with a range of 5.9 %, compared to a GFP expression of 0.14 % in the control. Notably, this is globally lower than the GFP expression values observed in the BM, suggesting there is smaller reduction in *Phd2* in the spleen **(Fig. 4-7E)**.

Overall, there was a trend of an increased LK population in the *shPh2/rtTA* mice versus the control. However, as shown in **Figure 4-9C**, the data, represented as a frequency of Lin^- cells, is spread, with two obvious outliers. Further analysis of this data revealed that an increase in spleen weight, which is an indicator of increased extramedullary haematopoiesis, results in a pronounced expansion of the LK progenitor compartment. This is best demonstrated when the flow cytometry analysis plots of a control mouse, with a spleen weight of 77 mg **(Fig. 4-9D),** is compared to a *shPh2/rtTA* mouse, with a spleen weight of 759.7 mg **(Fig. 4-9F)**. The LK population in the spleen is 1.18 % in the control mouse and 3.20 % in the mouse with reduced levels of *Phd2*. Notably, as represented in **Figure 4-9E**, there were multiple *shPhd2/rtTA* mice with an increased spleen weight (142.5 mg), but with equal or a decrease in the LK population when compared to the control mice. Thus, only under great extramedullary expansion is there a significant increase in the percentage of LK progenitor cells in the spleen. The disparity shown between *shPhd2/rtTA* mice, in both spleen weights and the frequency of LK cells, versus results from BM experiments in

Section 4-6, suggest that systemic ablation of *Phd2* levels results in a varied active extramedullary haematopoiesis response in the spleen.

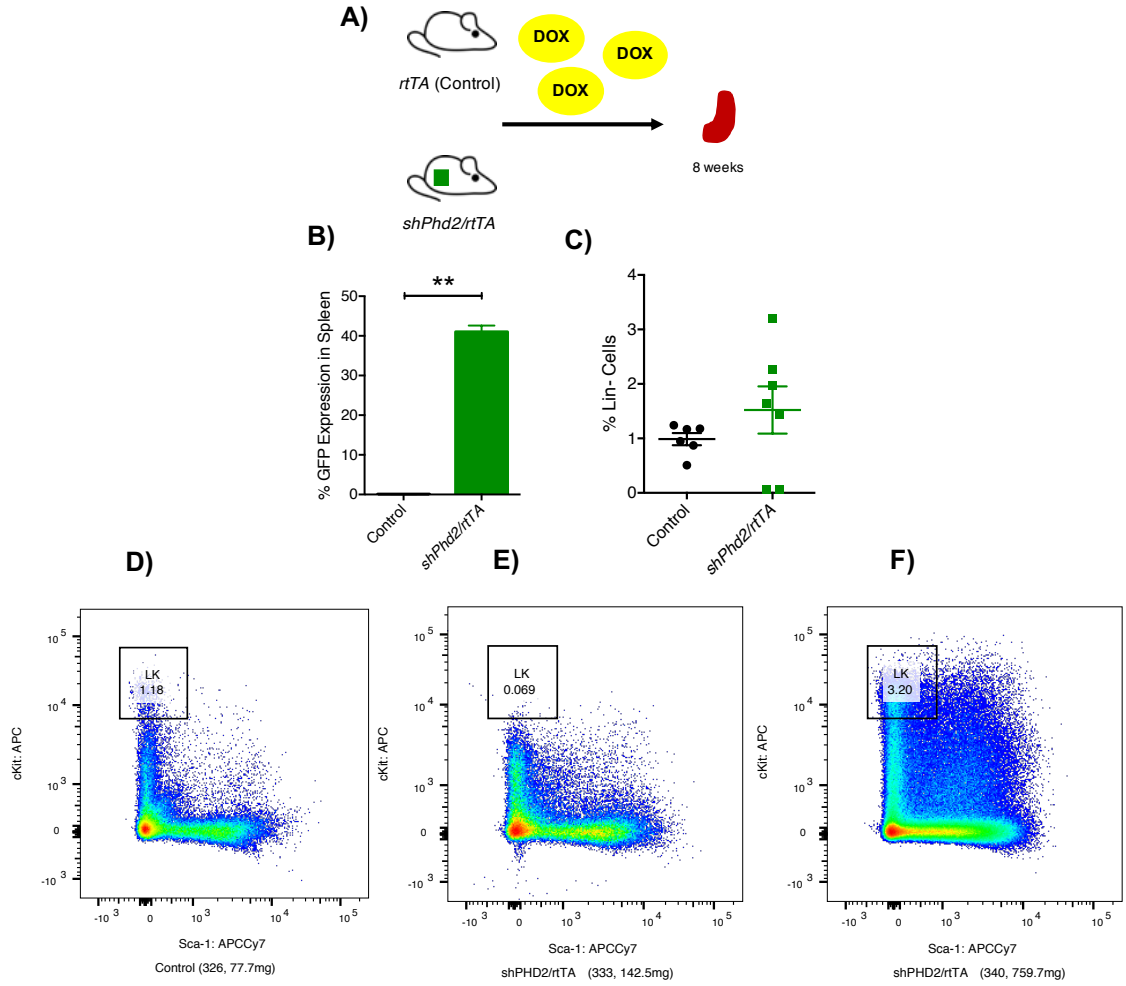

Figure 4-9 - Mice lacking *Phd2* show an increase in the LK progenitor compartment (A) Schematic representation of the *rtTA (*Control) and *shPhd2/rtTA* transgenic mice. Control and *shPhd2/rtTA* mice were treated with 2 mg/ml Dox in their drinking water for 8 weeks. **(B)** GFP expression in spleen. **(C)** Frequency of LK cells as a percentage of the Lin$^-$ compartment. **(D-F)** Representative flow cytometry plots of control and *shPhd2/rtTA* mice. Corresponding spleen are stated below each plot. n=6-7 biological replicates per genotype. Data are mean ± SEM. **, P < 0.01 (Mann-Whitney U test).

4.10 HSCs with *Phd2* knockdown are less fit than their control counterparts

After discovering that systemic reduction of *Phd2* levels under steady-state conditions results in contraction of the HSC compartment **(Fig 4-5D)**, I sought out to investigate the fitness of these *Phd2* deficient cells under extreme stress, using an HSC transplantation assay. Notably, HSC transplants are considered the "gold standard" to detect and characterise the functionality of HSCs as upon transplantation, quiescent HSCs are forced to exit dormancy to self-renew and differentiate into functional mature blood cells (Wilson et al., 2009).

In this experiment, 200 $CD45.2^+$ HSCs from *shPhd2/rtTA* and control mice were isolated by FACS and injected via the tail vein into sub-lethally irradiated (11Gy) $CD45.1^+/CD45.2^+$ syngeneic recipient mice. Notably, at this stage, neither the *shPhd2/rtTA* or control mice have been treated with Dox, so both have WT levels of *Phd2*. Importantly, transplantation of $CD45.2^+$ donor cells into $CD45.1^+/CD45.2^+$ recipient mice allows for the engraftment and differentiation potential of donor HSCs to be tracked by flow cytometry analysis of the CD45.2 cell-surface marker.

Multilineage reconstitution is considered to be stable approximately 3 - 6 weeks following transplantation, with WT HSCs able to sustain haematopoiesis in the recipient mouse for a minimum of 16 weeks (Ema et al., 2014; Morrison et al., 1997). To analyse the $CD45.2^+$ engraftment and multilineage repopulation potential of the transplanted HSCs, PB samples were collected from recipient mice at 4-, 6-, 8-, 10-, 14- and 18-weeks post-transplantation. At 6 weeks post-transplantation, the engraftment of $CD45.2^+$ cells had increased from analyses at week 4, and reached a mean value of 89.01 % in the control mice and 87.8 % in the *shPhd2/rtTA* **(Fig. 4-10B).** Given these significant levels of engraftment shown in the PB at week 6 post-transplantation, recipient mice transplanted with *shPhd2/rtTA* and control HSCs were given 2 mg/ml Dox in their drinking water to induce the transcription of a short-hairpin targeting *Phd2* and GFP. Thus, unlike previous experiments described in this chapter which induced systemic knockdown of *Phd2,* this experiment reduces *Phd2* levels specifically within

the transplanted HSCs and their progeny. These experiments, therefore, can investigate the effect of *Phd2* depletion on the biology of HSCs.

Following confirmation of stable $CD45.2^+$ engraftment at 6 weeks post-transplantation, mice were treated with 2 mg/ml Dox. PB samples were collected from recipient mice at 8-, 10-, 14- and 18- weeks post-transplantation, measuring GFP expression and $CD45.2^+$ engraftment by flow cytometry analysis. Prior to Dox induction, in PB samples taken at week 4 and week 6 post-transplantation, there was no expression of GFP in the PB of recipient mice transplanted with either *shPhd2/rtTA* or control HSCs. However, at week 8, following Dox treatment, there is significant GFP expression in the PB of mice transplanted with *shPhd2/rtTA* HSCs versus the control. This confirms successful transcription of the *GFP/shPhd2* cassette upon Dox induction. GFP expression remains in PB of mice transplanted with *shPhd2/rtTA* HSCs until the mice were sacrificed at 18 weeks post-transplantation. Notably, there is a slight but notable decrease in the percentage of GFP positive cells over time, suggesting a decrease in the number of HSCs lacking *Phd2*. **(Fig. 4-10C)**. Moreover, analysis of $CD45.2^+$ engraftment in the recipient mice, found that mice transplanted with HSCs with knockdown of *Phd2* had a decrease in engraftment versus control HSCs **(Fig. 4-10B)**.

Analysis of the WBC and RBC counts in the PB of recipient mice using the HEMAVET® 950 analyser found that there was no difference in the number of RBCs across all recipient mice **(Fig. 4-10E)**. Importantly, there were significant decreases in the WBC count at 8-, 10-, 14- and 18 weeks post-transplantation in the recipient mice transplanted with HSCs deficient in *Phd2* versus the control. There is, however, a global decrease in the number of WBC over time, across all recipient mice **(Fig. 4-10D)**. PB samples from all recipient mice were collected and analysed on the same day, so the general decrease in WBC count may be an artefact of measurement variations in the HEMAVET® 950 analyser. Conversely, global reductions in the WBC count may indicate that both the control and *shPhd2/rtTA* HSCs are exhausting over time under the transplantation stress. Thus, at all times, samples from recipient mice transplanted with *shPhd2/rtTA* or control HSCs are collected and analysed in parallel. This

ensures a direct comparison of the fitness and biology of the control and *Phd2* knockdown HSCs, eliminating other external factors where possible.

Overall, it is evident from the $CD45.2^+$ engraftment data and WBC counts from recipient mice, that reduction of *Phd2* levels impairs the fitness of HSCs under stress conditions.

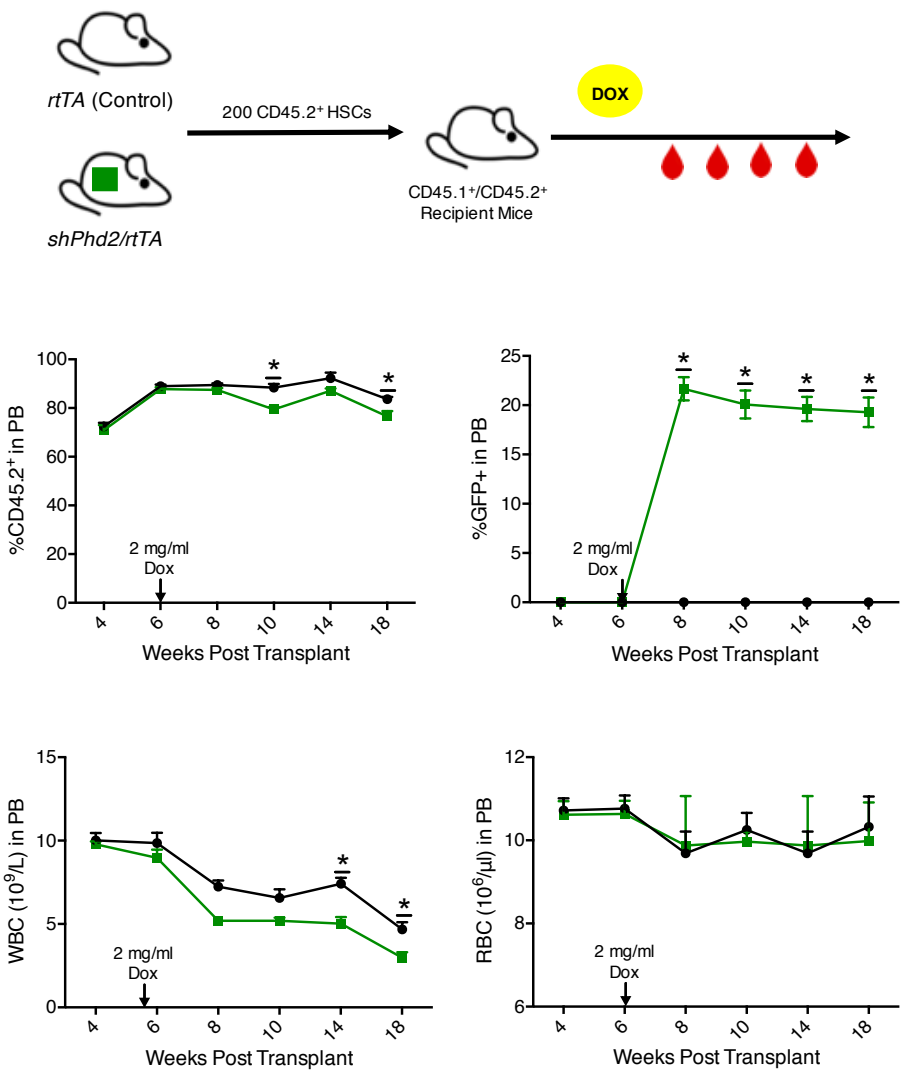

Figure 4-10 - HSCs deficient in *Phd2* have decreased engraftment and a decrease in WBC number in the PB (A) 200 CD45.2$^+$ LSK CD48$^-$CD150$^+$ HSCs from control *shPhd2/rtTA* mice were transplanted into lethally irradiated (11Gy) syngeneic CD45.1$^+$/CD45.2$^+$ recipient mice. Following stable CD45.2$^+$ engraftment at 6 weeks post-transplant, recipient mice were treated with 2 mg/ml Dox in their drinking water, driving production of a short-hairpin targeting *Phd2,* transcription of GFP. **(B)** Percentage of donor cells engraftment and GFP expression **(C)** measured by flow cytometry analysis at 4-, 6-, 8-, 10-, 14- and 18- weeks post-transplantation. **(D)** The number of White Blood Cells (WBC) and Red Blood Cells (RBC) **(E)** were measured using a HEMAVET® 950 analyser at 4-, 6-, 8-, 10-, 14- and 18- weeks post-transplantation. n=5 recipients per biological replicates (n=3-4). Data are mean ± SEM. *, P < 0.05 (Multiple t-test, statistical significance determined using the Holm-Sidak method).

4.11 HSCs with a knockdown of *Phd2* have an altered multilineage reconstitution potential

In order to address if HSCs lacking *Phd2* operate under a lineage bias upon transplantation, I analysed the percentage of B cells, T cells, monocytes and granulocytes in the PB of recipient mice by flow cytometry analysis.

As shown in **Figure 4-11**, the multilineage reconstitution was altered in HSCs with reduced levels of *Phd2*, resulting in an increase of T cells and granulocytes, and a decrease in the percentage of B cells in the PB. These results corroborate those found in the steady state analysis of the PB of non-transplanted *shPhd/rtTA* mice*,* which displayed an increase in the percentage of granulocytes, and a decrease in the B cell population following 8 weeks of Dox treatment **(Fig. 4-2F).**

Overall, these results suggest that *Phd2* does present a lineage bias, as reduction of *Phd2* levels consistently increases the granulocyte population, and decreases the B cell population, under both steady state and transplantation assay analysis.

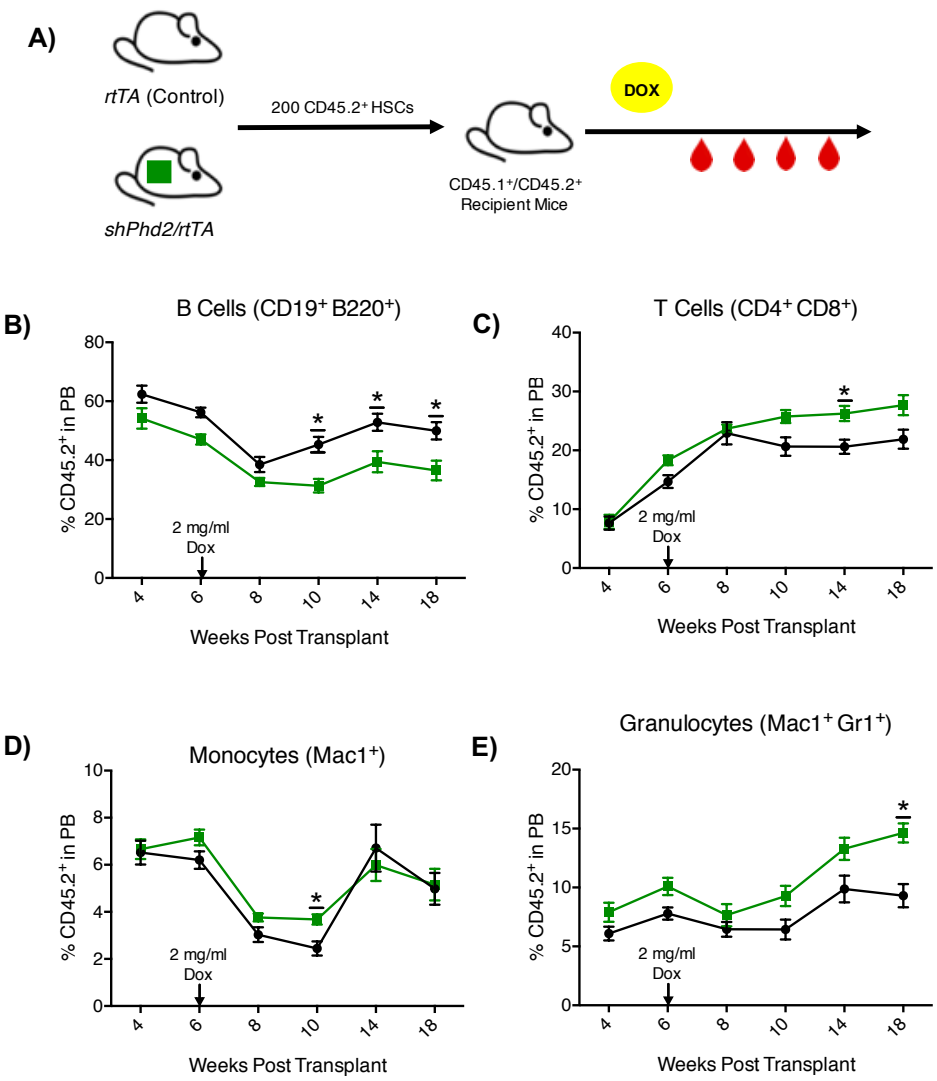

Figure 4-11 - Upon transplantation, HSCs with a knockdown of *Phd2* have altered multilineage haematopoietic differentiation (A) 200 CD45.2$^+$ LSK CD48$^-$CD150$^+$ HSCs from control *shPhd2/rtTA* mice were transplanted into lethally irradiated (11Gy) syngeneic CD45.1$^+$/CD45.2$^+$ recipient mice. Following stable CD45.2$^+$ engraftment at 6 weeks post-transplant, recipient mice were treated with 2 mg/ml Dox in their drinking water, driving production of a short-hairpin targeting *Phd2,* transcription of GFP. Mature blood cells (B cells (CD19$^+$B220$^+$) **(B)**, T cells (CD4$^+$CD8$^+$) **(C)**, monocytes (Mac1$^+$) **(D)** and granulocytes (Mac1$^+$Gr1$^+$)) **(E)** were analysed by flow cytometry at 4-, 6-, 8-, 10-, 14- and 18- weeks post-transplantation. n=5 recipients per biological replicates (n=3-4). Data are mean ± SEM. *, P < 0.05 (Multiple t-test, statistical significance determined using the Holm-Sidak method).

4.12 Reduction of *Phd2* in HSCs does not affect the repopulation of mature haematopoietic cells in the BM

In order to investigate the ability of HSCs deficient in *Phd2* to repopulate the differentiated haematopoietic cell compartment of the BM, I analysed the BM of recipient mice 18 weeks following the transplantation of 200 $CD45.2^+$ HSCs from control and *shPhd2/rtTA* mice.

I found that there was a significant GFP expression in the mice transplanted with *shPhd2/rtTA* HSCs when compared to recipient mice transplanted with control HSCs **(Fig. 4-12B).** In addition, despite significant decreases found in the PB samples **(Fig. 4-10B)**, there was no difference found in $CD45.2^+$ engraftment between recipient mice **(Fig. 4-12C).**

Flow cytometry analysis of the BM of recipient mice revealed that there was a decrease in the B cell population in mice transplanted with *Phd2* deficient HSCs versus those transplanted with control HSCs. Notably, this phenotype was also observed in the PB experiments. There were, however, no significant differences in either of the myeloid compartments **(Fig. 4-12D).**

As found in the steady state analysis experiments in the BM **(Fig. 4-4C)** and spleen **(Fig. 4-7B)** there is stable GFP expression in the B cell, T cell, monocyte and granulocyte compartments. There is an increased GFP expression in myeloid cells (monocytes and granulocytes), versus lymphoid cells (B cells and T cells), suggesting there is a reduced knockdown of *Phd2* in these cells **(Fig. 4-12E).** It is possible, that given a more significant knockdown, there would be an even greater decrease in the B cell compartment.

Overall, when transplanted into recipient mice, *shPhd2/rtTA* HSCs are able to successfully repopulate the BM of lethally irradiated recipient mice. In addition, *shPhd2/rtTA* HSCs present a lineage bias in both the PB and BM tissues, favouring granulocyte production over B cell differentiation.

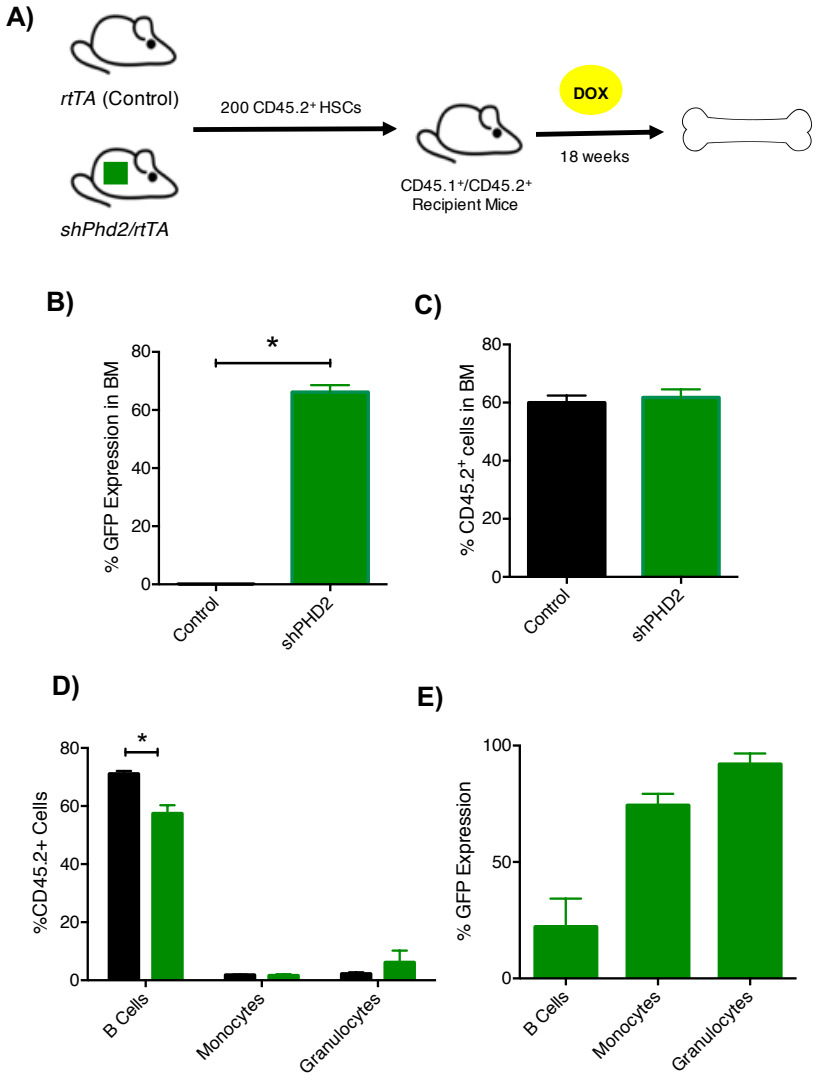

Figure 4-12 - HSCs lacking *Phd2* are able to repopulate the BM of recipient mice (A) 200 CD45.2$^+$ LSK CD48$^-$CD150$^+$ HSCs from control *shPhd2/rtTA* mice were transplanted into lethally irradiated (11Gy) syngeneic CD45.1$^+$/CD45.2$^+$ recipient mice. Following stable CD45.2$^+$ engraftment at 6 weeks post-transplant, recipient mice were treated with 2 mg/ml Dox in their drinking water, driving production of a short-hairpin targeting *Phd2,* transcription of GFP. **(B)** Percentage of GFP expression and CD45.2$^+$ engraftment **(C)** measured by flow cytometry analysis. **(D)** Mature blood cells (B cells (CD19$^+$B220$^+$), monocytes (Mac1$^+$) and granulocytes as a percentage of CD45.2$^+$ cells (Mac1$^+$Gr1$^+$)). **(E)** GFP expression in the B cell, monocyte and granulocyte compartments. n=5 recipients per biological replicates (n=3-4). Data are mean ± SEM. *, P < 0.05 (Mann-Whitney U test).

4.13 Upon transplantation, HSCs with reduced levels of *Phd2* generate an altered stem cell compartment

Previous experiments in this chapter provided evidence that systemic reduction of *Phd2* levels results in an altered stem cell compartment. These data show that under steady state haematopoietic conditions, a decrease in *Phd2* levels results in a decrease in the primitive HSC and MPP compartments, and a compensatory increase in less primitive HSPC cells; HPC-1 and HPC-2 **(Fig. 4-5)**. Given this interesting phenotype, I sought to investigate the effect of depletion specifically within transplanted HSCs and their progeny, and the influence this would have on the HSPC compartment of the recipient animals.

In concordance with the steady state BM analysis conducted in **Figure 4-5**, GFP expression is highest in the HSC compartment, and is significantly decreased in the LK and Lin^- populations. High expression of GFP in the primitive compartment, especially in the HSC, MPP, HPC-1 and HPC-2, proves that the HSCs lacking *Phd2* were indeed functional and able to self-renew and differentiate into primitive progenitor cells **(Fig. 4-13B)**.

In contrast with published results by Takeda et al in 2008, and experiments in this chapter **(Fig. 4-5C)**, there is no difference in the frequency of the LK or LSK compartments of mice transplanted with *shPhd2/rtTA* HSCs versus those transplanted with control HSCs. Flow cytometric analysis of the LSK compartment using CD48 and CD150 cell-surface markers, displayed an altered stem cell compartment, with a significant decrease in the HSC and MPP compartments (not significant). As before **(Fig. 4-5D)**, the reduction in the most primitive cells of the haematopoietic hierarchy is compensated by an increase in the progenitor population of HPC-1 **(Fig. 4-13D)**.

Thus, both a systemic decrease of *Phd2,* and a decrease of *Phd2* levels specifically within transplanted HSCs, both result in an altered HSPC compartment, with a significant decrease the HSC pool.

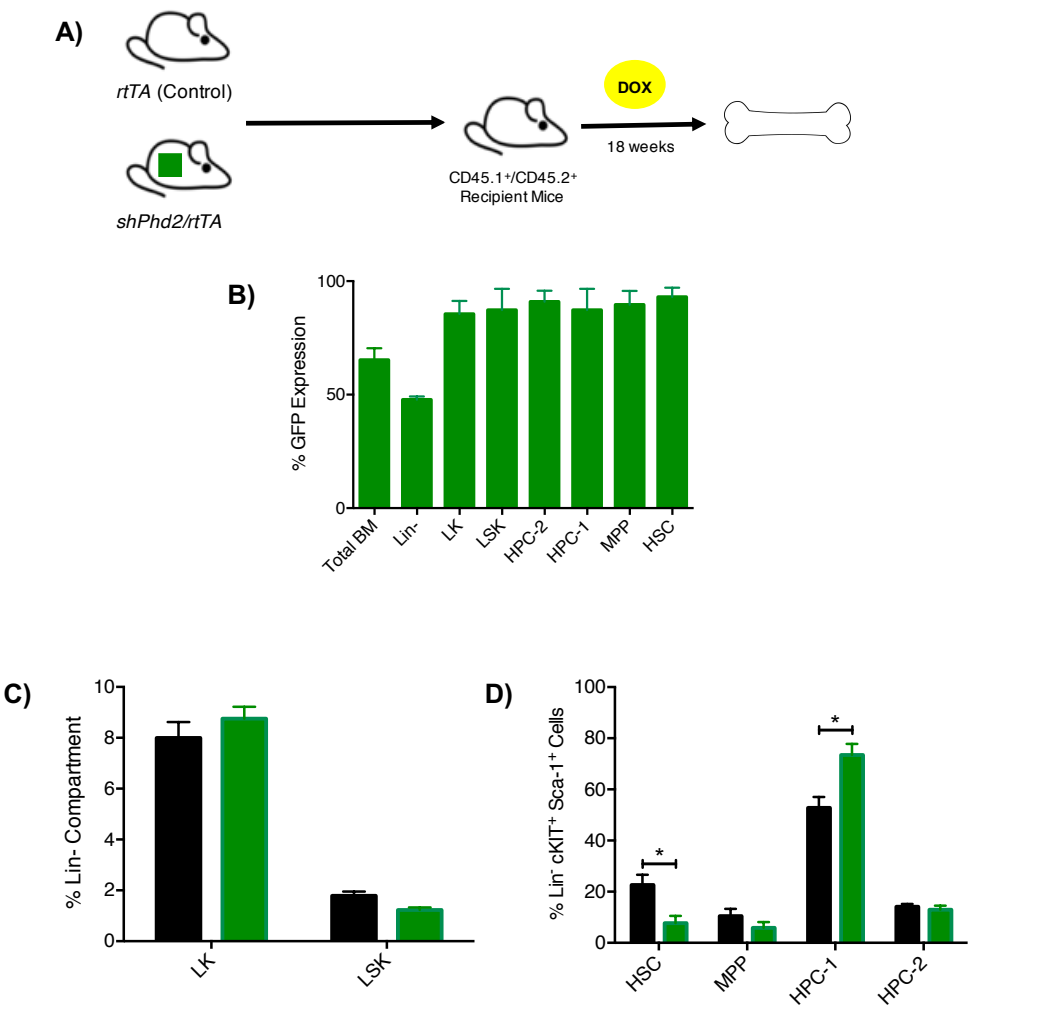

Figure 4-13 - HSCs with reduced levels of *Phd2* repopulate adult BM with an altered HSPC compartment (A) 200 CD45.2$^+$ LSK CD48$^-$CD150$^+$ HSCs from control *shPhd2/rtTA* mice were transplanted into lethally irradiated (11Gy) syngeneic CD45.1$^+$/CD45.2$^+$ recipient mice. Following stable CD45.2$^+$ engraftment at 6 weeks post-transplant, recipient mice were treated with 2 mg/ml Dox in their drinking water, driving production of a short-hairpin targeting *Phd2,* transcription of GFP. **(B)** GFP expression in total BM, Lin$^-$, LK (Lin$^-$ cKit$^+$), LSK (Lin$^-$ cKit$^+$ Sca-1$^+$), HSCs (LSK CD48$^-$CD150$^+$), MPPs (LSK CD48$^-$CD150$^-$), HPC-1s (LSK CD48$^+$CD150$^-$) and HPC-2s (LSK CD48$^+$CD150$^+$). **(C)** LK and LSK cells as a frequency of the Lin$^-$ compartment. **(D)** Percentage of haematopoietic stem and progenitor cells within the LSK compartment. n=5 recipients per biological replicates (n=3-4). Data are mean ± SEM. *, P < 0.05 (Mann-Whitney U test).

4.14 Discussion

Work in this chapter provides further insight into the role of *Phd2* in haematopoiesis. In particular, the *shPhd2/rtTA* transgenic mouse model used here allowed for timed and systemic depletion of *Phd2* when investigating steady state haematopoiesis, as well as reduction of *Phd2* levels within HSCs transplanted into recipient mice. Thus, the role of *Phd2* could be accurately investigated in non-cell-autonomous haematopoiesis, as paralleled in experiments conducted by Takeda and colleagues in 2008, and in addition, could also be used to dissect the role of *Phd2* in the biology of HSCs.

The *shPhd2/rtTA* transgenic mouse line used in this chapter is comparable to the *R26-rtTA* promoter driven tamoxifen-inducible $Phd2^{CKO}$ model used by Takeda et al in 2008. However, results shown in this chapter differ between the models. Notably, in the *shPhd2/rtTA* model, the reverse tetracycline trans-activator (*rtTA)* is placed under control of the *CAG* promoter, which is known to give stronger and increased ubiquitous expression than the *R26-rtTA* promoter (Dow et al., 2012). Importantly, the Dox-inducible model generates a short-hairpin targeting *Phd2,* thus, unlike the $Phd2^{CKO}$ mouse model, it does not eliminate the protein, but reduces *Phd2* expression. This model, however, is somewhat beneficial, as opposed to a knockout model, reduction of *Phd2* levels is considered to be more faithful to physiological levels, pathological levels and pharmaceutical intervention.

Experiments designed to validate the *shPhd2/rtTA* model found that, following Dox treatment for 5 weeks, *shPhd2/rtTA* mice had reduced levels of *Phd2* mRNA when compared to the Dox-treated control mice. In concordance with these findings, upon validating this novel mouse model, our collaborators at the University of Oxford found that the shRNA sequence used was effective at knocking down *Phd2* mRNA levels in all tissues. In addition, it was discovered that knockdown of *Phd2* was sufficient to upregulate *Phd3* and *Bnip3*, two HIF target genes. At a protein level, western blot analysis of Dox-treated liver tissue found that PHD2 levels were decreased and HIF-1α and HIF-2α were stabilised. This suggests that phenotypes observed are, at least in part, a result of HIF-α stabilisation. Notably, *in vivo* validation experiments at

the University of Oxford were also conducted with a second *shPhd2* construct, and agreed with those described (Yamamoto et al, in submission).

Investigations into the effect of the systemic depletion of *Phd2* on steady state haematopoiesis found a skewed lineage bias in the differentiation compartment in the PB, with a significant decrease in the B cell population, and an increase in the granulocyte population. Notably, this result was also shown in the HSC transplantation assay, with HSCs deficient in *Phd2* giving rise to an increased frequency of B cells, and a decreased frequency of granulocytes **(Fig. 4-11)**.

Moreover, in the PB samples analysed during the steady state experiments, there were significant decreases found in various haematological parameters including WBC count, RBC count, haemoglobin and haematocrit values in the mice with knockdown of *Phd2* versus the control **(Fig. 4-2)**. Previous published research using a systemic knockdown of *Phd2*, however, found a significant increase in WBC, RBC, haemoglobin and haematocrit values using the *Rosa-CreER Phd2*^{CKO} mouse model (Takeda et al., 2008). These stark differences in phenotype may be accounted for by the aforementioned differences in the *Rosa-CreER Phd2*^{CKO} versus *shPhd2/rtTA* transgenic models. Additionally, mice in the *in vivo* studies presented in **Figure 4-2** had reduced levels of *Phd2* for 8 weeks, versus 6 weeks in the Takeda 2008 paper. Thus, it is possible that between 6 and 8 weeks, prolonged deficiency of *Phd2* has a detrimental effect on the PB compartment.

In agreement with results published utilising the *Rosa-CreER Phd2*^{CKO} mice (Takeda et al., 2008), results presented in this chapter found that reduction of *Phd2* levels results in an increase in the LSK compartment **(Fig. 4-5C)**. Experiments in this chapter elaborated on this phenotype, analysing the LSK compartment using CD48 and CD150 cell-surface markers, and unveiled a reduction in the frequency of the HSC and MPP populations, accompanied by an increase in the frequency of HPC-1 progenitors **(Fig. 4-5D)**. Importantly, analyses of the BM of recipient mice transplanted with HSCs isolated from *shPhd2/rtTA* mice also found a decrease in the most primitive cells of the LSK compartment (HSC and MPP), and an increase

in the HPC-1 population **(Fig. 4-13D)**. This suggests that both systemic and HSC cell-autonomous levels of *Phd2* are essential for the maintenance of HSCs.

To investigate the role of *Phd2* in the fitness of HSCs*,* a transplantation experiment was performed with FACS isolated HSCs from *shPhd2/rtTA* and control mice. Once CD45.2^{+} engraftment was established in recipient mice, Dox treatment began, reducing *Phd2* levels specifically within the transplanted HSCs and their progeny. Under the stress of a transplantation assay, it was clear that the HSCs with a knockdown of *Phd2*, were significantly less fit than their control counterparts, exhibiting a reduction in CD45.2^{+} engraftment and WBC numbers **(Fig. 4-10)**. Notably, unpublished experiments conducted by Dr Guitart in the Kranc laboratory, found that HSCs isolated from *Phd2$^{fl/fl}$;Vav-iCre^{+}* (*Phd2^{CKO})* mice, also presented with a reduced CD45.2^{+} engraftment when transplanted into lethally irradiated mice. Moreover, in further agreement with results presented in this chapter, transplantation experiments published by Singh and colleagues in 2013 found that recipient mice injected with *Phd2$^{fl/fl}$;CD68-Cre^{+}* (*Phd2^{CKO})* LSK cells, had a significant reduction in CD45.2^{+} chimerism. Together, these results suggest that cell-autonomous depletion of *Phd2* fundamentally reduces the fitness of HSCs.

Interestingly, systemic depletion of *Phd2* has a substantial effect on extramedullary haematopoiesis, with significant increases in the spleen weight, WBC count and RBC count in Dox-treated *shPhd2/rtTA* mice versus the control **(Fig. 4-6).** Additionally, analysis of the HSPC compartment by flow cytometry found that, overall, splenic tissue isolated from *shPhd2/rtTA* mice exhibited significant increases in the LK compartment versus the control mice **(Fig. 4-9)**. This increase, however, was strongly related to an increase in spleen weight, suggesting that an increase in *Phd2* deficient extramedullary haematopoiesis directly results in expansion of haematopoietic progenitor cells in the spleen. Notably, experiments by Takeda et al in 2008 found that there was an increase colony formation in splenic tissue derived from *Phd2^{CKO}* mice versus the control. Importantly, this result suggests that these expanded HSPC cells are also functional as they are able to form colonies in CFC assay. Notably, these results somewhat

parallel the haematological disorder polycythaemia vera, a condition which is also evident in patients with a somatic point mutation in the *PHD2* gene (Barradas et al., 2018; Percy et al., 2006; Spivak et al.). As a result, this phenotype merits further investigation such as more detailed analysis of this tissues and transplantation of these splenic cells. Overall, these data confirm that systemic depletion of *Phd2* results in extramedullary haematopoiesis in the spleen, leading to an increase in the HSPC compartment.

In addition, qPCR analysis of *Phd2,* as well HIF-target genes such as *Aldoa*, *Pdk1*, *Bnip3*, and *Egln3* in spleen, BM and blood tissues would demonstrate if the phenotypes observed were related to the level of *Phd2* knockdown, and its relation to HIF activity. Further molecular analysis of FACS isolated haematopoietic compartments such as LK, LSK and HSCs could indicate the mechanism through which HSCs lacking *Phd2* have a reduction in fitness, as well as the expansion of extramedullary haematopoiesis in the spleen.

In conclusion, this chapter has successfully dissected the role of *Phd2* in haematopoiesis utilising a novel CAG-promoter driven *shPhd/rtTA* mouse model. Importantly, given that systemic depletion of *Phd2,* and transplantation-induced stress in HSCs lacking *Phd2,* both lead to decrease in the frequency and functionality of the HSC compartment, further investigations into the role of *Phd2* in the biology HSCs is merited. Such research is of therapeutic and clinical importance, especially in regards to the production and utilisation of *Phd2* inhibitors for multiple pathological conditions.

CHAPTER 5

The role of Prolyl Hydroxylase Domain enzymes in AML

Chapter 5 The role of Prolyl Hydroxylase Domain enzymes in Acute Myeloid Leukaemia

5.1 Introduction

Acute Myeloid Leukaemia (AML) is a complex, heterogeneous disease characterised by uncontrolled overproduction of immature leukocytes (Papaemmanuil et al., 2016). In the UK, AML is the second most common form of leukaemia in adults and children, with an increase in disease incidence of 30 % since the 1990s, versus an increase in incidence of just 15 % in all other leukaemias (CRUK; www.cancerresearchuk.org). Long-term outcomes have not improved significantly for over 3 decades, with a median survival rate of 1 year (Döhner et al., 2015). Current conventional chemotherapy achieves disease remission in > 70 % of patients, but the majority will relapse within 5 years (Appelbaum et al., 2006). This clinical challenge derives from the stem-cell source of AML, first identified by John Dick et al in 1994. Studies into the biology of LSCs have unveiled their stem cell characteristics such as self-renewal, quiescence and low rate of apoptosis. In addition, these cells have an increased drug efflux, which gives them strong resistance to chemotherapies aimed at eradicating bulk AML disease (Wulf et al., 2001). As such, there is a significant research effort to further dissect the biology of LSCs, aiming to expose vulnerabilities, with the ultimate aim of targeting LSCs in conjunction with current chemotherapies to eradicate AML.

5.1.1 Hypoxia pathway in AML

Multiple studies, including that of Spencer et al in 2014 and Passaro et al in 2017, have shown that normal and malignant haematopoiesis occurs under hypoxic conditions within the bone marrow niche. Moreover, this hypoxic niche is thought to promote LSC self-renewal, as well as quiescence, which is believed to be one mechanism through which LSCs evade chemotherapy (Ishikawa et al., 2007). Given these findings, the Kranc laboratory focused on the role of oxygen sensing pathways in leukaemic transformation and development.

Cellular responses to hypoxia are predominantly orchestrated by the hypoxia-inducible factors Hif-1 and Hif-2, which regulate gene expression, facilitating the hypoxia response. Several studies have investigated the roles of Hif-1*α* and Hif-2*α* in human and murine models of AML, unveiling both oncogenic and tumour-suppressor roles. *HIF-2α* knockdown in AML patient samples led to a reduction in $CD34^{+}$ engraftment, and a reduction of AML disease upon transplantation into recipient mice (Rouault-Pierre et al., 2013). Additionally, Wang et al in 2011 found that reduction of HIF levels, through the inhibitor echinomycin, reduced the self-renewal capacity of AML cells. However, a recent study using a *Mx1-Cre* driven *Hif-1α* conditional knockout mouse model showed that there was no effect on the development or maintenance of AML in the absence of *Hif-1α* (Velasco-Hernandez et al., 2014). Moreover, new research in the field has demonstrated that MLL-AF9 driven AML with deletion of *Hif-1α* accelerates the progression of chemotherapy treated disease *in vivo* (in press; personal communications with Profs K. Kranc and J. Cammenga). These findings corroborate experiments published by the Kranc laboratory, which found that while deletion of *Hif-1α* and *Hif-2α* had no impact on normal stem cell self-renewal (Guitart et al., 2013; Vukovic et al., 2016), it dramatically enhanced LSC formation and AML leukaemogenesis in a *Meis1/Hoxa9* model of murine AML (Vukovic et al., 2015).

5.1.2 The role of PHDs in AML

Given the evidence of the tumour suppressor function of *Hif-1α* and *Hif-2α* in AML, it can be hypothesised that stabilisation of *Hif-1α* and *Hif-2α,* through the inhibition of *Phds* may hold therapeutic potential in the targeting of LSCs. Notably, when compared to research focusing on *Hif-1α* and *Hif-2α,* there is little published on the role of *Phds* in AML.

Micro-array gene expression profiling used in the MILE (Microarray Innovations in Leukaemia) study of AML patient samples show both up-regulation and down-regulation of Phd1 (ELGN2) when compared to control BM (Labaj et al., 2017). Interestingly, the same dataset shows a significant fold-change increase in Phd2 (ELGN1) expression in AML, and multiple forms of ALL (Haferlach et al., 2010). Conversely, a recent paper published in Molecular Cell found that PHD3 expression is significantly decreased in some cancers, including AML. Mechanistic studies discovered that over-expression of PHD3 in AML limits leukaemia cell proliferation through a reliance on fat catabolism (German et al., 2016).

Notably, murine *in vivo* work by Leite et al in 2012 demonstrated that systemic inhibition of *Phd2* during chemotherapy-based AML treatment has a therapeutic benefit *in vivo*, increasing survival and reducing drug toxicity. Thus, dissection of the roles of *Phd1* and *Phd2* in AML is essential and will reveal if PHDs are in fact tumour suppressors or oncogenes, and therefore, most importantly, if they can function as therapeutic targets in AML.

5.1.3 Meis1/Hoxa9 retroviral model

The *Meis1/Hoxa9* retroviral AML mouse model is well characterised and widely used in *in vivo* AML studies, with both genes being implicated in leukaemic transformation in murine and human AML. Early studies by Kroon et al in 1998 showed that retroviral infection of over-expression vectors for *Meis1 and Hoxa9* gave rise to AML < 3 months after transplantation, whereas overexpression of either *Meis1* or *Hoxa9* alone failed to give AML even 6 months post-transplantation. Notably, in murine AML, it was shown that *Hoxa9* promotes immortal self-renewal of haematopoietic progenitors, whereas *Meis1* activates leukaemogenicity and transcription of multiple stem-cell genes including *Flt3* (Morgado et al., 2007). Further studies confirmed this, and showed that only when there is co-expression of both *Meis1* and *Hoxa9* specifically within the primitive or progenitor haematopoietic compartment will mice develop blood cancer with the characteristics of AML (Krivtsov et al., 2006; Lessard and Sauvageau, 2003; Wong et al., 2007).

5.2 Aims and objectives of Chapter 5

Evidence from previous work in the Kranc laboratory demonstrated that deletion of *Hif-1α* and *Hif-2α* increased LSC formation and AML leukaemogenesis, thus reducing disease latency and survival *in vivo* (Vukovic et al., 2015). This led to the hypothesis that constitutive activation of the HIF system, through inhibition of *Phd1, Phd2,* or both *Phd1* and *Phd2* will reduce leukaemogenesis *in vitro* and inhibit leukaemia development and maintenance *in vivo.* The role of PHDs in leukaemogenesis was investigated using a *Vav-iCre* conditional knock-out model (as explored in **Chapter 3**), as well as a *shPhd2* doxycycline inducible model (as explored in **Chapter 4**). This allowed the study both the impact of *Phd* gene deletion on the development and maintenance of AML, as well as the effect of the reduction of *Phd2* levels on established AML disease.

5.3 Experimental design

A *Meis1/Hoxa9* retroviral model was used to investigate the role of the PHD enzymes in the development and maintenance of AML. In this model, primitive, or haematopoietic stem and progenitor cells (HSPCs) were isolated from $CD45.2^+$ 14.5 dpc embryo FL cells, enriched for the $cKit^+$ cell population, and infected with retroviruses overexpressing *Meis1* and *Hoxa9.* The cells over-expressing *Meis1* and *Hoxa9* were then positively selected based on their antibiotic resistance to puromycin and neomycin, respectively. These cells then underwent serial re-plating in semi-solid methylcellulose media, and after 3 re-plating assays, only the most primitive and oncogenic cells survived, generating pre-leukaemic stem cells (pre-LSCs). Following this, a primary transplant was performed, with 100 000 pre-LSCs mixed with 200 000 WT $CD45.1^+$ unfractionated BM cells, and injected into sub-lethally irradiated (11Gy) $CD45.1^+/CD45.2^+$ syngeneic recipient mice in order to follow leukaemic disease development *in vivo*. Once mice developed AML, they were sacrificed and secondary transplants were performed with 50 000 bone marrow (BM) cells (containing LSCs).

5.3.1 *Vav-iCre*-mediated conditional knockout model

In order to address the role of PHDs in the development of murine AML, the *Meis1/Hoxa9* model described above was used with FLs of control embryos (*Vav-iCre^{-})*, and embryos with *Vav-iCre* conditional deletions of *Phd1* (*Phd1$^{fl/fl}$;Vav-iCre^{+}*), *Phd2* (*Phd2$^{fl/fl}$;Vav-iCre^{+}*), or both (*Phd1$^{fl/fl}$; Phd2$^{fl/fl}$;Vav-iCre^{+}*) **(Fig. 5-1)**. Notably, each experiment using conditional knockout embryos with deletion of *Phd1, Phd2*, or both *Phd1* or *Phd2* was conducted in parallel with their appropriate *Vav-iCre^{-}* littermate controls, e.g. Control (*Phd1$^{fl/fl}$;Vav-iCre^{-})* and *Phd1*^{CKO} (*Phd1$^{fl/fl}$;Vav-iCre^{+}*); Control (*Phd2$^{fl/fl}$;Vav-iCre^{-})* and *Phd2*^{CKO} (*Phd2$^{fl/fl}$;Vav-iCre^{+}*); Control (*Phd1$^{fl/fl}$; Phd2$^{fl/fl}$;Vav-iCre^{-}*) and *Phd1/2*^{CKO} (*Phd1$^{fl/fl}$; Phd2$^{fl/fl}$;Vav-iCre^{+}*). This ensured tight control of the *Vav-iCre* conditional knock-out system, with all embryos containing a floxed *Phd* allele. Importantly, control and conditional knock out cells were all genotyped at various stages to ensure correct results were recorded. Cells were genotyped; after CFC1, after CFC3 prior to primary transplantation, and BM samples from sacrificed primary recipient mice.

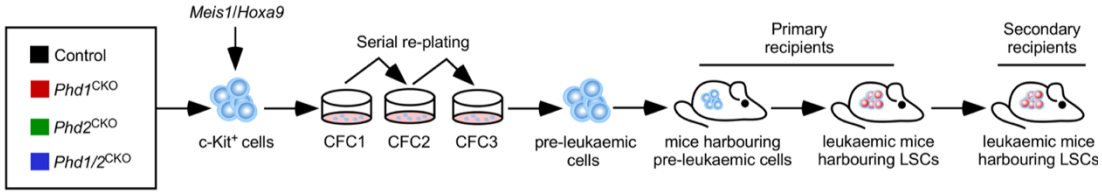

Figure 5-1 - *Meis1/Hoxa9* retroviral model using *Vav-iCre* conditional knock out mice. Schematic representation of the *Meis1/Hoxa9* retroviral model. Foetal liver (FL) cells from Control (*Vav-iCre^{-})*, *Phd1*^{CKO} (*Phd1$^{fl/fl}$;Vav-iCre^{+}*); *Phd2*^{CKO} (*Phd2$^{fl/fl}$;Vav-iCre^{+}*); or both *Phd1/2*^{CKO} (*Phd1$^{fl/fl}$; Phd2$^{fl/fl}$;Vav-iCre^{+}*) embryos were enriched for cKit^{+} and infected with *Meis1* and *Hoxa9* over-expressing retroviruses and serially re-plated, generating pre-leukaemic stem cells (pre-LSCS). pre-LSC cells were then transplanted into primary recipient mice, which developed murine AML. Once mice showed signs of leukaemic disease, they were sacrificed, and secondary transplants were performed.

5.3.2 Inducible *shPhd2*-mediated knockdown model

To further dissect the role of PHD2 in leukaemia, the *Meis1/Hoxa9* retroviral model was followed, using FL tissue taken from *rtTA* (Control) and *shPhd2/rtTA* embryos. As previously described in Chapter 4, upon Dox treatment, *shPhd2/rtTA* mice transcribe a short-hairpin targeting *Phd2,* as well as *GFP*. This model allows the further investigation the role of *Phd2* on AML development, but also, more importantly, the inducible nature of the system allows the study of *Phd2* on established leukaemic disease, reducing *Phd2* levels at multiple stages of leukaemia development. GFP expression was measured via flow cytometry at all stages as a read-out of *shPhd2* expression, and to ensure correct identification of samples. As shown below in **Figure 5-2A**, this model was initially tested *in vitro* to investigate the effect of acute reduction of *Phd2* levels in pre-LSCs. Following this, the *shPhd2* doxycycline-inducible model was used *in vivo* to address the role of *Phd2* in AML disease progression (**Figure 5-2B)**.

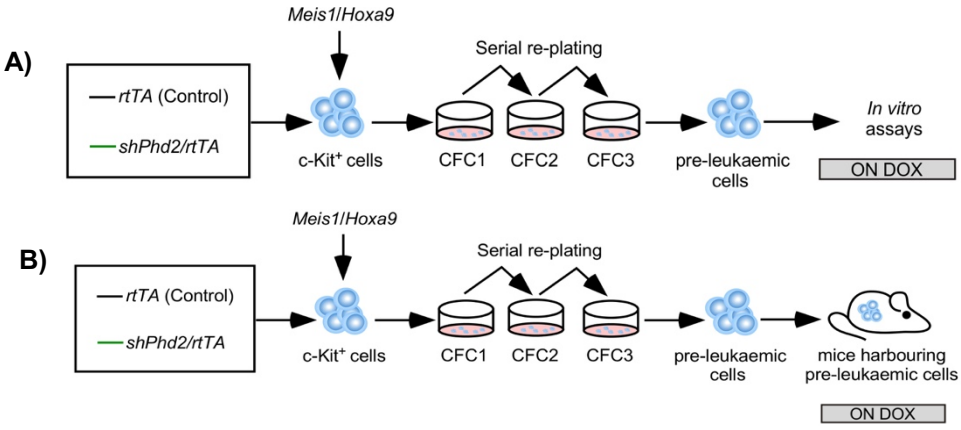

Figure 5-2 - *Meis1/Hoxa9* retroviral model using inducible *shPhd2* mice. Schematic representation of the *Meis1/Hoxa9* retroviral model. Foetal liver (FL) cells from *rtTA* (Control) or *shPhd2/rtTA* embryos were enriched for cKit$^+$ and infected with *Mesi1* and *Hoxa9* over-expressing retroviruses and serially re-plated, generating pre-leukaemic stem cells (pre-LSCS). **(A)** These cells were then used for doxycycline titration experiments *in vitro* and in *in vitro* assays. **(B)** pre-LSC cells, not exposed to doxycycline were transplanted into primary recipient mice, which developed murine AML. Once mice showed signs of leukaemic disease, they were sacrificed and analysed.

5.4 Loss of *Phd1, Phd2,* or both results in a reduction in cell number and colony formation

In order to determine the role of PHD1 and PHD2 in leukaemic transformation, I employed the *Meis1/Hoxa9* retroviral model using *Vav-iCre*$^{+}$ conditional knock-out cells. As described in **Figure 5-1**, haematopoietic stem and progenitor cells isolated from the foetal liver of 14.5 dpc Control (*Vav-iCre*$^{-}$), *Phd1*^{CKO} (*Phd1*$^{fl/fl}$*;Vav-iCre*$^{+}$), *Phd2*^{CKO} (*Phd2*$^{fl/fl}$*;Vav-iCre*$^{+}$), or both *Phd1/2*^{CKO} (*Phd1*$^{fl/fl}$*; Phd2*$^{fl/fl}$*;Vav-iCre*$^{+}$) embryos were enriched for cKit^{+} and infected with *Meis1* and *Hoxa9* over-expressing retroviruses and plated into methyl-cellulose to perform a Colony Forming Cell (CFC) assay, with antibiotic selection for both *Meis1* and *Hoxa9* (puromycin and neomycin respectively). The *Meis1/Hoxa9* transformed cells were then serially re-plated from CFC1 into CFC2, and CFC2 into CFC3. Importantly, the cells remain in antibiotic selection throughout the CFC assay to ensure all live cells remain fully transformed with retrovirus. After every CFC, live cells were counted using the Trypan Blue exclusion method, and 2500 live cells were plated at each stage into semi-solid methylcellulose. This was important, as shown in **Figure 5-3**, there are significant differences in live cell number after each CFC. After each stage, i.e. CFC1, CFC2 and CFC3 colonies were counted. After CFC3, these cells are referred to as pre-LSCs. Importantly, for all repeat experiments, each PHD isoform, as well as its *Vav-iCre*$^{-}$ control, was infected with the same batch of *Meis1* and *Hoxa9* viruses. This ultimately results variability in cell number and colony number between PHD isoform experiments, but ensures paired comparisons between the specific *Phd*^{CKO} and its appropriate control.

As mentioned above, following CFC assay, there was a significant decrease in live cell number in the *Phd1*^{CKO}*, Phd2*^{CKO} and *Phd1/2*^{CKO} cells versus their appropriate controls (**Fig. 5-3**). This suggests that the lack of either *Phd1, Phd2,* or both, reduces the leukaemic potential of cells over-expressing *Meis1* and *Hoxa9*. Notably, there does not seem to be a synergistic effect between *Phd1* and *Phd2*, as loss of both *Phd1* and *Phd2* together (*Phd1/2*^{CKO}) produces a less significant cell number reduction than that of either *Phd1* or *Phd2* alone. This suggests that PHD1 and PHD2 isoforms are independently required for leukaemic transformation.

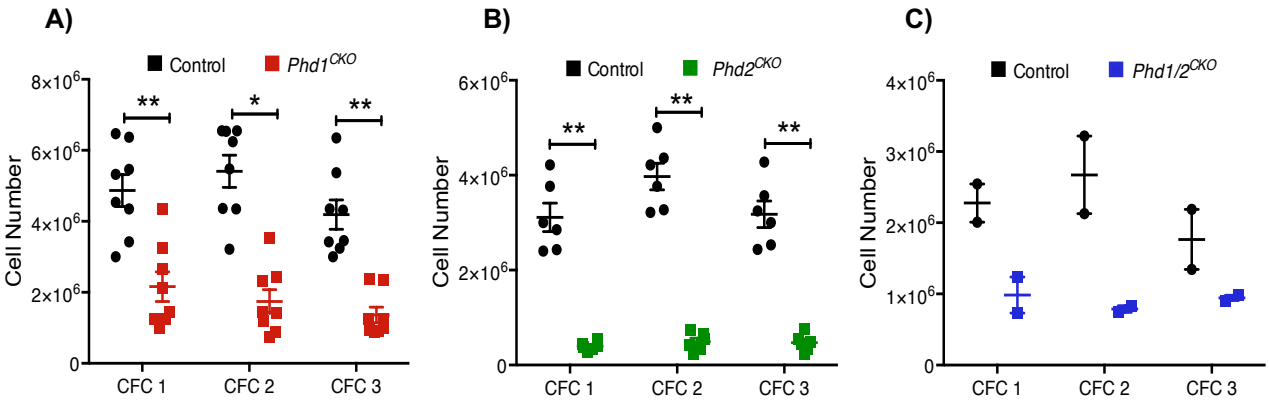

Figure 5-3 - Cells lacking *Phd1, Phd2,* or both show reduced cell number Live cell counts via Trypan-Blue exclusion after Colony Forming Cell (CFC) assay, per 2500 cells plated. *Phd1*^{CKO} **(A)**, *Phd2*^{CKO} **(B)**, and *Phd1/2*^{CKO} **(C)**, versus their *Vav-iCre*$^{-}$ littermate controls. n=2-8 biological replicates per genotype, in 1-4 independent experiments. Data are mean ± SEM. *, P < 0.05; **, P < 0.01 (Mann-Whitney U test).

Additionally, perhaps as expected, re-plating of these cells results in a reduction in colony formation in *Phd1*^{CKO}, *Phd2*^{CKO} and both *Phd1/2*^{CKO} when compared to their *Vav-iCre*$^{-}$ littermate controls. These results suggest that loss of either *Phd1* or *Phd2* reduces leukaemic transformation in a *Meis1/Hoxa9* murine model of AML, especially with regards to their stem-cell regenerative capacity. Notably, the reduction in colony formation is more pronounced in *Phd2*^{CKO}, when compared to either the single *Phd1*^{CKO} or both *Phd1/2*^{CKO}. This suggests that *Phd2* may be the principal *Phd* isoform in leukaemic transformation. Additionally, as previously shown in **Figure 5-3**, there is no evidence of a synergistic effect between *Phd1* and *Phd2*, with no further reduction in the *Phd1/2*^{CKO} versus that of *Phd1*^{CKO} or *Phd2*^{CKO} alone. However, *Phd1/2*^{CKO} experiments are n=2, whereas *Phd1*^{CKO} is n=8, and *Phd2*^{CKO} n=6 per biological genotype, thus further experiments with the *Phd1/2*^{CKO} genetic model could be used to confirm this result.

Overall, these results suggest that PHDs have a significant role in leukaemic transformation *in vitro*, with reductions in both live cell number and colony formation from CFC assay.

Furthermore, these results suggest an important pro-oncogenic role for PHDs in *Meis1/Hoxa9* mediated AML.

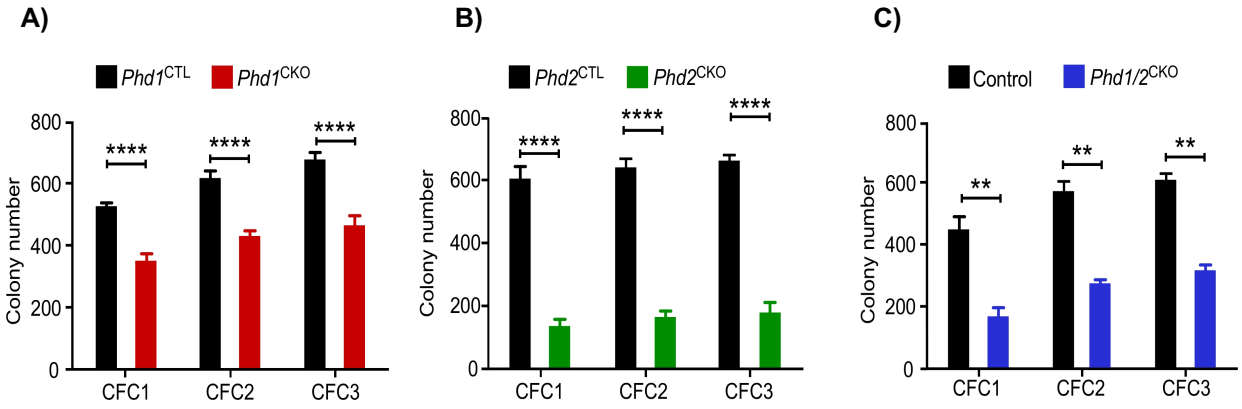

Figure 5-4 - Cells deficient in *Phd1, Phd2,* or both show reduced colony formation Colony forming cell (CFC) counts (colony number) at each re-plating per 2 500 live cells plated. *Phd1*^{CKO} **(A)**, *Phd2*^{CKO} **(B)**, and *Phd1/2*^{CKO} **(C)**, versus their *Vav-iCre*$^{-}$ littermate controls. n=2-8 biological replicates per genotype, in 1-4 independent experiments. Data are mean ± SEM. **, P < 0.01; ****, P < 0.0001 (Mann-Whitney U test).

5.5 *Phd*-deficient cells exhibit a reduction in cell growth

In order to determine whether the *Meis1/Hoxa9* pre-LSCs deficient for *Phd* displayed a growth disadvantage *in vitro*, I conducted a proliferation assay with *Phd*^{CKO} cells, and their control counterparts. Following CFC3, the pre-LSCs were harvested from methylcellulose and placed in liquid culture to measure the proliferation capacity of the fully transformed cells. All cells were plated at the same concentration and live cells counted using Trypan Blue exclusion method at 24, 48 and 72 hours. As shown below in **Figure 5-5**, cells lacking *Phd1, Phd2,* or both *Phd1* and *Phd2*, have reduced proliferation rates in comparison to their *Vav-iCre*$^{-}$ controls. This suggests that although viable, these cells have a reduced mitotic capacity, a valuable asset in an anti-leukaemic target. Moreover, *Phd2*^{CKO} cells show the most significant decrease in proliferation when compared to the control, further confirming its significance in the anti-oncogenic activity of PHD inhibition. Additionally, there is no evidence of a collaborative role between *Phd1* and *Phd2*, with *Phd1/2*^{CKO} cells showing a less significant reduction than that of the *Phd1* ^{CKO} or *Phd2* ^{CKO} alone. Therefore, it can be concluded that *Phd1* and *Phd2* act in an independent manner regarding leukaemic growth *in vitro.*

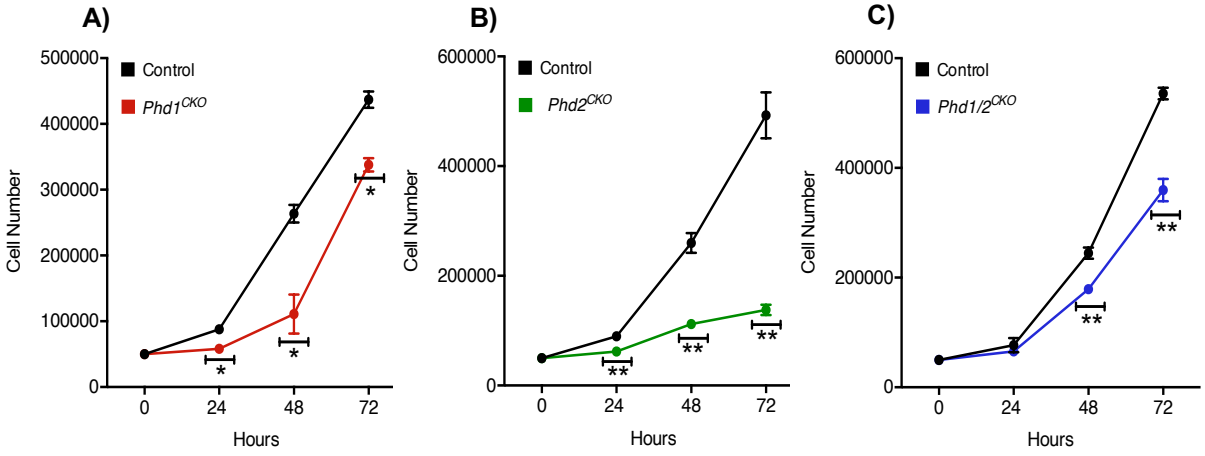

Figure 5-5 - *Phd1* and *Phd2* are essential in the proliferation activity of pre-LSCs 50 000 live pre-LSCs were plated and counted at 24 hrs, 48 hrs and 72 hrs (Trypan-Blue exclusion). *Phd1*^{CKO} **(A)**, *Phd2*^{CKO} **(B)**, and *Phd1/2*^{CKO} **(C)**, versus their *Vav-iCre*$^{-}$ controls. Data are mean ± SEM. n=2-3 biological replicates per genotype, cells plated in triplicate. *, $P < 0.05$; **, $P < 0.01$ (Mann-Whitney U test).

5.6 Expression of *Phd1 and Phd2* increases leukaemic burden *in vivo*

To investigate whether the deletion of *Phd1, Phd2*, or both, impacts leukaemia development *in vivo*, I performed transplantation assays with the *Meis1/Hoxa9* transformed pre-LSCs. 100 000 CD45.2$^+$ pre-LSCs from CFC3 were isolated and mixed with 200 000 WT CD45.1$^+$ unfractionated BM cells, and transplanted into sub-lethally irradiated (11Gy) CD45.1$^+$/CD45.2$^+$ syngeneic recipient mice in order to follow leukaemic disease development *in vivo*. This experimental design allows tracking of leukaemic disease as it develops *in vivo* through the flow cytometric analysis on CD45.2$^+$ expression in the peripheral blood (PB) of recipient mice. Given correct transformation and transplantation of *Meis1/Hoxa9*-transduced cells, the CD45.2$^+$ expression will increase over time. We chose to take PB samples from recipient mice at 4 weeks, 8 weeks and 12 weeks. This is due to the fact that murine haematopoietic cells often take 2-3 weeks to fully engraft (Zijlmans et al., 1998), and as shown by Kroon et al, the *Meis1/Hoxa9* retroviral model should give rise to AML < 3 months after transplantation. Once recipient mice showed signs of leukaemic disease such as weight loss, shortness of breath, a hunched position, impaired motion or pale paws, they were sacrificed and the date of death recorded. Death from an AML-like disease was confirmed by high CD45.2$^+$ Mac-1$^+$Gr1$^+$ expression through flow-cytometry analysis in the BM of deceased mice. All transplanted mice developed an AML-like disease and were sacrificed by 105 days post-transplant, with an average survival of 84 days.

Peripheral blood samples taken at 4 weeks and 8 weeks post-transplant show a significant decrease in CD45.2$^+$ cell engraftment in the mice transplanted with *Phd1*^{CKO}*, Phd2*^{CKO} and *Phd1/2*^{CKO} cells compared to their controls (**Fig. 5-6)**. Again, there seems to be no co-operation between of *Phd1* and *Phd2*, with recipient mice transplanted with *Phd1/2*^{CKO} cells showing much lower engraftment than that of either *Phd1*^{CKO} or *Phd2*^{CKO} cells. Notably, the *in vivo* transplantation of *Phd1/2*^{CKO} and control cells was conducted in one independent experiment using n=2 biological replicate donors, each donor being transplanted into 6 recipient mice. In comparison, both the *Phd1*^{CKO} *and Phd2*^{CKO} experiments feature 2 independent experiments,

of n=3-4 biological replicates into 5 recipient mice. Repetition of the *Phd1/2*^{CKO} will shed further light and confirm the role and interaction of Phd1 and Phd2 in the development of murine AML in vivo.

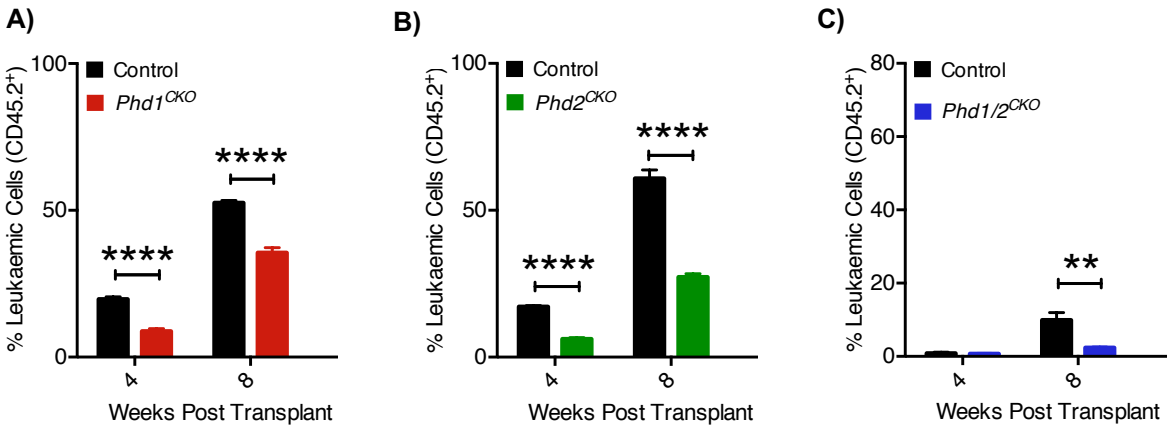

Figure 5-6 - Transplantation of cells lacking *Phd1, Phd2,* or both show reduced engraftment Percentage of leukaemic cells (% CD45.2$^+$ engraftment) following primary transplantation of 100 000 pre-leukaemic stem cells. Peripheral blood samples taken at 4 weeks and 8 weeks post-transplant and CD45.2$^+$ engraftment measured by flow cytometry analysis. *Phd1*^{CKO} **(A)**, *Phd2*^{CKO} **(B)**, and *Phd1/2*^{CKO} **(C)**, versus their *Vav-iCre*$^-$ controls. n=5-6 recipients per biological replicates (n=2-4), 1-2 independent experiments. Data are mean ± SEM. **, P < 0.01; ****, P < 0.0001 (Mann-Whitney U test)

5.7 Loss of *Phd1, Phd2,* or both decreases LSC development *in vivo*

In addition to leukaemic cell engraftment analysis, *in vivo* transplantation experiments were also used to investigate the role of PHDs in development of leukaemic disease *in vivo*. Following transplantation of pre-LSCs, once recipient mice showed signs of ill-health, they were sacrificed and analysed to confirm their AML disease, and date of death was recorded. As is shown in **Figure 5-7**, loss of *Phd1, Phd2,* or both extended survival in a *Meis1/Hoxa9* model of leukaemia. Recipient mice transplanted with *Phd1* ^{CKO} cells had a mean survival rate of 82 days versus mice transplanted with *Phd1* control cells with a survival rate of 58.5 days. Meanwhile, mice transplanted with *Phd2* ^{CKO} cells had a mean survival rate of 80.5 days versus mice transplanted with *Phd2* control cells with a survival rate of 59 days. Finally, mice transplanted with cells lacking both *Phd1* and *Phd2* had a mean survival of 84.5 days versus 63.5 days in their control counterparts. Overall, the increase in mean survival is very similar with 23.5 days, 21.5 days and 21 days for *Phd1* ^{CKO}, *Phd2* ^{CKO} and *Phd1/2* ^{CKO} respectively.

Although there were differences *in vitro*, notably with *Phd2* presenting the most significant phenotype in leukaemic transformation, when translated *in vivo*, this effect is lost, with all isoforms resulting in the same increase in survival when compared to their appropriate controls.

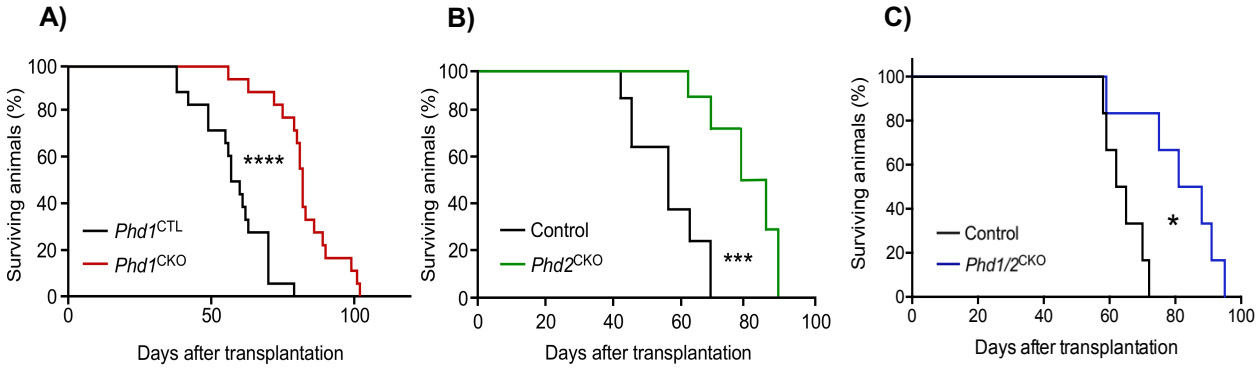

Figure 5-7 - Deletion of *Phd1, Phd2,* or both increases survival *in vivo* Kaplan-Meier survival curve of recipients transplanted with 100 000 pre-leukaemic stem cells. *Phd1*^{CKO} **(A)**, *Phd2*^{CKO} **(B)**, and *Phd1/2*^{CKO} **(C)**, versus their *Vav-iCre*$^{-}$ controls. n=5-6 recipients per biological replicates (n=2-4), 1-2 independent experiments. *, P < 0.05; ***, P < 0.001; ****, P < 0.0001 (Mantel-Cox test).

5.8 LSCs lacking *Phd1* have reduced stem-cell potential

In vitro and *in vivo* experiments conducted using pre-LSCs found that deletion of *Phd1, Phd2,* or both has a significant anti-leukaemic effect. Following this, I sought to investigate the role of *Phds* in the propagation of *Meis1-Hoxa9* driven AML using LSCs isolated from the recipient mice used in the primary transplantation experiments described in **Section 5-6** and **5-7**. Following the development of leukaemic disease, recipient mice were sacrificed and BM samples were analysed to confirm AML. Notably, these leukaemic cells derived from adult BM, having generated AML in the murine recipients are now said to be leukaemic stem cells (LSCs). These cells give an interesting insight into the biological processes behind the development of pre-LSCs into LSCs *in vivo*, and further functional assays can unveil the role of the *Phds* in leukaemia maintenance.

Total BM cells from recipient mice transplanted with control (*Vav-iCre^{-})* and *Phd1*^{CKO} cells were first placed in CFC assay to isolate the transformed colony forming cells for further studies. In addition, the CFC assay can also be used experimentally to compare the potency of *Phd1* ^{CKO} LSCs versus the control LSCs. As shown in **Figure 5-8A**, LSCs with a deficiency of *Phd1* exhibit a significant decrease in colony formation versus control LSCs. This suggests that although all recipient mice eventually succumbed to AML, with BM CD45.2^{+} engraftment of between 98.9 % and 100 % for both *Phd1* ^{CKO} and control experiments (**Fig 5-8C**), there is an apparent decrease in stem-cell and self-renewal potential in LSCs lacking *Phd1*.

After harvesting LSCs from the CFC assay, a proliferation experiment was conducted to study the growth of these cells lacking *Phd1*. Mirroring the result of the pre-LSC proliferation curve (**Fig 5-5A)**, cells with a deficiency of *Phd1*, although viable, showed a pronounced growth stagnation when compared to control LSCs **(Fig 5-5B).** Additionally, harvested LSC cells were immunophenotypically analysed by flow cytometry and *Phd1* ^{CKO} LSCs showed a significant decrease in cKit expression, a marker of primitive haematopoiesis, as well as a dramatic increase in Mac1^{+} expression, which marks differentiated monocytes **(Fig 5-5C).** This, in combination with results from **Figure 5-8A** and **Figure 5-B** gives strong evidence that the

phenotype shown in primary transplant *in vivo* is due to a loss of *Meis1/Hoxa9* derived stem-cell activity. Notably, there is a marked decrease in the $Gr1^+$ and $Mac1^+Gr1^+$ compartments, which are also markers of differentiated myeloid cells, this may be a $Gr1^+$ specific phenotype. Histology and molecular analysis would unravel this phenotype.

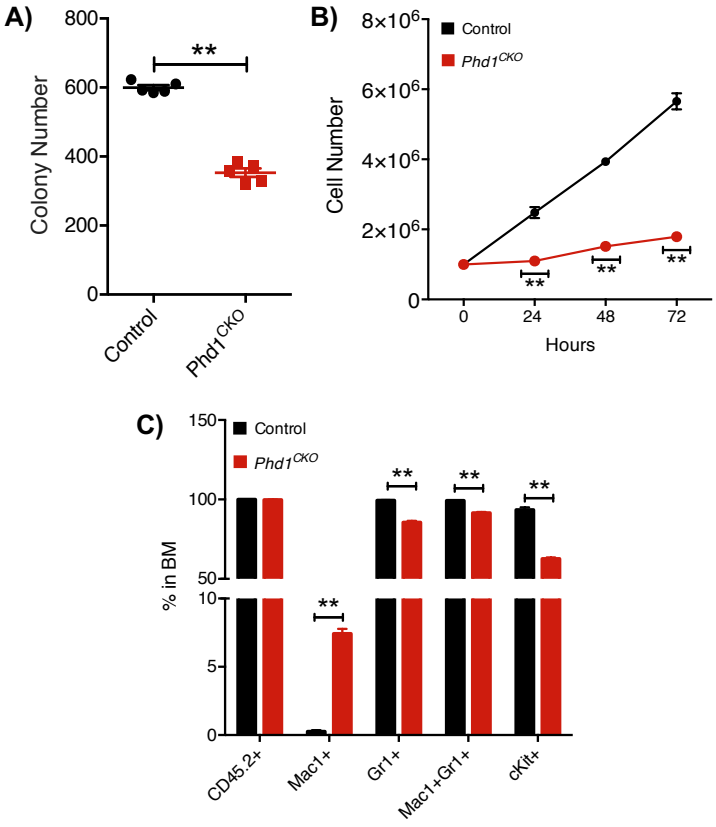

Figure 5-8 - LSCs deficient in *Phd1* have reduced stem-cell activity (A) 2 500 BM LSCs were plated in CFC assay and counted after 6 days **(B)** 50 000 LSCs were plated in triplicate and counted by Trypan-Blue exclusion 24 hrs, 48 hrs and 72 hrs later **(C)** Flow cytometry analysis of Control and *Phd1* ^{CKO} LSCs. Data are mean ± SEM. n=3-5 biological replicates per genotype. **, $P < 0.01$ (Mann-Whitney U test).

5.9 *Phd1* promotes AML maintenance

To investigate the ability of *Phd1*-deficient LSCs to propagate AML, a secondary transplantation experiment was performed. 50 000 LSCs were transplanted into sub-lethally irradiated (11Gy) $CD45.1^+/CD45.2^+$ syngeneic secondary recipient mice to functionally test the role of *Phd1* in AML maintenance. As before, mice were serially bled at 4, 8- and 12-weeks post-transplantation to track development of the disease. These experiments showed that there is a decrease in leukaemic cell engraftment in the mice transplanted with LSCs lacking *Phd1* versus the control **(Fig. 5-9A)**. As such, all control mice succumbed to AML and were sacrificed by week 12, whereas a large number of *Phd1* ^{CKO} recipient mice remained. Notably, although statistically significant, the engraftment data is noticeably more variable than that of the primary transplant experiment **(Fig. 5-7A)**. This is due to the *in vivo* source of the LSCs which are inherently more biologically divergent than *in vitro* cultured pre-LSCs. As such, a significant decrease in engraftment in secondary transplant gives real strength to the hypothesis that a deficit in *Phd1* impairs AML *in vivo.*

All recipient mice in the secondary transplant succumbed to AML disease, with LSC infiltration present in the BM and spleen of all animals. The latency of the disease was drastically increased in mice transplanted with *Phd1* ^{CKO} LSCs with an average survival of 85 days, versus 52.5 days in control mice. Additionally, the longest surviving mouse transplanted with *Phd1* ^{CKO} LSCs mice remained alive for 136 days, versus just 61 days in the control group **(Fig. 5-9B)**. At 61 days, 76.9 % of the mice transplanted with *Phd1* ^{CKO} LSCs were still alive. Thus, it is evident, that in addition to the importance of *Phd1* in the transformation and development of AML, it also serves a vital role in the long-term self-renewal capacity of LSCs. This is especially important when exploring therapeutic targets for AML as patients will often present with advanced disease fuelled by LSCs that must be eradicated.

Notably, although these experiments have proved successful with *Phd1* ^{CKO} LSCs, they must be repeated with *Phd2* and *Phd1/2* in order to fully dissect the role of *Phds* in AML maintenance. As demonstrated with *Phd1*^{CKO} LSCs, it is possible that the reduction in

proliferation and colony growth shown in the *Phd2* ^{CKO} pre-LSCs **(Figs 5-5B, 5-6B)** will translate to an even more significant defect in *Phd2* ^{CKO} LSCs. Further *in vivo* and mechanistic studies on *Phd1* ^{CKO}, *Phd2* ^{CKO} and *Phd1/2* ^{CKO} LSCs will unveil the role of each *Phd* isoform in LSC biology, and potentially expose which isoforms can be optimised for targeted AML therapy.

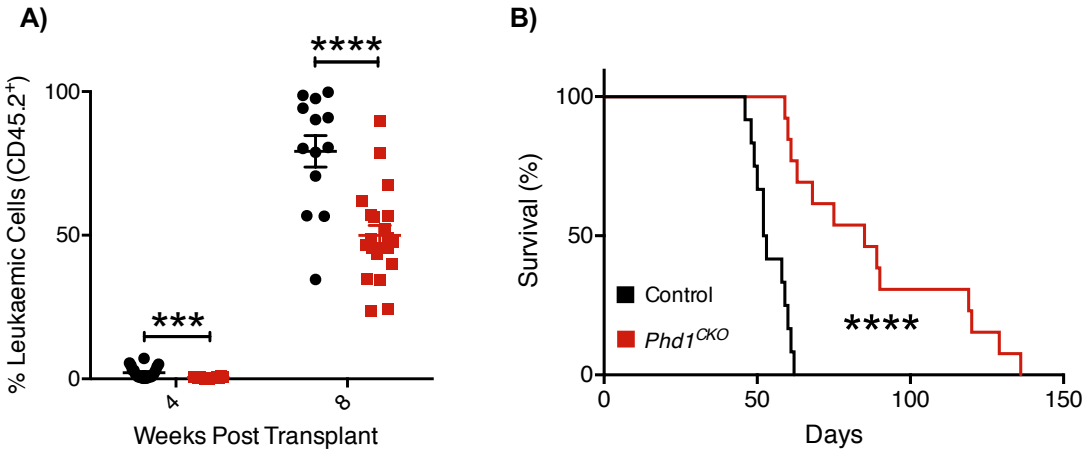

Figure 5-9 - LSCs deficient in *Phd1* have reduced engraftment and increased survival following transplantation assay (A) Percentage of leukaemic cells (% CD45.2$^+$ engraftment) following secondary transplantation of 50 000 BM LSCs. Peripheral blood samples taken at 4 weeks, 8 weeks and 12 weeks post-transplant, and CD45.2$^+$ engraftment measured by flow cytometry analysis. At 12 weeks, all control mice were sacrificed having developed AML. n=5 recipients per biological replicates (n=3-4), 1 independent experiment. Data are mean ± SEM. ****, P < 0.0001 (Mann-Whitney U test). **(B)** Kaplan-Meier survival curve of recipients transplanted with *Phd1*^{CKO} LSCs versus the *Vav-iCre*$^-$ control. n=5 recipients per biological replicates (n=3-4), 1 independent experiment. Data are mean ± SEM. ****, P < 0.0001 (Mantel-Cox test).

5.10 Inducible *Phd2* knockdown in *Meis1/Hoxa9-transformed cells* results in increased cell death *in vitro*

After discovering that deletion of *Phd1, Phd2,* or both results in decreased leukaemogenesis both *in vitro* and *in vivo*, the *shPhd2* doxycycline inducible model was employed (as described in **Chapter 4**) to knockdown *Phd2* at different stages of leukaemic disease progression. As described in **Section 5.3.2**, the *Meis1/Hoxa9* retroviral model was further utilised, using FL cells taken from *rtTA* (Control) and *shPhd2/rtTA* embryos. Upon treatment with Dox, *shPhd2/rtTA* cells will transcribe a short-hairpin targeting *Phd2,* as well as GFP, whereas when treated with Dox, *rtTA* (Control) cells will not transcribe a short-hairpin targeting *Phd2,* or GFP. Experiments began by testing this model *in vitro* to investigate the effect of acute reduction of *Phd2* levels in pre-LSCs. Following this, the model was used *in vivo* to address the role of *Phd2* in AML disease evolution. This mouse model offers great insight into the therapeutic potential of inhibition of *Phd2*, as *Phd2* levels can be decreased, even once leukaemic engraftment has been established *in vivo.*

Following infection with *Meis1* and *Hoxa9* over-expressing retroviruses, and antibiotic selection, control and *shPhd2/rtTA* were plated in CFC assay to select for the most oncogenic and primitive pre-LSC clones. As shown in **Figure 5-11A**, when plated in CFC assay in the absence of Dox, there is no difference in colony formation between the control and *shPhd2/rtTA* mice. As such, there is no evidence of activation of the *shPhd2/rtTA* construct in the *Meis1/Hoxa9* transformed *shPhd2/rtTA* cells.

Notably, there is some evidence that Dox itself can have a cytotoxic effect in human leukaemia cell lines including HL-60 (AML), KG1a (acute myelogenous leukaemia) and K562 (chronic myelogenous leukaemia), promoting apoptosis through caspase activation and cleavage of PARP and Bcl-2 (Mouratidis et al., 2007; Onoda et al., 2006). This effect, however, is slight, and uses significantly higher concentrations 0.5–100 μg/ml for 24 hr (Song et al., 2014). Regardless, to ensure the effect is from acute deletion of *Phd2* and not Dox, both control and

shPhd2/rtTA cells are consistently treated with the same concentration of antibiotic. Thus, all phenotypes observed in experiments with Dox-treated shPhd2/rtTA cells versus Dox-treated control cells, are a direct consequence of *Phd2* knockdown.

After harvesting cells from CFC3, a Dox titration experiment was performed to determine the correct concentration of antibiotic to use *in vitro* to activate transcription of the short-hairpin targeting *Phd2*. All *in vitro* experiments used 2 biological replicates plated in triplicate, with both control and shPhd2/rtTA cells treated with Dox for 48 hrs before flow cytometry analysis. This ensured there was no Dox-specific effect on the *Meis1/Hoxa9* transformed cells. Additionally, GFP expression was measured as a direct read-out of *shPhd2* expression, and ensured the correct identification of control and *shPhd2/rtTA* cells. To investigate the role of *Phd2* in *Meis1/Hoxa9* driven AML, the rate of apoptosis was measured in *shPhd2/rtTA* and control cells after treatment with Dox for 48 hrs. For this TO-PRO^{TM}-3 Iodide (referred to as ToPro) was used. Notably To-Pro is a carbocyanine monomeric nucleic acid stain, which is regularly used as a dead cell indicator. Thus, it was chosen to measure the rate of cell death *in vitro.*

Primary Dox titration experiments using concentrations of 1.56 ng/ml to 100 ng/ml of Dox show a steady increase in GFP expression, with 100 ng/ml showing a maximum GFP expression of 84.2 %. Importantly, as expected, there is no GFP in the control group, or when *shPhd2/rtTA* cells were in the absence of Dox **(Fig 5-10A).** There is no difference in the percentage of ToPro^{+} cells at lower concentrations of Dox, but a significant increase in apoptosis at 100 ng/ml **(Fig 5-10 B)**. However, there is a noticeably high level of apoptosis in all experiments, including cells that were not exposed to Dox in both the control and *shPhd2/rtTA.* As such, a new batch of *Mesi1/Hoxa9*-transformed control and *shPhd2/rtTA* cells were thawed, and the Dox titration experiment was repeated, this time at higher concentrations of Dox.

As before, control and *shPhd2/rtTA* cells were exposed to increasing concentrations of Dox, from 62.5 ng/ml to 1000 ng/ml. These concentrations were chosen to include 100 ng/ml, where

there was a marked increase in apoptosis in *shPhd2/rtTA* pre-LSCs. Importantly, there is a significantly lower level of background apoptosis in this experiment, with an average of 3.29 % To-Pro$^+$ cells in the control and non-treated samples 48 hr after plating **(Fig 5-10D)**. This result allows for a more accurate measurement of apoptosis in the Dox treated *shPhd2/rtTA* pre-LSCs. In addition, in concordance with the previous experiment, there is no GFP expression in either the non-treated cells, or the control cells lacking the *shPhd2* construct. The GFP expression reaches its maximum when *shPhd2/rtTA* cells are treated with 250 ng/ml Dox, suggesting a peak in *shPhd2* activity **(Fig 5-10C).** Moreover, in addition to a peak in GFP expression, To-Pro$^+$ expression is at its highest when *shPhd2/rtTA* pre-LSCs are treated with 250 ng/ml Dox, with an average of 33.45 % To-Pro$^+$ cells, versus 3.27 % To-Pro$^+$ cells in the treated control. Increasing the Dox concentration above 250 ng/ml has no increased effect on apoptosis, with 500 ng/ml and 1000 ng/ml showing a decrease in both GFP and To-Pro expression. This suggests concentrations above 250 ng/ml may saturate the system, moderately decreasing *shPhd2* transcription, and thus significantly decreasing its cytotoxic effect.

Taken together, these experiments indicate that knockdown of *Phd2 in vitro* results in an increase in apoptosis in *Meis1/Hoxa9* leukaemia. Based on these results, all further *in vitro* experiments used a Dox concentration of 250 ng/ml.

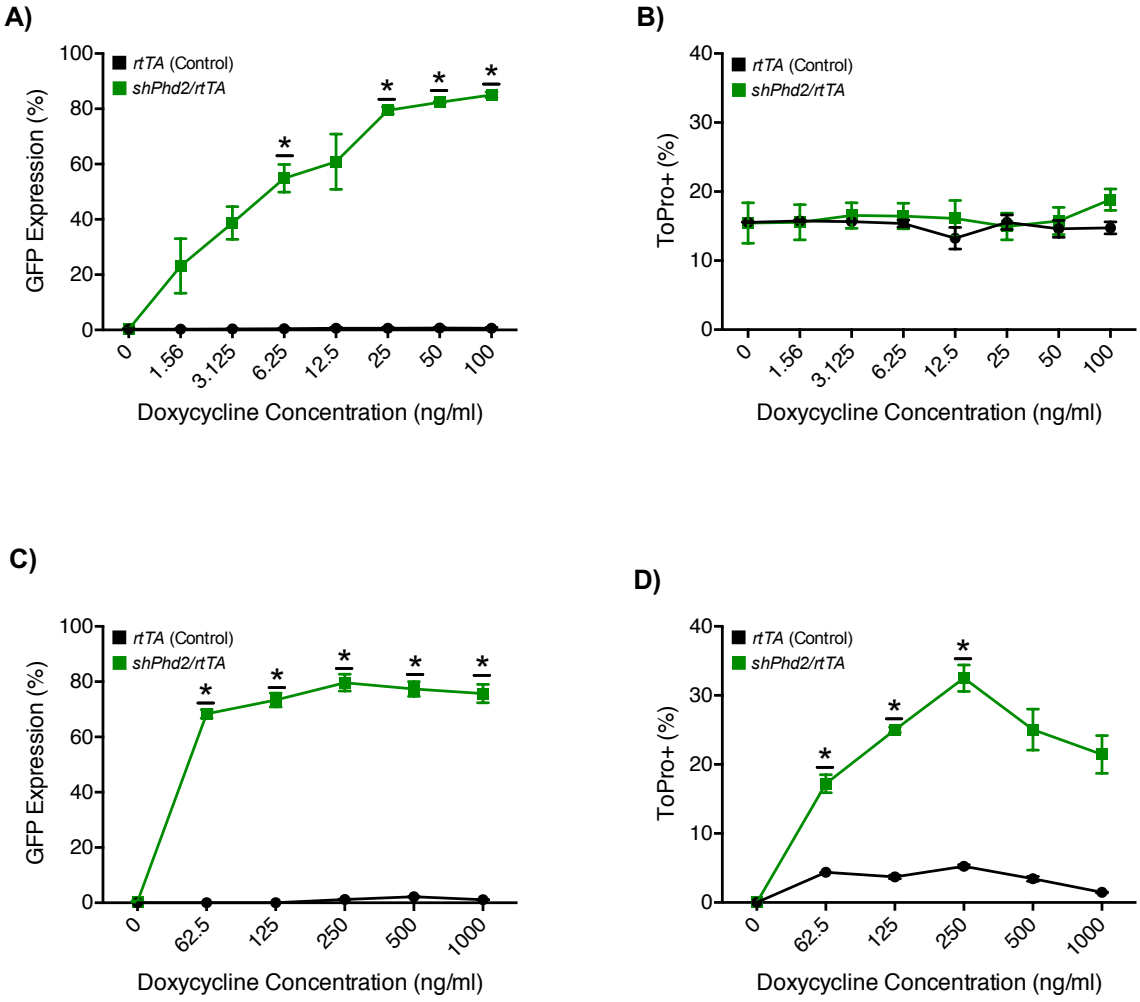

Figure 5-10 - Dox treatment of *shPhd2/rtTA* pre-LSCs results in increased GFP expression and apoptosis *Meis1Hoxa9* pre-LSCs from control (*rtTA)* and *shPhd2/rtTA* mice were harvested from CFC3 and treated with increasing concentrations of Dox as described. 48 hr later, GFP **(A, C)** and To-Pro^{+} cells **(B, D)** were measured by flow cytometry. Data are mean ± SEM. n=2 biological replicates plated in triplicate. *, $P < 0.05$ (Multiple t-test, statistical significance determined using the Holm-Sidak method).

5.11 Suppression of *Phd2* reduces the potency of pre-LSCs

After determining the appropriate Dox concentration to use *in vitro*, a CFC assay was performed on control and *shPhd2/rtTA* pre-LSCs in the presence and absence of Dox. As shown in **Figure 5-11A**, in the absence of Dox, there is no difference in colony number between control and *shPhd2/rtTA* pre-LSCs. Interestingly, however, when the CFC assay was repeated, and both groups were treated with 250 ng/ml Dox, the cells with a deficiency in *Phd2* showed a significant decrease in colony number **(Fig 5-11B)**. This suggests acute knockdown of *Phd2* in potent pre-LSCs can significantly reduce their leukaemic activity.

In addition, when imaged with the Operetta high-content automated microscope, colonies derived from *shPhd2/rtTA* cells were GFP+ and were significantly smaller and more dispersed than the control. Notably, large, dense, compact colonies, as represented in the bottom panel of **Figure 5-11C**, are known to contain more stem cells, resembling that of colonies generated by primitive haematopoietic cells. Smaller colonies like that shown in middle panel of **Figure 5-11C** have a compact centre, surrounded by differentiated cells. These are thought to derive from haematopoietic progenitors, with a lower stem-cell capacity. Finally, looser colonies, as represented in the top panel of **Figure 5-11C**, are comprised of long-term myeloid progenitor cells, and, as such, are considered to be more differentiated haematopoietic cells. These colonies are classified as Type 1, Type 2, and Type 3 respectively (Lavau et al., 1997). Moreover, these phenotypes have a clinical relevance as Somervaille et al in 2006 showed that murine models of aggressive human leukaemias induced by MLL-AF9 or MLL-ENL produced compact colonies, with a higher proportion of stem-cell derived, "blast-like" cells when compared to less aggressive murine models of human leukaemias.

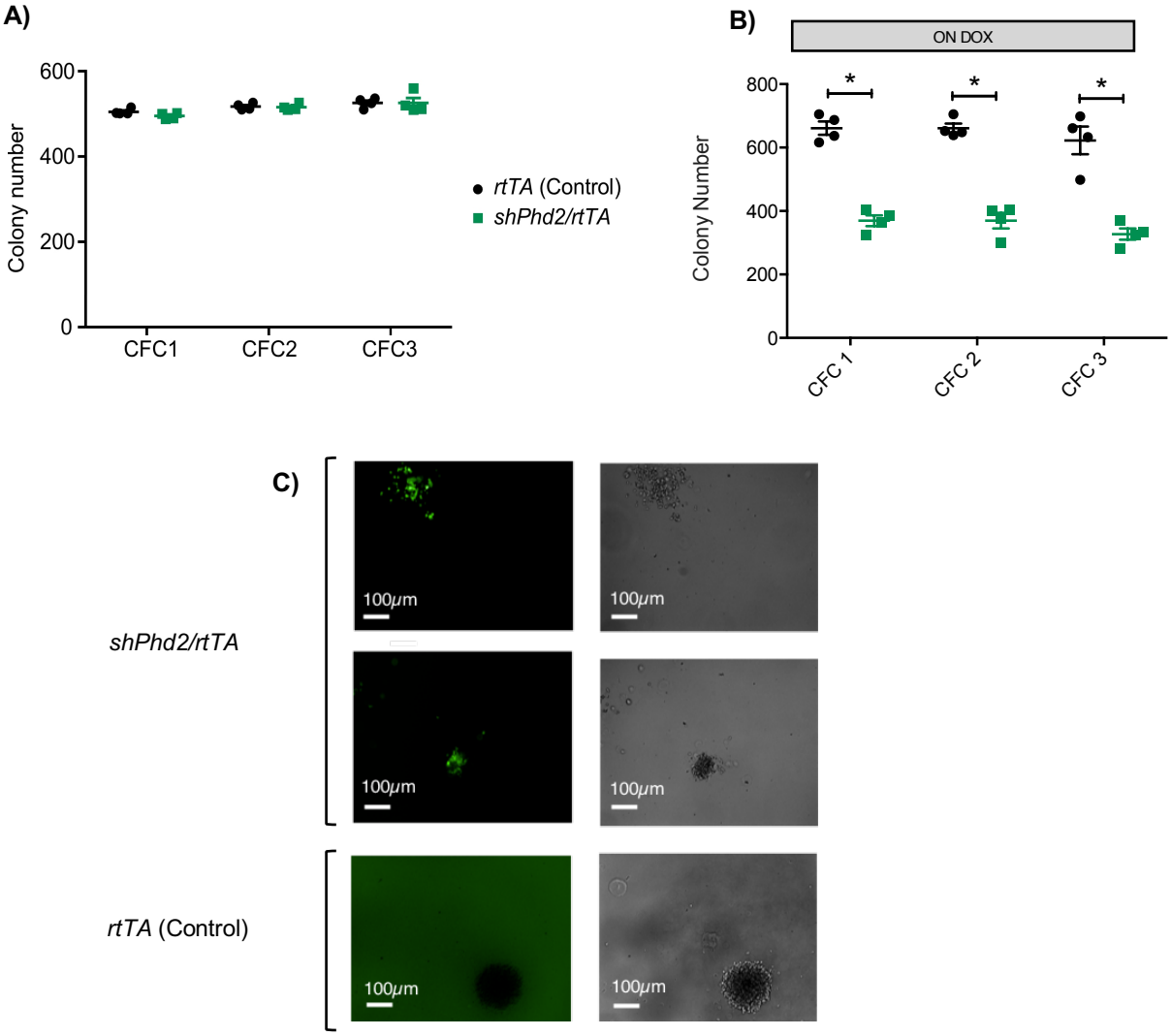

Figure 5-11 - Acute reduction of *Phd2* results in reduced colony number and size (A) *Meis1Hoxa9* pre-LSCs from control (*rtTA)* and *shPhd2/rtTA* mice were plated into CFC assay, and in parallel plated into a CFC assay with 250 ng/ml Dox **(B)**, counted 6 days after plating. Imaging was performed using the Perkin Elmer Operetta high content imaging system 6 days after plating. **(C)** Representative images of Type 1 (bottom panel), Type 2 (middle panel) and Type 3 (top panel) colonies are shown, taken with a 585 - 605 nm and brightfield filter respectively. Data are mean ± SEM. n=2 biological replicates plated in duplicate. *, $P < 0.05$ (Mann-Whitney U test).

5.12 Knockdown of Phd2 in established AML decreases engraftment and LSC development *in vivo*

To investigate the effect of acute *Phd2* knockdown in established AML disease, I transplanted control and *shPhd2/rtTA* pre-LSCs into primary recipient mice and induced *shPhd2* expression following marked AML engraftment. 100 000 $CD45.2^+$ *Meis1/Hoxa9* pre-LSCs from CFC3, unexposed to Dox, were isolated and mixed with 200 000 WT $CD45.1^+$ unfractionated BM cells and transplanted into sub-lethally irradiated (11Gy) $CD45.1^+/CD45.2^+$ syngeneic recipient mice. Mice were serially bled at 4 weeks (30 days) and 8 weeks (60 days) to measure leukaemic engraftment prior to Dox induction. After 60 days, recipient mice transplanted with control and *shPhd2/rtTA* pre-LSCs showed robust CD45.2 engraftment with an average of 11.4 % and 16.5 % respectively. Given this result, at 60 days post-transplantation, recipient mice were treated with 2 mg/ml Dox in their drinking water to activate transcription of a short-hairpin targeting *Phd2.*

As shown in **Figure 5-12A**, after only 10 days on Dox, *shPhd2/rtTA* recipient mice have a significantly lower engraftment than that of recipient mice transplanted with control pre-LSCs. This result is especially powerful given that *shPhd2/rtTA* recipient mice had a notably higher CD45.2 engraftment at 60 days. Although the percentage of CD45.2 increases from day 60 to day 70, there is an evident slowing of leukaemia progression **(Fig 5-12A)**. Moreover, this translates into an increase in disease latency, with an average survival of 127 days versus 72 days in mice transplanted with control cells **(Fig 5-12B)**. Notably, there is increased survival in the *rt/TA* control group versus comparative controls in the *Vav-iCre* transplantation experiments **(Fig 5-7)**. This is due to differing batches of *Meis1/Hoxa9* virus, and this experiment should be repeated with new virus to corroborate this result. Despite this, the experiment described in **Figure 5-12** gives promising evidence that inhibition of *Phd2,* in an established form of aggressive AML, can prolong survival *in vivo.* Additionally, this result suggests that pharmacological inhibition of *Phd2*, and possibly other *Phd* isoforms may hold therapeutic potential in the eradication of LSCs in human patients.

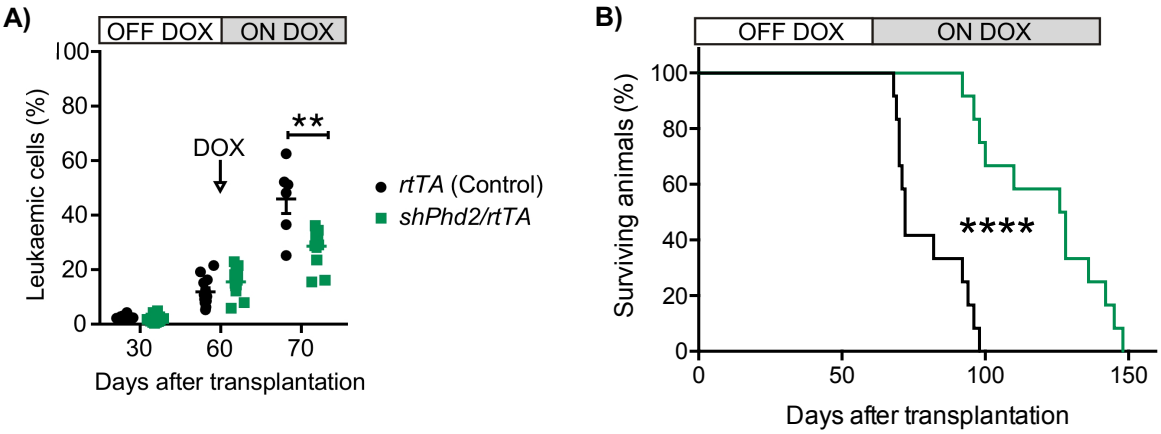

Figure 5-12 - Inhibition of *Phd2* reduces engraftment and increases survival *in vivo* (A) Percentage of leukaemic cells (% CD45.2^{+} engraftment) following primary transplantation of 100 000 *rtTA (*Control) or *shPhd2/rtTA* pre-leukaemic stem cells into recipient mice. Peripheral blood samples taken at 30 days, 60 days and 70 days post-transplant. Engraftment measured by flow cytometry analysis. **, P < 0.01 (Mann-Whitney U test) **(B)** Kaplan-Meier survival curve of recipients. n=6 recipients per biological replicates (n=2). ****, P < 0.0001 (Mantel-Cox test).

5.13 Discussion

This work offers new insights into the role of PHD enzymes in AML, identifying *Phd1* and *Phd2* as oncogenes in a *Meis1/Hoxa9* retroviral model of AML. From this chapter, it is evident that inhibition of *Phd1* and *Phd2* has a detrimental effect on potency of LSCs, effecting their growth and self-renewal potential.

Genetic deletions of *Phd1* and *Phd2* in *Meis1/Hoxa9* transformed pre-LSCs showed a significant reduction in growth in CFC assay. This result is corroborated in the Dox-inducible *shPhd2* experiments, which also show a pronounced decrease in colony growth in pre-LSCs with an acute deletion in *Phd2*. Notably, in addition to a reduced colony number, *shPhd2/rtTA* pre-LSCs treated with Dox have a smaller and more dispersed morphology, consisting of myeloid progenitor and differentiated cells, so called "Type 3" colonies (Lavau et al., 1997). Somervialle et al in 2006 expanded upon the work conducted by Lavau and colleagues, and showed that a Type 3 morphological phenotype *in vitro* is synonymous with less potent AML MLL-subtypes, such as *MLL-AF10* or *MLL-AF1p*. In contrast, colonies produced by *MLL-AF9* and *MLL-ENL*, produce large, 'blast-like' colonies, which contain a high frequency of aberrantly self-renewing LSCs. Translating these findings to the clinic, there was a direct link between poor prognosis and LSC frequency. As such, there is much academic and pharmacological research into promoting the differentiation of LSCs, overcoming the so-called "differentiation block" (Bose and Konopleva, 2018). This evidence reveals *Phd2* as a promising therapeutic candidate, as it indeed decreases the self-renewal capacity of pre-LSCs, pushing them instead to a more differentiated state.

Repeating imaging experiments with $Phd1^{CKO}$, $Phd2^{CKO}$ and $Phd1/2^{CKO}$ cells, as well as selective PHD inhibitors would give further insight into this hypothesis. Use of machine learning processes, like that published by the Kranc laboratory in 2018, allow for high-throughput screening and multi-parameter analysis of CFC assays, ideally suited to quantify colony morphology and differentiation (O'Duibhir et al., 2018). This study using retrovirally transformed *Meis1/Hoxa9* cells, and the human AML cell line THP-1, identified that IOX2, a

PHD inhibitor, decreased colony formation and increased differentiation, albeit less significantly than other hits in the screen. A notable hit was GSK-LSD1, a LSD1 (also known as KDM1A) inhibitor was found in the screen to drastically increase differentiation, and is currently in phase I clinical trials in patients with relapsed AML (under the generic name GSK2879552, https://www.gsk-clinicalstudyregister.com/study/200200#ps). Notably, IOX2 is a PHD inhibitor, but also inhibits multiple other 2-OG oxygenases (Chowdhury et al., 2013), some of which are already known to increase LSC activity, and are likely to have reduced the anti-oncogenic effect of inhibition of PHDs (Sepulveda et al., in preparation). Using specific PHD inhibitors, or further short-hairpin studies, will help to determine the self-renewal effect of PHDs in AML. In addition to murine AML, established human AML cell lines, or patient samples should also be used to verify the therapeutic potential of PHDs.

When *Meis1/Hoxa9* transformed pre-LSCs were transplanted into syngeneic primary recipient mice, cells deficient in *Phd1, Phd2,* or both showed a decrease in leukaemic engraftment, resulting in an increase in disease latency. This result was confirmed by acute deletion of *Phd2* in established AML, leading to a reduction in disease progression, shown in both engraftment and survival data. Thus, as shown in the *in vitro* assays, ablation of PHDs reduces the oncogenic and self-renewal potential of pre-LSCs. Moreover, *in vitro* and *in vivo* assays on $Phd1^{CKO}$ and control LSCs showed a decline in LSC potential. To further investigate this, the $Phd1^{CKO}$ secondary transplant should be repeated, and similar experiments with $Phd2^{CKO}$ and $Phd1/2^{CKO}$ LSCs conducted. Moreover, to test the hypothesis that PHDs help promote LSC activity, a limiting dilution assay (or LDA), whereby recipient mice are transplanted with a bulk leukemic population (as in the secondary transplantation described in **5.9**), but replicates are conducted with multiple dilutions of cell number, until a dose with no response is achieved (in this case murine survival) would support these findings (Hu and Smyth, 2009). This technique should be employed to accurately quantify the active LSC frequency in *Phd*-deficient and control leukaemic cells, and to confirm the hypothesis that deletion of *Phds* decreases LSC potency and self-renewal capacity.

Furthermore, this work supports further exploration of the *Meis1Hoxa9* retroviral model using the *shPhd2/rtTA* mice. From experiments shown in sections **5-10** to **5-12**, there is strong evidence to show that acute depletion of *Phd2* can have marked effect on pre-LSC and LSC biology. Primary transplantations, as described in **Fig 5-12** should be repeated, and Dox removed following a decrease in *shPhd2/rtTA* engraftment. This will reveal if acute knockdown of *Phd2* has a lasting effect on LSCs. Notably, to expose this phenomenon, it is possible that fewer LSCs will have to be transplanted in this experiment to extend disease latency. Additionally, secondary transplantations with this model should be conducted with two cohorts of *shPhd2/rtTA* recipient mice which in primary transplantation were either in the absence or presence of Dox. This will unveil the role of *Phd2* at multiple levels of AML disease maintenance.

Experiments focusing on chemotherapy in murine models of AML, have shown that deletion of *Hif-1α* in MLL-AF9 driven AML accelerates disease in mice when treated with cytarabine and doxorubicin (in press; personal communications with Profs K. Kranc and J. Cammenga). This emerging research, in addition to previous studies by the Kranc laboratory, demonstrate the negative impact of HIF deletion in AML, especially in regards to chemotherapy treatment. In concordance to this hypothesis, systemic genetic deletion of *Phd2* decreased drug toxicity and increased survival in mice, with $Phd2^{+/-}$ mice surviving for 20 days with doxorubicin treatment, versus a survival of only 5 days in WT mice. The authors found that the abnormal vasculature found in multiple cancer types is somewhat corrected in $Phd2^{+/-}$ mice, allowing more efficient delivery of anti-cancer drugs, at lower concentrations (Leite de Oliveira et al., 2012). It is possible, therefore, that *Phd2* inhibitors may hold a dual function in AML therapy, both eradicating LSCs, and enhancing the efficacy of chemotherapy. Using this chemotherapy model (Zuber et al., 2009), control (*rtTA)* and *shPhd2/rtTA* mice should be transplanted with *Meis1/Hoxa9* transformed *shPhd2/rtTA* and control cells, and treated with Dox, as well as chemotherapy. This will dissect the multiple roles of *Phd2* in AML therapy, and using the Dox-inducible system, investigate the efficacy of combined pharmacological *Phd2* inhibition with standard chemotherapy.

Notably, *Meis1* and *Hoxa9* as downstream effectors of MLL, serve as an accurate retroviral overexpression model of human AML, deriving from a stem-cell source, with significant self-renewal and clonogenic capacity. However, there are multiple other murine AML models, such as retroviral induction of MLL-AF9 and MLL-ENL translocations (described in (Somervaille et al., 2009)), as well as multiple MLL-AF9 transgenic mouse models, such as the Dox inducible *rtTA;*MLL-AF9 model engineered by the Schwaller laboratory (Stavropoulou et al., 2016). Notably, other groups studying the role of either HIF or PHD in AML have used other AML models, and these studies confirm our hypothesis and results (Leite de Oliveira et al., 2012; Velasco-Hernandez et al., 2014). However, it is important to explore other models of AML, as it is possible that current anti-leukaemogenic phenotypes resulting from Phd deletion are specific to *Meis1/Hoxa9* AML model.

Vukovic et al in 2015 provided evidence that deletion of both *Hif-1α* and *Hif-2α* increases leukaemic disease *in vivo*. As such, the initial hypothesis was that deletion of both *Phd1* and *Phd2,* stabilising both *Hif-1α* and *Hif-2α,* would have the most significant effect on AML. As shown in **Figures 5-3, 5-4, 5-5, 5-6 and 5-7**, deletion of both *Phd1* and *Phd2* has no additive effect on the reduction of leukaemic cell growth, colony formation, or engraftment and survival *in vivo.* From this result, it is possible that the effects shown in *Phd1* and *Phd2* in AML may be HIF-*α* independent, or stabilisation of one HIF-*α* isoform is sufficient. Western blot analysis should be performed to investigate HIF-stabilisation in $Phd1^{CKO}$, $Phd2^{CKO}$ and $Phd1/2^{CKO}$ cells, as well as RNA-seq analysis to identify if other HIF-*α* independent mechanisms are at play.

Overall, the results shown in this chapter demonstrate that *Phd1* and *Phd2* have significant roles in AML. Deletion of *Phd1* or *Phd2* results in decreased leukaemogenesis, through the reduction in LSC activity. Further genetic and pharmacological studies of *Phd1 and Phd2,* with special focus on human AML cell lines and samples, are essential to determine if *Phd1* and *Phd2* are valid as more general therapeutic targets in AML. Moreover, mechanistic studies are required to establish if these anti-leukaemic effects are HIF-*α* dependent or independent.

CHAPTER 6

Discussion

Chapter 6 Discussion

Normal and malignant haematopoiesis occur within the hypoxic environment of the BM niche. Following characterisation of the various components of this HSC niche, a number of studies focused the role and biological significance of the cell-cell interactions in this protective environment (Mendez-Ferrer et al., 2008; Morrison and Scadden, 2014). Seminal studies by Schofield in 1978 found that the hypoxic BM niche protects HSCs from exhaustion and DNA damage, by retaining them in a quiescent state. In addition, experiments by Dexter and colleagues in 1977 unveiled that BM stromal cells isolated from the HSC niche have a beneficial effect on HSPCs in long-term cultures *ex vivo.* Interestingly, the LSCs which drive leukaemic disease, have been shown to modulate their own BM niche. LSC-induced changes in the stroma are consistent with pro-survival and growth-stimulatory signals, theorised to contribute to their therapy resistance (Zhou et al., 2016). A recent paper by Cheloni and colleagues in 2017 found that leukaemic cell lines cultured in hypoxic conditions equivalent to those observed in the stem cell niche, had reduced levels of driver oncogenic proteins. Under these conditions, growth is impaired, and suggests that hypoxia may have an impact on LSC function (Giuntoli et al., 2007).

Following the discovery of the molecular mechanisms behind the cellular hypoxic response, there have been significant research efforts to investigate if this system plays any role in the regulation of haematopoiesis (Guitart et al., 2017; Guitart et al., 2013; Semenza, 2000; Takeda et al., 2008; Takeda et al., 2007; Vukovic et al., 2016). The cellular response to hypoxia is orchestrated by the master transcription factor HIF, which binds to the HRE (hypoxia response element) in over 200 genes, facilitating the adaption to low oxygen conditions. This hypoxia signalling pathway is controlled by the HIF-prolyl hydroxylase domain enzymes (PHDs), which under normoxic conditions hydroxylate specific proline residues on the HIF-α subunit, marking it for degradation (Epstein et al., 2001; Jaakkola et al., 2001; Masson et al., 2001).

Research papers published by the Kranc laboratory found that cell autonomous deletion of *Hif-1α, Hif-2α,* or both *Hif-1α* and *Hif-2α* had no effect on haematopoiesis in both steady state,

or transplantation-induced stress conditions (Guitart et al., 2013; Vukovic et al., 2015). Notably, when *Hif-1α* and *Hif-2α* were deleted in pre-LSCs, it was unveiled that HIFs had a strong tumour suppressive role in AML (Vukovic et al., 2015).

Given these results, and the emerging roles of hypoxia in HSC biology and AML, the general aim of this thesis was to investigate the role of the HIF-PHDs in normal and malignant hematopoiesis.

6.1 PHDs in normal haematopoiesis

Experiments in **Chapters 3 & 4** investigated the role of *Phd1* and *Phd2* in normal haematopoiesis using state-of-the-art transgenic mouse models. Opposing published research in the field (Takeda et al., 2007; Takeda et al, 2008; Singh et al., 2013), it was found that deletion of *Phd2* specifically within the haematopoietic system using *Vav-iCre* had no effect on the differentiated blood lineages or the HSPC compartment. Notably, previous research that found a fundamental role for *Phd2* in the haematopoietic system, used transgenic models which deleted *Phd2* either systemically, or in other tissues as well as the haematopoietic system. Given the role of stromal tissues within the hypoxic BM niche, this result it to be expected.

In addition to the *Vav-iCre* model, I also investigated the role of acute *Phd2* knockdown in haematopoiesis using Dox inducible *shPhd2/rtTA* transgenic mice. Here I found an altered differentiation compartment in the PB and BM of mice with reduced levels of *Phd2.* Additionally, within the HSPC compartment, systemic reduction of *Phd2* levels lead to a decrease in primitive haematopoietic cells, accompanied by an increase in the progenitor population. Given the systemic and acute nature of this gene knockdown experiment, it is possible that the protective HSC BM niche is altered by reduced *Phd2* levels, yielding a stress-like haematopoietic response, and thus HSC emergence.

Following this, as there was a notable effect of *Phd2* depletion in the HSC compartment, a transplantation experiment was performed with FACS isolated HSCs from *shPhd2/rtTA* and control mice. Under the stress of a transplantation assay, it was clear that the HSCs with a knockdown of *Phd2* were significantly less fit than their control counterparts. Due to the experimental design of this experiment, *Phd2* levels were only reduced in the transplanted HSCs, not systemically. This suggests that the stem cell compartment is affected both by acute systemic and cell-autonomous depletion of *Phd2.* This may be a result of *Phd1* or *Phd3* compensation in the hypoxia signalling pathway, or a HIF-independent affect.

Notably, this thesis unveiled an undiscovered role for *Phd1* in haematopoiesis. Ablation of *Phd1* within the haematopoietic system resulted in a significant decrease in BM cellularity. This phenotype was also shown in mice with deletion of both *Phd1* and *Phd2,* but not in mice with deletion of *Phd2* alone. Additionally, mice with deletion of both *Phd1* and *Phd2* had a dramatic expansion of the HSC compartment, which was not recorded in the single *Phd1* knockout or *Phd2* knockout mice. This suggests as cell-autonomous synergistic role between *Phd1* and *Phd2* in the HSC compartment.

6.2 PHDs in AML

Previous published research in the Kranc laboratory found that deletion of *Hif-1α* and *Hif-2α* accelerated AML disease in a *Meis1/Hoxa9* retroviral model of leukaemia (Vukovic et al., 2015). As such, in **Chapter 5** this thesis explored the effect of HIF-*α* stabilisation on AML through deletion of its inhibitor PHD.

Phd1^{CKO}, *Phd2*^{CKO} and *Phd1/2*^{CKO} pre-LSCs derived from *Meis1/Hoxa9* transformed foetal liver cells were tested for their proliferative and colony forming ability. These assays revealed that deletion of *Phd1, Phd2* or both *Phd1* and *Phd2,* reduces the potency of pre-LSCs, when compared to the control. Transplantation of these cells into lethally irradiated recipient mice resulted in a significant increase in disease latency.

To further dissect the role of *Phd2* in murine AML, I transformed foetal liver cells from *shPhd2/rtTA* and control embryos with *Meis/Hoxa9* viruses. This experimental model allowed for the depletion of *Phd2* levels at any point in the development or maintenance of AML. In concordance with the results shown in the conditional knockout experiments, acute reduction of *Phd2* levels resulted in a decrease in colony formation and an increase in disease latency *in vivo.* Given that acute deletion of *Phd2* reduces leukaemic burden, even in established disease, shows significant promise for the use pharmacological PHD inhibitors in AML.

6.3 Final conclusions and future directions

As described in this thesis, there is desperate need for new, targeted AML therapies. Whilst a large proportion of the field endeavours to target the genetic mutations and translocations that generate AML, others have hypothesised that current chemotherapies in conjunction with drugs that specifically target LSCs will reduce the risk of relapse, significantly improving the outcome for patients with AML (Kumar, 2011; Pollyea and Jordan, 2017).

Given the intimate relationship between HSC and LSC biology, it is essential that any therapeutic option must successfully eliminate LSCs, but does not harm the fundamental process of haematopoiesis. Here I describe that deletion of *Phd1, Phd2* or both has no significant detrimental effect on normal haematopoiesis, but does reduce leukaemic burden and extend survival in a retroviral model of AML. In addition to this encouraging data, evidence from the labs of Dr Mazzone and Prof Cammenga show that reduction of *Phd2* levels also improve the efficiency of chemotherapy, and alleviate some of the cytotoxic side effects. Furthermore, PHD inhibitors are already safely used in the clinic for diseases such as stroke, anaemia and chronic kidney disease (Haase et al., 2017; Ogle et al., 2012; Nangaku et al., 2007).

As such, there is a substantial case for further exploration into the therapeutic potential of PHDs in AML. RNA-seq analysis of $Phd1^{CKO}$, $Phd2^{CKO}$ and $Phd1/2^{CKO}$ pre-LSCs and LSCs will unveil the mechanism through which *Phd* deletion impacts LSC biology. Importantly, these experiments will also disclose if these encouraging phenotypes work through a HIF-dependent of HIF-independent mechanism. Given the heterogeneity of AML, it is vital to explore the role of PHDs in other transgenic AML mouse models, as well as human patient samples. Finally, other leukaemias and cancers such as CML, pancreatic cancer and glioblastoma are known to be driven by cancer stem cells, and reside in a hypoxic environment. As such, the therapeutic significance of PHDs may extend beyond AML, and have potential in multiple other forms of cancer (Holyoake and Vetrie, 2017; Lathia et al., 2015; Li et al.)

References

Abram, C.L., Roberge, G.L., Hu, Y., and Lowell, C.A. (2014). Comparative analysis of the efficiency and specificity of myeloid-Cre deleting strains using ROSA-EYFP reporter mice. Journal of immunological methods *408*, 89-100.

Abramson, S., Miller, R.G., and Phillips, R.A. (1977). The identification in adult bone marrow of pluripotent and restricted stem cells of the myeloid and lymphoid systems. J Exp Med *145*, 1567-1579.

Acar, M., Kocherlakota, K.S., Murphy, M.M., Peyer, J.G., Oguro, H., Inra, C.N., Jaiyeola, C., Zhao, Z., Luby-Phelps, K., and Morrison, S.J. (2015). Deep imaging of bone marrow shows non-dividing stem cells are mainly perisinusoidal. Nature *526*, 126-130.

Adolfsson, J., Borge, O.J., Bryder, D., Theilgaard-Monch, K., Astrand-Grundstrom, I., Sitnicka, E., Sasaki, Y., and Jacobsen, S.E. (2001). Upregulation of Flt3 expression within the bone marrow Lin(-)Sca1(+)c-kit(+) stem cell compartment is accompanied by loss of self-renewal capacity. Immunity *15*, 659-669.

Adolfsson, J., Mansson, R., Buza-Vidas, N., Hultquist, A., Liuba, K., Jensen, C.T., Bryder, D., Yang, L., Borge, O.J., Thoren, L.A.*, et al.* (2005). Identification of Flt3+ lympho-myeloid stem cells lacking erythro-megakaryocytic potential a revised road map for adult blood lineage commitment. Cell *121*, 295-306.

Alemany, A., Florescu, M., Baron, C.S., Peterson-Maduro, J., and van Oudenaarden, A. (2018). Whole-organism clone tracing using single-cell sequencing. Nature *556*, 108-112.

Alvarez-Silva, M., Belo-Diabangouaya, P., Salaun, J., and Dieterlen-Lievre, F. (2003). Mouse placenta is a major hematopoietic organ. Development (Cambridge, England) *130*, 5437-5444.

Andersen, S., Donnem, T., Stenvold, H., Al-Saad, S., Al-Shibli, K., Busund, L.T., and Bremnes, R.M. (2011). Overexpression of the HIF hydroxylases PHD1, PHD2, PHD3 and FIH are individually and collectively unfavorable prognosticators for NSCLC survival. PLoS One *6*, e23847.

Appelbaum, F.R., Gundacker, H., Head, D.R., Slovak, M.L., Willman, C.L., Godwin, J.E., Anderson, J.E., and Petersdorf, S.H. (2006). Age and acute myeloid leukemia. Blood *107*, 3481-3485.

Appelhoff, R.J., Tian, Y.M., Raval, R.R., Turley, H., Harris, A.L., Pugh, C.W., Ratcliffe, P.J., and Gleadle, J.M. (2004). Differential function of the prolyl hydroxylases PHD1, PHD2, and PHD3 in the regulation of hypoxia-inducible factor. J Biol Chem *279*, 38458-38465.

Arai, F., Hirao, A., Ohmura, M., Sato, H., Matsuoka, S., Takubo, K., Ito, K., Koh, G.Y., and Suda, T. (2004). Tie2/angiopoietin-1 signaling regulates hematopoietic stem cell quiescence in the bone marrow niche. Cell *118*, 149-161.

Arai, F., and Suda, T. (2007). Regulation of hematopoietic stem cells in the osteoblastic niche. Adv Exp Med Biol *602*, 61-67.

Argiropoulos, B., Yung, E., and Humphries, R.K. (2007). Unraveling the crucial roles of Meis1 in leukemogenesis and normal hematopoiesis. Genes Dev *21*, 2845-2849.

B'Chir, W., Maurin, A.C., Carraro, V., Averous, J., Jousse, C., Muranishi, Y., Parry, L., Stepien, G., Fafournoux, P., and Bruhat, A. (2013). The eIF2alpha/ATF4 pathway is essential for stress-induced autophagy gene expression. Nucleic Acids Res *41*, 7683-7699.

Barradas, J., Rodrigues, C.D., Ferreira, G., Rocha, P., Constanco, C., Andrade, M.R., Bento, C., and Silva, H.M. (2018). Congenital erythrocytosis - discover of a new mutation in the EGLN1 gene. Clinical case reports *6*, 1109-1111.

Begley, C.G., Aplan, P.D., Denning, S.M., Haynes, B.F., Waldmann, T.A., and Kirsch, I.R. (1989). The gene SCL is expressed during early hematopoiesis and encodes a differentiation-related DNA-binding motif. Proc Natl Acad Sci U S A *86*, 10128-10132.

Benveniste, P., Frelin, C., Janmohamed, S., Barbara, M., Herrington, R., Hyam, D., and Iscove, N.N. (2010). Intermediate-term hematopoietic stem cells with extended but time-limited reconstitution potential. Cell Stem Cell *6*, 48-58.

Bernard, O., Guglielmi, P., Jonveaux, P., Cherif, D., Gisselbrecht, S., Mauchauffe, M., Berger, R., Larsen, C.J., and Mathieu-Mahul, D. (1990). Two distinct mechanisms for the SCL gene activation in the t(1;14) translocation of T-cell leukemias. Genes Chromosomes Cancer *1*, 194-208.

Berra, E., Benizri, E., Ginouves, A., Volmat, V., Roux, D., and Pouyssegur, J. (2003). HIF prolyl-hydroxylase 2 is the key oxygen sensor setting low steady-state levels of HIF-1alpha in normoxia. EMBO J *22*, 4082-4090.

Blank, U., and Karlsson, S. (2015). TGF-beta signaling in the control of hematopoietic stem cells. Blood *125*, 3542-3550.

Bohensky, J., Shapiro, I.M., Leshinsky, S., Terkhorn, S.P., Adams, C.S., and Srinivas, V. (2007). HIF-1 regulation of chondrocyte apoptosis: induction of the autophagic pathway. Autophagy *3*, 207-214.

Bonnefoy-Berard, N., Munshi, A., Yron, I., Wu, S., Collins, T.L., Deckert, M., Shalom-Barak, T., Giampa, L., Herbert, E., Hernandez, J.*, et al.* (1996). Vav: function and regulation in hematopoietic cell signaling. Stem cells (Dayton, Ohio) *14*, 250-268.

Bose, P., and Konopleva, M.Y. (2018). ORY-1001: Overcoming the Differentiation Block in AML. Cancer Cell *33*, 342-343.

Boulais, P.E., and Frenette, P.S. (2015). Making sense of hematopoietic stem cell niches. Blood *125*, 2621-2629.

Briggs, J.A., Weinreb, C., Wagner, D.E., Megason, S., Peshkin, L., Kirschner, M.W., and Klein, A.M. (2018). The dynamics of gene expression in vertebrate embryogenesis at single-cell resolution. Science *360*.

Bruick, R.K., and McKnight, S.L. (2001). A conserved family of prolyl-4-hydroxylases that modify HIF. Science *294*, 1337-1340.

Bruns, I., Lucas, D., Pinho, S., Ahmed, J., Lambert, M.P., Kunisaki, Y., Scheiermann, C., Schiff, L., Poncz, M., Bergman, A.*, et al.* (2014). Megakaryocytes regulate hematopoietic stem cell quiescence through CXCL4 secretion. Nat Med *20*, 1315-1320.

Buenrostro, J.D., Corces, M.R., Lareau, C.A., Wu, B., Schep, A.N., Aryee, M.J., Majeti, R., Chang, H.Y., and Greenleaf, W.J. (2018). Integrated Single-Cell Analysis Maps the Continuous Regulatory Landscape of Human Hematopoietic Differentiation. Cell *173*, 1535-1548.e1516.

Bur, H., Haapasaari, K.M., Turpeenniemi-Hujanen, T., Kuittinen, O., Auvinen, P., Marin, K., Soini, Y., and Karihtala, P. (2018). Strong Prolyl Hydroxylase Domain 1 Expression Predicts

Poor Outcome in Radiotherapy-treated Patients with Classical Hodgkin's Lymphoma. Anticancer research *38*, 329-336.

Busch, K., Klapproth, K., Barile, M., Flossdorf, M., Holland-Letz, T., Schlenner, S.M., Reth, M., Hofer, T., and Rodewald, H.R. (2015). Fundamental properties of unperturbed haematopoiesis from stem cells in vivo. Nature *518*, 542-546.

Cabezas-Wallscheid, N., Klimmeck, D., Hansson, J., Lipka, D.B., Reyes, A., Wang, Q., Weichenhan, D., Lier, A., von Paleske, L., Renders, S.*, et al.* (2014). Identification of regulatory networks in HSCs and their immediate progeny via integrated proteome, transcriptome, and DNA methylome analysis. Cell Stem Cell *15*, 507-522.

Calvi, L.M., Adams, G.B., Weibrecht, K.W., Weber, J.M., Olson, D.P., Knight, M.C., Martin, R.P., Schipani, E., Divieti, P., Bringhurst, F.R.*, et al.* (2003). Osteoblastic cells regulate the haematopoietic stem cell niche. Nature *425*, 841-846.

Chan, D.A., Kawahara, T.L., Sutphin, P.D., Chang, H.Y., Chi, J.T., and Giaccia, A.J. (2009). Tumor vasculature is regulated by PHD2-mediated angiogenesis and bone marrow-derived cell recruitment. Cancer Cell *15*, 527-538.

Cheloni, G., Poteti, M., Bono, S., Masala, E., Mazure, N.M., Rovida, E., Lulli, M., and Dello Sbarba, P. (2017). The Leukemic Stem Cell Niche: Adaptation to "Hypoxia" versus Oncogene Addiction. Stem cells international *2017*, 4979474.

Chen, M.J., Yokomizo, T., Zeigler, B.M., Dzierzak, E., and Speck, N.A. (2009). Runx1 is required for the endothelial to haematopoietic cell transition but not thereafter. Nature *457*, 887-891.

Chow, D.C., Wenning, L.A., Miller, W.M., and Papoutsakis, E.T. (2001). Modeling pO(2) distributions in the bone marrow hematopoietic compartment. I. Krogh's model. Biophysical journal *81*, 675-684.

Chowdhury, R., Candela-Lena, J.I., Chan, M.C., Greenald, D.J., Yeoh, K.K., Tian, Y.M., McDonough, M.A., Tumber, A., Rose, N.R., Conejo-Garcia, A.*, et al.* (2013). Selective small molecule probes for the hypoxia inducible factor (HIF) prolyl hydroxylases. ACS chemical biology *8*, 1488-1496.

Clapp, D.W., Freie, B., Lee, W.H., and Zhang, Y.Y. (1995). Molecular evidence that in situ-transduced fetal liver hematopoietic stem/progenitor cells give rise to medullary hematopoiesis in adult rats. Blood *86*, 2113-2122.

Clevers, H. (2005). Stem cells, asymmetric division and cancer. Nature genetics *37*, 1027-1028.

Copley, M.R., Beer, P.A., and Eaves, C.J. (2012). Hematopoietic stem cell heterogeneity takes center stage. Cell Stem Cell *10*, 690-697.

Cozzio, A., Passegué, E., Ayton, P.M., Karsunky, H., Cleary, M.L., and Weissman, I.L. (2003). Similar MLL-associated leukemias arising from self-renewing stem cells and short-lived myeloid progenitors. Genes Dev *17*, 3029-3035.

Cummins, E.P., Berra, E., Comerford, K.M., Ginouves, A., Fitzgerald, K.T., Seeballuck, F., Godson, C., Nielsen, J.E., Moynagh, P., Pouyssegur, J.*, et al.* (2006). Prolyl hydroxylase-1 negatively regulates IkappaB kinase-beta, giving insight into hypoxia-induced NFkappaB activity. Proc Natl Acad Sci U S A *103*, 18154-18159.

Danet, G.H., Pan, Y., Luongo, J.L., Bonnet, D.A., and Simon, M.C. (2003). Expansion of human SCID-repopulating cells under hypoxic conditions. J Clin Invest *112*, 126-135.

de Boer, J., Williams, A., Skavdis, G., Harker, N., Coles, M., Tolaini, M., Norton, T., Williams, K., Roderick, K., Potocnik, A.J.*, et al.* (2003). Transgenic mice with hematopoietic and lymphoid specific expression of Cre. European journal of immunology *33*, 314-325.

Deguchi, K., Yagi, H., Inada, M., Yoshizaki, K., Kishimoto, T., and Komori, T. (1999). Excessive extramedullary hematopoiesis in Cbfa1-deficient mice with a congenital lack of bone marrow. Biochem Biophys Res Commun *255*, 352-359.

Dexter, T.M., Wright, E.G., Krizsa, F., and Lajtha, L.G. (1977). Regulation of haemopoietic stem cell proliferation in long term bone marrow cultures. Biomedicine / [publiee pour l'AAICIG] *27*, 344-349.

Dick, J.E. (2003). Breast cancer stem cells revealed. Proc Natl Acad Sci U S A *100*, 3547-3549.

Ding, L., Saunders, T.L., Enikolopov, G., and Morrison, S.J. (2012). Endothelial and perivascular cells maintain haematopoietic stem cells. Nature *481*, 457-462.

Doe, C.Q., and Bowerman, B. (2001). Asymmetric cell division: fly neuroblast meets worm zygote. Current opinion in cell biology *13*, 68-75.

Dohner, H., Estey, E.H., Amadori, S., Appelbaum, F.R., Buchner, T., Burnett, A.K., Dombret, H., Fenaux, P., Grimwade, D., Larson, R.A.*, et al.* (2010). Diagnosis and management of acute myeloid leukemia in adults: recommendations from an international expert panel, on behalf of the European LeukemiaNet. Blood *115*, 453-474.

Domen, J., Cheshier, S.H., and Weissman, I.L. (2000). The role of apoptosis in the regulation of hematopoietic stem cells: Overexpression of Bcl-2 increases both their number and repopulation potential. J Exp Med *191*, 253-264.

Doulatov, S., Notta, F., Laurenti, E., and Dick, J.E. (2012). Hematopoiesis: a human perspective. Cell Stem Cell *10*, 120-136.

Dow, L.E., Premsrirut, P.K., Zuber, J., Fellmann, C., McJunkin, K., Miething, C., Park, Y., Dickins, R.A., Hannon, G.J., and Lowe, S.W. (2012). A pipeline for the generation of shRNA transgenic mice. Nature protocols *7*, 374-393.

Draenert, K., and Draenert, Y. (1980). The vascular system of bone marrow. Scanning electron microscopy, 113-122.

Duran, R.V., MacKenzie, E.D., Boulahbel, H., Frezza, C., Heiserich, L., Tardito, S., Bussolati, O., Rocha, S., Hall, M.N., and Gottlieb, E. (2013). HIF-independent role of prolyl hydroxylases in the cellular response to amino acids. Oncogene *32*, 4549-4556.

Elvidge, G.P., Glenny, L., Appelhoff, R.J., Ratcliffe, P.J., Ragoussis, J., and Gleadle, J.M. (2006). Concordant regulation of gene expression by hypoxia and 2-oxoglutarate-dependent dioxygenase inhibition: the role of HIF-1alpha, HIF-2alpha, and other pathways. J Biol Chem *281*, 15215-15226.

Ema, H., Morita, Y., and Suda, T. (2014). Heterogeneity and hierarchy of hematopoietic stem cells. Exp Hematol *42*, 74-82.e72.

Eppert, K., Takenaka, K., Lechman, E.R., Waldron, L., Nilsson, B., van Galen, P., Metzeler, K.H., Poeppl, A., Ling, V., Beyene, J.*, et al.* (2011). Stem cell gene expression programs influence clinical outcome in human leukemia. Nat Med *17*, 1086-1093.

Epstein, A.C., Gleadle, J.M., McNeill, L.A., Hewitson, K.S., O'Rourke, J., Mole, D.R., Mukherji, M., Metzen, E., Wilson, M.I., Dhanda, A.*, et al.* (2001). C. elegans EGL-9 and mammalian homologs define a family of dioxygenases that regulate HIF by prolyl hydroxylation. Cell *107*, 43-54.

Essers, M.A., Offner, S., Blanco-Bose, W.E., Waibler, Z., Kalinke, U., Duchosal, M.A., and Trumpp, A. (2009). IFNalpha activates dormant haematopoietic stem cells in vivo. Nature *458*, 904-908.

Fan, L., Li, J., Yu, Z., Dang, X., and Wang, K. (2014). The hypoxia-inducible factor pathway, prolyl hydroxylase domain protein inhibitors, and their roles in bone repair and regeneration. Biomed Res Int *2014*, 239356.

Farrell, J.A., Wang, Y., Riesenfeld, S.J., Shekhar, K., Regev, A., and Schier, A.F. (2018). Single-cell reconstruction of developmental trajectories during zebrafish embryogenesis. Science *360*.

Ferraro, F., Celso, C.L., and Scadden, D. (2010). Adult stem cels and their niches. Adv Exp Med Biol *695*, 155-168.

Fong, G.H., and Takeda, K. (2008). Role and regulation of prolyl hydroxylase domain proteins. Cell Death Differ *15*, 635-641.

Forsberg, E.C., Serwold, T., Kogan, S., Weissman, I.L., and Passegue, E. (2006). New evidence supporting megakaryocyte-erythrocyte potential of flk2/flt3+ multipotent hematopoietic progenitors. Cell *126*, 415-426.

Franke, K., Gassmann, M., and Wielockx, B. (2013). Erythrocytosis: the HIF pathway in control. Blood *122*, 1122-1128.

Frei, C., and Edgar, B.A. (2004). Drosophila cyclin D/Cdk4 requires Hif-1 prolyl hydroxylase to drive cell growth. Developmental cell *6*, 241-251.

Frei, C., Galloni, M., Hafen, E., and Edgar, B.A. (2005). The Drosophila mitochondrial ribosomal protein mRpL12 is required for Cyclin D/Cdk4-driven growth. Embo j *24*, 623-634.

Fu, J., Menzies, K., Freeman, R.S., and Taubman, M.B. (2007). EGLN3 prolyl hydroxylase regulates skeletal muscle differentiation and myogenin protein stability. J Biol Chem *282*, 12410-12418.

Gekas, C., Dieterlen-Lievre, F., Orkin, S.H., and Mikkola, H.K. (2005). The placenta is a niche for hematopoietic stem cells. Developmental cell *8*, 365-375.

German, N.J., Yoon, H., Yusuf, R.Z., Murphy, J.P., Finley, L.W., Laurent, G., Haas, W., Satterstrom, F.K., Guarnerio, J., Zaganjor, E.*, et al.* (2016). PHD3 Loss in Cancer Enables Metabolic Reliance on Fatty Acid Oxidation via Deactivation of ACC2. Molecular cell *63*, 1006-1020.

Gezer, D., Vukovic, M., Soga, T., Pollard, P.J., and Kranc, K.R. (2014). Concise review: genetic dissection of hypoxia signaling pathways in normal and leukemic stem cells. Stem cells (Dayton, Ohio) *32*, 1390-1397.

Giuntoli, S., Rovida, E., Gozzini, A., Barbetti, V., Cipolleschi, M.G., Olivotto, M., and Dello Sbarba, P. (2007). Severe hypoxia defines heterogeneity and selects highly immature progenitors within clonal erythroleukemia cells. Stem cells (Dayton, Ohio) *25*, 1119-1125.

Goardon, N., Marchi, E., Atzberger, A., Quek, L., Schuh, A., Soneji, S., Woll, P., Mead, A., Alford, K.A., Rout, R.*, et al.* (2011). Coexistence of LMPP-like and GMP-like leukemia stem cells in acute myeloid leukemia. Cancer Cell *19*, 138-152.

Goldberg, M.A., Dunning, S.P., and Bunn, H.F. (1988). Regulation of the erythropoietin gene: evidence that the oxygen sensor is a heme protein. Science *242*, 1412-1415.

Goldie, J.H., and Coldman, A.J. (1984). The genetic origin of drug resistance in neoplasms: implications for systemic therapy. Cancer Res *44*, 3643-3653.

Goodell, M.A., Brose, K., Paradis, G., Conner, A.S., and Mulligan, R.C. (1996). Isolation and functional properties of murine hematopoietic stem cells that are replicating in vivo. J Exp Med *183*, 1797-1806.

Gottgens, B. (2015). Regulatory network control of blood stem cells. Blood *125*, 2614-2620.

Gough, P.J., Gordon, S., and Greaves, D.R. (2001). The use of human CD68 transcriptional regulatory sequences to direct high-level expression of class A scavenger receptor in macrophages in vitro and in vivo. Immunology *103*, 351-361.

Greenbaum, A., Hsu, Y.M., Day, R.B., Schuettpelz, L.G., Christopher, M.J., Borgerding, J.N., Nagasawa, T., and Link, D.C. (2013). CXCL12 in early mesenchymal progenitors is required for haematopoietic stem-cell maintenance. Nature *495*, 227-230.

Greijer, A.E., van der Groep, P., Kemming, D., Shvarts, A., Semenza, G.L., Meijer, G.A., van de Wiel, M.A., Belien, J.A., van Diest, P.J., and van der Wall, E. (2005). Up-regulation of gene expression by hypoxia is mediated predominantly by hypoxia-inducible factor 1 (HIF-1). J Pathol *206*, 291-304.

Guinn, B.A., Tobal, K., and Mills, K.I. (2007). Comparison of the survival implications of tumour-associated versus cancer-testis antigen expression in acute myeloid leukaemia. Br J Haematol *136*, 510-512.

Guitart, A.V., Panagopoulou, T.I., Villacreces, A., Vukovic, M., Sepulveda, C., Allen, L., Carter, R.N., van de Lagemaat, L.N., Morgan, M., Giles, P.*, et al.* (2017). Fumarate hydratase is a critical metabolic regulator of hematopoietic stem cell functions. J Exp Med *214*, 719-735.

Guitart, A.V., Subramani, C., Armesilla-Diaz, A., Smith, G., Sepulveda, C., Gezer, D., Vukovic, M., Dunn, K., Pollard, P., Holyoake, T.L.*, et al.* (2013). Hif-2alpha is not essential for cell-autonomous hematopoietic stem cell maintenance. Blood *122*, 1741-1745.

Gupta, P., Gurudutta, G.U., Saluja, D., and Tripathi, R.P. (2009). PU.1 and partners: regulation of haematopoietic stem cell fate in normal and malignant haematopoiesis. Journal of cellular and molecular medicine *13*, 4349-4363.

Haase, V.H. (2017). Therapeutic targeting of the HIF oxygen-sensing pathway: Lessons learned from clinical studies. Experimental cell research *356*, 160-165.

Haferlach, T., Kohlmann, A., Wieczorek, L., Basso, G., Kronnie, G.T., Béné, M.C., De Vos, J., Hernández, J.M., Hofmann, W.K., Mills, K.I.*, et al.* (2010). Clinical utility of microarray-based gene expression profiling in the diagnosis and subclassification of leukemia: report from the International Microarray Innovations in Leukemia Study Group. J Clin Oncol *28*, 2529-2537.

Hancock, R.L., Dunne, K., Walport, L.J., Flashman, E., and Kawamura, A. (2015). Epigenetic regulation by histone demethylases in hypoxia. Epigenomics *7*, 791-811.

Harris, A.L. (2002). Hypoxia--a key regulatory factor in tumour growth. Nature reviews Cancer *2*, 38-47.

Heimfeld, S., and Weissman, I.L. (1991). Development of mouse hematopoietic lineages. Current topics in developmental biology *25*, 155-175.

Hermitte, F., Brunet de la Grange, P., Belloc, F., Praloran, V., and Ivanovic, Z. (2006). Very low O2 concentration (0.1%) favors G0 return of dividing CD34+ cells. Stem cells (Dayton, Ohio) *24*, 65-73.

Hewitson, K.S., Lienard, B.M., McDonough, M.A., Clifton, I.J., Butler, D., Soares, A.S., Oldham, N.J., McNeill, L.A., and Schofield, C.J. (2007). Structural and mechanistic studies on the inhibition of the hypoxia-inducible transcription factor hydroxylases by tricarboxylic acid cycle intermediates. J Biol Chem *282*, 3293-3301.

Hirsila, M., Koivunen, P., Xu, L., Seeley, T., Kivirikko, K.I., and Myllyharju, J. (2005). Effect of desferrioxamine and metals on the hydroxylases in the oxygen sensing pathway. FASEB journal : official publication of the Federation of American Societies for Experimental Biology *19*, 1308-1310.

Hiwatashi, Y., Kanno, K., Takasaki, C., Goryo, K., Sato, T., Torii, S., Sogawa, K., and Yasumoto, K. (2011). PHD1 interacts with ATF4 and negatively regulates its transcriptional activity without prolyl hydroxylation. Experimental cell research *317*, 2789-2799.

Holyoake, T.L., and Vetrie, D. (2017). The chronic myeloid leukemia stem cell: stemming the tide of persistence. Blood *129*, 1595-1606.

Hu, Y., and Smyth, G.K. (2009). ELDA: extreme limiting dilution analysis for comparing depleted and enriched populations in stem cell and other assays. Journal of immunological methods *347*, 70-78.

Ikuta, K., and Weissman, I.L. (1992). Evidence that hematopoietic stem cells express mouse c-kit but do not depend on steel factor for their generation. Proc Natl Acad Sci U S A *89*, 1502-1506.

Ishikawa, F., Yoshida, S., Saito, Y., Hijikata, A., Kitamura, H., Tanaka, S., Nakamura, R., Tanaka, T., Tomiyama, H., Saito, N.*, et al.* (2007). Chemotherapy-resistant human AML stem cells home to and engraft within the bone-marrow endosteal region. Nat Biotechnol *25*, 1315-1321.

Ivan, M., Kondo, K., Yang, H., Kim, W., Valiando, J., Ohh, M., Salic, A., Asara, J.M., Lane, W.S., and Kaelin, W.G., Jr. (2001). HIFalpha targeted for VHL-mediated destruction by proline hydroxylation: implications for O2 sensing. Science *292*, 464-468.

Jaakkola, P., Mole, D.R., Tian, Y.M., Wilson, M.I., Gielbert, J., Gaskell, S.J., von Kriegsheim, A., Hebestreit, H.F., Mukherji, M., Schofield, C.J.*, et al.* (2001). Targeting of HIF-alpha to the von Hippel-Lindau ubiquitylation complex by O2-regulated prolyl hydroxylation. Science *292*, 468-472.

Jacobson, L.O., Simmons, E.L., Marks, E.K., and Eldredge, J.H. (1951). Recovery from radiation injury. Science *113*, 510-511.

Jang, Y.Y., and Sharkis, S.J. (2007). A low level of reactive oxygen species selects for primitive hematopoietic stem cells that may reside in the low-oxygenic niche. Blood *110*, 3056-3063.

Joharapurkar, A.A., Pandya, V.B., Patel, V.J., Desai, R.C., and Jain, M.R. (2018). Prolyl Hydroxylase Inhibitors: A Breakthrough in the Therapy of Anemia Associated with Chronic Diseases. Journal of medicinal chemistry *61*, 6964-6982.

Johnson, G.R., and Moore, M.A. (1975). Role of stem cell migration in initiation of mouse foetal liver haemopoiesis. Nature *258*, 726-728.

Jokilehto, T., and Jaakkola, P.M. (2010). The role of HIF prolyl hydroxylases in tumour growth. Journal of cellular and molecular medicine *14*, 758-770.

Jung, Y., Wang, J., Schneider, A., Sun, Y.X., Koh-Paige, A.J., Osman, N.I., McCauley, L.K., and Taichman, R.S. (2006). Regulation of SDF-1 (CXCL12) production by osteoblasts; a possible mechanism for stem cell homing. Bone *38*, 497-508.

Kadrmas, J.L., and Beckerle, M.C. (2004). The LIM domain: from the cytoskeleton to the nucleus. Nature reviews Molecular cell biology *5*, 920-931.

Kaelin, W.G., Jr., and Ratcliffe, P.J. (2008). Oxygen sensing by metazoans: the central role of the HIF hydroxylase pathway. Molecular cell *30*, 393-402.

Katayama, Y., Hidalgo, A., Furie, B.C., Vestweber, D., Furie, B., and Frenette, P.S. (2003). PSGL-1 participates in E-selectin-mediated progenitor homing to bone marrow: evidence for cooperation between E-selectin ligands and alpha4 integrin. Blood *102*, 2060-2067.

Kato, H., Inoue, T., Asanoma, K., Nishimura, C., Matsuda, T., and Wake, N. (2006). Induction of human endometrial cancer cell senescence through modulation of HIF-1alpha activity by EGLN1. Int J Cancer *118*, 1144-1153.

Katzav, S., Martin-Zanca, D., and Barbacid, M. (1989). vav, a novel human oncogene derived from a locus ubiquitously expressed in hematopoietic cells. Embo j *8*, 2283-2290.

Khwaja, A., Bjorkholm, M., Gale, R.E., Levine, R.L., Jordan, C.T., Ehninger, G., Bloomfield, C.D., Estey, E., Burnett, A., Cornelissen, J.J*., et al.* (2016). Acute myeloid leukaemia. Nature reviews Disease primers *2*, 16010.

Kiel, M.J., Yilmaz, O.H., Iwashita, T., Yilmaz, O.H., Terhorst, C., and Morrison, S.J. (2005). SLAM family receptors distinguish hematopoietic stem and progenitor cells and reveal endothelial niches for stem cells. Cell *121*, 1109-1121.

Kim, I., He, S., Yilmaz, O.H., Kiel, M.J., and Morrison, S.J. (2006). Enhanced purification of fetal liver hematopoietic stem cells using SLAM family receptors. Blood *108*, 737-744.

Kingston, R.E., Chen, C.A., and Okayama, H. (2003). Calcium phosphate transfection. Curr Protoc Cell Biol *Chapter 20*, Unit 20 23.

Koditz, J., Nesper, J., Wottawa, M., Stiehl, D.P., Camenisch, G., Franke, C., Myllyharju, J., Wenger, R.H., and Katschinski, D.M. (2007). Oxygen-dependent ATF-4 stability is mediated by the PHD3 oxygen sensor. Blood *110*, 3610-3617.

Koivunen, P., Tiainen, P., Hyvarinen, J., Williams, K.E., Sormunen, R., Klaus, S.J., Kivirikko, K.I., and Myllyharju, J. (2007). An endoplasmic reticulum transmembrane prolyl 4-hydroxylase is induced by hypoxia and acts on hypoxia-inducible factor alpha. J Biol Chem *282*, 30544-30552.

Kondo, M., Weissman, I.L., and Akashi, K. (1997). Identification of clonogenic common lymphoid progenitors in mouse bone marrow. Cell *91*, 661-672.

Kranc, K.R., Schepers, H., Rodrigues, N.P., Bamforth, S., Villadsen, E., Ferry, H., Bouriez-Jones, T., Sigvardsson, M., Bhattacharya, S., Jacobsen, S.E.*, et al.* (2009). Cited2 is an essential regulator of adult hematopoietic stem cells. Cell Stem Cell *5*, 659-665.

Krivtsov, A.V., Figueroa, M.E., Sinha, A.U., Stubbs, M.C., Feng, Z., Valk, P.J., Delwel, R., Dohner, K., Bullinger, L., Kung, A.L.*, et al.* (2013). Cell of origin determines clinically relevant subtypes of MLL-rearranged AML. Leukemia *27*, 852-860.

Krivtsov, A.V., Twomey, D., Feng, Z., Stubbs, M.C., Wang, Y., Faber, J., Levine, J.E., Wang, J., Hahn, W.C., Gilliland, D.G.*, et al.* (2006). Transformation from committed progenitor to leukaemia stem cell initiated by MLL-AF9. Nature *442*, 818-822.

Kroon, E., Krosl, J., Thorsteinsdottir, U., Baban, S., Buchberg, A.M., and Sauvageau, G. (1998). Hoxa9 transforms primary bone marrow cells through specific collaboration with Meis1a but not Pbx1b. EMBO J *17*, 3714-3725.

Kumar, C.C. (2011). Genetic abnormalities and challenges in the treatment of acute myeloid leukemia. Genes & cancer *2*, 95-107.

Kumaravelu, P., Hook, L., Morrison, A.M., Ure, J., Zhao, S., Zuyev, S., Ansell, J., and Medvinsky, A. (2002). Quantitative developmental anatomy of definitive haematopoietic stem cells/long-term repopulating units (HSC/RUs): role of the aorta-gonad-mesonephros (AGM) region and the yolk sac in colonisation of the mouse embryonic liver. Development (Cambridge, England) *129*, 4891-4899.

Kunisaki, Y., Bruns, I., Scheiermann, C., Ahmed, J., Pinho, S., Zhang, D., Mizoguchi, T., Wei, Q., Lucas, D., Ito, K.*, et al.* (2013). Arteriolar niches maintain haematopoietic stem cell quiescence. Nature *502*, 637-643.

Kunisato, A., Chiba, S., Saito, T., Kumano, K., Nakagami-Yamaguchi, E., Yamaguchi, T., and Hirai, H. (2004). Stem cell leukemia protein directs hematopoietic stem cell fate. Blood *103*, 3336-3341.

Labaj, W., Papiez, A., Polanski, A., and Polanska, J. (2017). Comprehensive Analysis of MILE Gene Expression Data Set Advances Discovery of Leukaemia Type and Subtype Biomarkers. Interdisciplinary sciences, computational life sciences *9*, 24-35.

Laslo, P., Spooner, C.J., Warmflash, A., Lancki, D.W., Lee, H.J., Sciammas, R., Gantner, B.N., Dinner, A.R., and Singh, H. (2006). Multilineage transcriptional priming and determination of alternate hematopoietic cell fates. Cell *126*, 755-766.

Lathia, J.D., Mack, S.C., Mulkearns-Hubert, E.E., Valentim, C.L., and Rich, J.N. (2015). Cancer stem cells in glioblastoma. Genes Dev *29*, 1203-1217.

Laurenti, E., and Gottgens, B. (2018). From haematopoietic stem cells to complex differentiation landscapes. Nature *553*, 418-426.

Lavau, C., Szilvassy, S.J., Slany, R., and Cleary, M.L. (1997). Immortalization and leukemic transformation of a myelomonocytic precursor by retrovirally transduced HRX-ENL. Embo j *16*, 4226-4237.

Lee, S., Nakamura, E., Yang, H., Wei, W., Linggi, M.S., Sajan, M.P., Farese, R.V., Freeman, R.S., Carter, B.D., Kaelin, W.G., Jr.*, et al.* (2005). Neuronal apoptosis linked to EglN3 prolyl hydroxylase and familial pheochromocytoma genes: developmental culling and cancer. Cancer Cell *8*, 155-167.

Leite de Oliveira, R., Deschoemaeker, S., Henze, A.T., Debackere, K., Finisguerra, V., Takeda, Y., Roncal, C., Dettori, D., Tack, E., Jonsson, Y.*, et al.* (2012). Gene-targeting of Phd2 improves tumor response to chemotherapy and prevents side-toxicity. Cancer Cell *22*, 263-277.

Lemischka, I.R., Raulet, D.H., and Mulligan, R.C. (1986). Developmental potential and dynamic behavior of hematopoietic stem cells. Cell *45*, 917-927.

Lessard, J., and Sauvageau, G. (2003). Polycomb group genes as epigenetic regulators of normal and leukemic hemopoiesis. Exp Hematol *31*, 567-585.

Li, C., Heidt, D.G., Dalerba, P., Burant, C.F., Zhang, L., Adsay, V., Wicha, M., Clarke, M.F., and Simeone, D.M.

Li, C.L., and Johnson, G.R. (1995). Murine hematopoietic stem and progenitor cells: I. Enrichment and biologic characterization. Blood *85*, 1472-1479.

Lieb, M.E., Menzies, K., Moschella, M.C., Ni, R., and Taubman, M.B. (2002). Mammalian EGLN genes have distinct patterns of mRNA expression and regulation. Biochemistry and cell biology = Biochimie et biologie cellulaire *80*, 421-426.

Ling, K.W., Ottersbach, K., van Hamburg, J.P., Oziemlak, A., Tsai, F.Y., Orkin, S.H., Ploemacher, R., Hendriks, R.W., and Dzierzak, E. (2004). GATA-2 plays two functionally distinct roles during the ontogeny of hematopoietic stem cells. J Exp Med *200*, 871-882.

Liu, B., Yang, R., Wong, K.A., Getman, C., Stein, N., Teitell, M.A., Cheng, G., Wu, H., and Shuai, K. (2005). Negative regulation of NF-kappaB signaling by PIAS1. Molecular and cellular biology *25*, 1113-1123.

Lo, C.C., Wu, J.W., and Lin, C.P. In vivo imaging of hematopoietic stem cells and their microenvironment.

Lo Celso, C., Wu, J.W., and Lin, C.P. (2009). In vivo imaging of hematopoietic stem cells and their microenvironment. Journal of biophotonics *2*, 619-631.

Lorenz, E., Uphoff, D., Reid, T.R., and Shelton, E. (1951). Modification of irradiation injury in mice and guinea pigs by bone marrow injections. Journal of the National Cancer Institute *12*, 197-201.

Lowenberg, B., Downing, J.R., and Burnett, A. (1999). Acute myeloid leukemia. N Engl J Med *341*, 1051-1062.

Mansson, R., Hultquist, A., Luc, S., Yang, L., Anderson, K., Kharazi, S., Al-Hashmi, S., Liuba, K., Thoren, L., Adolfsson, J.*, et al.* (2007). Molecular evidence for hierarchical transcriptional lineage priming in fetal and adult stem cells and multipotent progenitors. Immunity *26*, 407-419.

Markolovic, S., Wilkins, S.E., and Schofield, C.J. (2015). Protein Hydroxylation Catalyzed by 2-Oxoglutarate-dependent Oxygenases. J Biol Chem *290*, 20712-20722.

Masson, N., and Ratcliffe, P.J. (2003). HIF prolyl and asparaginyl hydroxylases in the biological response to intracellular O(2) levels. Journal of cell science *116*, 3041-3049.

Masson, N., Willam, C., Maxwell, P.H., Pugh, C.W., and Ratcliffe, P.J. (2001). Independent function of two destruction domains in hypoxia-inducible factor-alpha chains activated by prolyl hydroxylation. Embo j *20*, 5197-5206.

Maxwell, P.H., Wiesener, M.S., Chang, G.W., Clifford, S.C., Vaux, E.C., Cockman, M.E., Wykoff, C.C., Pugh, C.W., Maher, E.R., and Ratcliffe, P.J. (1999). The tumour suppressor protein VHL targets hypoxia-inducible factors for oxygen-dependent proteolysis. Nature *399*, 271-275.

Mazzone, M., Dettori, D., de Oliveira, R.L., Loges, S., Schmidt, T., Jonckx, B., Tian, Y.M., Lanahan, A.A., Pollard, P., de Almodovar, C.R.*, et al.* (2009). Heterozygous deficiency of PHD2 restores tumor oxygenation and inhibits metastasis via endothelial normalization. Cell *136*, 839-851.

McMahon, K.A., Hiew, S.Y., Hadjur, S., Veiga-Fernandes, H., Menzel, U., Price, A.J., Kioussis, D., Williams, O., and Brady, H.J. (2007). Mll has a critical role in fetal and adult hematopoietic stem cell self-renewal. Cell Stem Cell *1*, 338-345.

Medvinsky, A., and Dzierzak, E. (1996). Definitive hematopoiesis is autonomously initiated by the AGM region. Cell *86*, 897-906.

Mendelson, A., and Frenette, P.S. (2014). Hematopoietic stem cell niche maintenance during homeostasis and regeneration. Nat Med *20*, 833-846.

Mendez-Ferrer, S., Lucas, D., Battista, M., and Frenette, P.S. (2008). Haematopoietic stem cell release is regulated by circadian oscillations. Nature *452*, 442-447.

Metzeler, K.H., Herold, T., Rothenberg-Thurley, M., Amler, S., Sauerland, M.C., Gorlich, D., Schneider, S., Konstandin, N.P., Dufour, A., Braundl, K.*, et al.* (2016). Spectrum and prognostic relevance of driver gene mutations in acute myeloid leukemia. Blood *128*, 686-698.

Milne, T.A., Briggs, S.D., Brock, H.W., Martin, M.E., Gibbs, D., Allis, C.D., and Hess, J.L. (2002). MLL targets SET domain methyltransferase activity to Hox gene promoters. Molecular cell *10*, 1107-1117.

Milyavsky, M., Gan, O.I., Trottier, M., Komosa, M., Tabach, O., Notta, F., Lechman, E., Hermans, K.G., Eppert, K., Konovalova, Z.*, et al.* (2010). A distinctive DNA damage response in human hematopoietic stem cells reveals an apoptosis-independent role for p53 in self-renewal. Cell Stem Cell *7*, 186-197.

Minamishima, Y.A., Moslehi, J., Bardeesy, N., Cullen, D., Bronson, R.T., and Kaelin, W.G., Jr. (2008). Somatic inactivation of the PHD2 prolyl hydroxylase causes polycythemia and congestive heart failure. Blood *111*, 3236-3244.

Mohrin, M., Bourke, E., Alexander, D., Warr, M.R., Barry-Holson, K., Le Beau, M.M., Morrison, C.G., and Passegué, E. (2010). Hematopoietic stem cell quiescence promotes error-prone DNA repair and mutagenesis. Cell Stem Cell *7*, 174-185.

Mole, D.R., Blancher, C., Copley, R.R., Pollard, P.J., Gleadle, J.M., Ragoussis, J., and Ratcliffe, P.J. (2009). Genome-wide association of hypoxia-inducible factor (HIF)-1alpha and HIF-2alpha DNA binding with expression profiling of hypoxia-inducible transcripts. J Biol Chem *284*, 16767-16775.

Moore, M.A., Williams, N., and Metcalf, D. (1972). Purification and characterisation of the in vitro colony forming cell in monkey hemopoietic tissue. Journal of cellular physiology *79*, 283-292.

Morgado, E., Albouhair, S., and Lavau, C. (2007). Flt3 is dispensable to the Hoxa9/Meis1 leukemogenic cooperation. Blood *109*, 4020-4022.

Morita, Y., Ema, H., and Nakauchi, H. (2010). Heterogeneity and hierarchy within the most primitive hematopoietic stem cell compartment. J Exp Med *207*, 1173-1182.

Morrison, S.J., Hemmati, H.D., Wandycz, A.M., and Weissman, I.L. (1995). The purification and characterization of fetal liver hematopoietic stem cells. Proc Natl Acad Sci U S A *92*, 10302-10306.

Morrison, S.J., Lagasse, E., and Weissman, I.L. (1994). Demonstration that Thy(lo) subsets of mouse bone marrow that express high levels of lineage markers are not significant hematopoietic progenitors. Blood *83*, 3480-3490.

Morrison, S.J., and Scadden, D.T. (2014). The bone marrow niche for haematopoietic stem cells. Nature *505*, 327-334.

Morrison, S.J., Wright, D.E., and Weissman, I.L. (1997). Cyclophosphamide/granulocyte colony-stimulating factor induces hematopoietic stem cells to proliferate prior to mobilization. Proc Natl Acad Sci U S A *94*, 1908-1913.

Moskow, J.J., Bullrich, F., Huebner, K., Daar, I.O., and Buchberg, A.M. (1995). Meis1, a PBX1-related homeobox gene involved in myeloid leukemia in BXH-2 mice. Molecular and cellular biology *15*, 5434-5443.

Mouratidis, P.X., Colston, K.W., and Dalgleish, A.G. (2007). Doxycycline induces caspase-dependent apoptosis in human pancreatic cancer cells. Int J Cancer *120*, 743-752.

Muller-Sieburg, C.E., Sieburg, H.B., Bernitz, J.M., and Cattarossi, G. (2012). Stem cell heterogeneity: implications for aging and regenerative medicine. Blood *119*, 3900-3907.

Na Nakorn, T., Traver, D., Weissman, I.L., and Akashi, K. (2002). Myeloerythroid-restricted progenitors are sufficient to confer radioprotection and provide the majority of day 8 CFU-S. J Clin Invest *109*, 1579-1585.

Nangaku, M., Izuhara, Y., Takizawa, S., Yamashita, T., Fujii-Kuriyama, Y., Ohneda, O., Yamamoto, M., van Ypersele de Strihou, C., Hirayama, N., and Miyata, T. (2007). A novel class of prolyl hydroxylase inhibitors induces angiogenesis and exerts organ protection against ischemia. Arteriosclerosis, thrombosis, and vascular biology *27*, 2548-2554.

Nilsson, S.K., Johnston, H.M., and Coverdale, J.A. (2001). Spatial localization of transplanted hemopoietic stem cells: inferences for the localization of stem cell niches. Blood *97*, 2293-2299.

Nombela-Arrieta, C., Pivarnik, G., Winkel, B., Canty, K.J., Harley, B., Mahoney, J.E., Park, S.Y., Lu, J., Protopopov, A., and Silberstein, L.E. (2013). Quantitative imaging of haematopoietic stem and progenitor cell localization and hypoxic status in the bone marrow microenvironment. Nature cell biology *15*, 533-543.

North, T.E., Stacy, T., Matheny, C.J., Speck, N.A., and de Bruijn, M.F. (2004). Runx1 is expressed in adult mouse hematopoietic stem cells and differentiating myeloid and lymphoid cells, but not in maturing erythroid cells. Stem cells (Dayton, Ohio) *22*, 158-168.

Notta, F., Zandi, S., Takayama, N., Dobson, S., Gan, O.I., Wilson, G., Kaufmann, K.B., McLeod, J., Laurenti, E., Dunant, C.F*., et al.* (2016). Distinct routes of lineage development reshape the human blood hierarchy across ontogeny. Science *351*, aab2116.

O'Duibhir, E., Paris, J., Lawson, H., Sepulveda, C., Shenton, D.D., Carragher, N.O., and Kranc, K.R. (2018). Machine Learning Enables Live Label-Free Phenotypic Screening in Three Dimensions. Assay and drug development technologies *16*, 51-63.

Ogilvy, S., Elefanty, A.G., Visvader, J., Bath, M.L., Harris, A.W., and Adams, J.M. (1998). Transcriptional regulation of vav, a gene expressed throughout the hematopoietic compartment. Blood *91*, 419-430.

Ogilvy, S., Metcalf, D., Gibson, L., Bath, M.L., Harris, A.W., and Adams, J.M. (1999). Promoter elements of vav drive transgene expression in vivo throughout the hematopoietic compartment. Blood *94*, 1855-1863.

Ogle, M.E., Gu, X., Espinera, A.R., and Wei, L. (2012). Inhibition of prolyl hydroxylases by dimethyloxaloylglycine after stroke reduces ischemic brain injury and requires hypoxia inducible factor-1α. Neurobiology of disease *45*, 733-742.

Oguro, H., Ding, L., and Morrison, S.J. (2013). SLAM family markers resolve functionally distinct subpopulations of hematopoietic stem cells and multipotent progenitors. Cell Stem Cell *13*, 102-116.

Okuda, T., van Deursen, J., Hiebert, S.W., Grosveld, G., and Downing, J.R. (1996). AML1, the target of multiple chromosomal translocations in human leukemia, is essential for normal fetal liver hematopoiesis. Cell *84*, 321-330.

Olive, P.L., Durand, R.E., Raleigh, J.A., Luo, C., and Aquino-Parsons, C. (2000). Comparison between the comet assay and pimonidazole binding for measuring tumour hypoxia. Br J Cancer *83*, 1525-1531.

Onoda, T., Ono, T., Dhar, D.K., Yamanoi, A., and Nagasue, N. (2006). Tetracycline analogues (doxycycline and COL-3) induce caspase-dependent and -independent apoptosis in human colon cancer cells. Int J Cancer *118*, 1309-1315.

Orford, K., Kharchenko, P., Lai, W., Dao, M.C., Worhunsky, D.J., Ferro, A., Janzen, V., Park, P.J., and Scadden, D.T. (2008). Differential H3K4 methylation identifies developmentally poised hematopoietic genes. Developmental cell *14*, 798-809.

Orkin, S.H., and Zon, L.I. (2008). Hematopoiesis: an evolving paradigm for stem cell biology. Cell *132*, 631-644.

Ottersbach, K., and Dzierzak, E. (2005). The murine placenta contains hematopoietic stem cells within the vascular labyrinth region. Developmental cell *8*, 377-387.

Ozer, A., and Bruick, R.K. (2005). Regulation of HIF by prolyl hydroxylases: recruitment of the candidate tumor suppressor protein ING4. Cell cycle (Georgetown, Tex) *4*, 1153-1156.

Palis, J., Robertson, S., Kennedy, M., Wall, C., and Keller, G. (1999). Development of erythroid and myeloid progenitors in the yolk sac and embryo proper of the mouse. Development (Cambridge, England) *126*, 5073-5084.

Pan, Y., Mansfield, K.D., Bertozzi, C.C., Rudenko, V., Chan, D.A., Giaccia, A.J., and Simon, M.C. (2007). Multiple factors affecting cellular redox status and energy metabolism modulate hypoxia-inducible factor prolyl hydroxylase activity in vivo and in vitro. Molecular and cellular biology *27*, 912-925.

Papaemmanuil, E., Dohner, H., and Campbell, P.J. (2016). Genomic Classification in Acute Myeloid Leukemia. N Engl J Med *375*, 900-901.

Parmar, K., Mauch, P., Vergilio, J.A., Sackstein, R., and Down, J.D. (2007). Distribution of hematopoietic stem cells in the bone marrow according to regional hypoxia. Proc Natl Acad Sci U S A *104*, 5431-5436.

Passaro, D., Di Tullio, A., Abarrategi, A., Rouault-Pierre, K., Foster, K., Ariza-McNaughton, L., Montaner, B., Chakravarty, P., Bhaw, L., Diana, G.*, et al.* (2017). Increased Vascular Permeability in the Bone Marrow Microenvironment Contributes to Disease Progression and Drug Response in Acute Myeloid Leukemia. Cancer Cell *32*, 324-341.e326.

Patterson, L.J., Gering, M., Eckfeldt, C.E., Green, A.R., Verfaillie, C.M., Ekker, S.C., and Patient, R. (2007). The transcription factors Scl and Lmo2 act together during development of the hemangioblast in zebrafish. Blood *109*, 2389-2398.

Pearce, D.J., Taussig, D., Simpson, C., Allen, K., Rohatiner, A.Z., Lister, T.A., and Bonnet, D. (2005). Characterization of cells with a high aldehyde dehydrogenase activity from cord blood and acute myeloid leukemia samples. Stem cells (Dayton, Ohio) *23*, 752-760.

Percy, M.J., Zhao, Q., Flores, A., Harrison, C., Lappin, T.R., Maxwell, P.H., McMullin, M.F., and Lee, F.S. (2006). A family with erythrocytosis establishes a role for prolyl hydroxylase domain protein 2 in oxygen homeostasis. Proc Natl Acad Sci U S A *103*, 654-659.

Pietras, E.M., Reynaud, D., Kang, Y.A., Carlin, D., Calero-Nieto, F.J., Leavitt, A.D., Stuart, J.M., Gottgens, B., and Passegue, E. (2015). Functionally Distinct Subsets of Lineage-Biased Multipotent Progenitors Control Blood Production in Normal and Regenerative Conditions. Cell Stem Cell *17*, 35-46.

Pineault, N., Helgason, C.D., Lawrence, H.J., and Humphries, R.K. (2002). Differential expression of Hox, Meis1, and Pbx1 genes in primitive cells throughout murine hematopoietic ontogeny. Exp Hematol *30*, 49-57.

Plass, M., Solana, J., Wolf, F.A., Ayoub, S., Misios, A., Glazar, P., Obermayer, B., Theis, F.J., Kocks, C., and Rajewsky, N. (2018). Cell type atlas and lineage tree of a whole complex animal by single-cell transcriptomics. Science *360*.

Pollyea, D.A., and Jordan, C.T. (2017). Therapeutic targeting of acute myeloid leukemia stem cells. Blood *129*, 1627-1635.

Pronk, C.J., Rossi, D.J., Mansson, R., Attema, J.L., Norddahl, G.L., Chan, C.K., Sigvardsson, M., Weissman, I.L., and Bryder, D. (2007). Elucidation of the phenotypic, functional, and molecular topography of a myeloerythroid progenitor cell hierarchy. Cell Stem Cell *1*, 428-442.

Pugh, C.W., and Ratcliffe, P.J. (2017). New horizons in hypoxia signaling pathways. Experimental cell research *356*, 116-121.

Qian, H., Buza-Vidas, N., Hyland, C.D., Jensen, C.T., Antonchuk, J., Mansson, R., Thoren, L.A., Ekblom, M., Alexander, W.S., and Jacobsen, S.E. (2007). Critical role of thrombopoietin in maintaining adult quiescent hematopoietic stem cells. Cell Stem Cell *1*, 671-684.

Ramos-Mejia, V., Navarro-Montero, O., Ayllon, V., Bueno, C., Romero, T., Real, P.J., and Menendez, P. (2014). HOXA9 promotes hematopoietic commitment of human embryonic stem cells. Blood *124*, 3065-3075.

Rasmussen, K.D., Simmini, S., Abreu-Goodger, C., Bartonicek, N., Di Giacomo, M., Bilbao-Cortes, D., Horos, R., Von Lindern, M., Enright, A.J., and O'Carroll, D. (2010). The miR-144/451 locus is required for erythroid homeostasis. J Exp Med *207*, 1351-1358.

Rhodes, J., Hagen, A., Hsu, K., Deng, M., Liu, T.X., Look, A.T., and Kanki, J.P. (2005). Interplay of pu.1 and gata1 determines myelo-erythroid progenitor cell fate in zebrafish. Developmental cell *8*, 97-108.

Robb, L., Lyons, I., Li, R., Hartley, L., Kontgen, F., Harvey, R.P., Metcalf, D., and Begley, C.G. (1995). Absence of yolk sac hematopoiesis from mice with a targeted disruption of the scl gene. Proc Natl Acad Sci U S A *92*, 7075-7079.

Rouault-Pierre, K., Lopez-Onieva, L., Foster, K., Anjos-Afonso, F., Lamrissi-Garcia, I., Serrano-Sanchez, M., Mitter, R., Ivanovic, Z., de Verneuil, H., Gribben, J*., et al.* (2013). HIF-2alpha protects human hematopoietic stem/progenitors and acute myeloid leukemic cells from apoptosis induced by endoplasmic reticulum stress. Cell Stem Cell *13*, 549-563.

Ruas, J.L., Poellinger, L., and Pereira, T. (2005). Role of CBP in regulating HIF-1-mediated activation of transcription. Journal of cell science *118*, 301-311.

Sanjuan-Pla, A., Macaulay, I.C., Jensen, C.T., Woll, P.S., Luis, T.C., Mead, A., Moore, S., Carella, C., Matsuoka, S., Bouriez Jones, T*., et al.* (2013). Platelet-biased stem cells reside at the apex of the haematopoietic stem-cell hierarchy. Nature *502*, 232-236.

Sarkozy, C., Gardin, C., Gachard, N., Merabet, F., Turlure, P., Malfuson, J.V., Pautas, C., Micol, J.B., Thomas, X., Quesnel, B*., et al.* (2013). Outcome of older patients with acute myeloid leukemia in first relapse. American journal of hematology *88*, 758-764.

Sauvageau, G., Lansdorp, P.M., Eaves, C.J., Hogge, D.E., Dragowska, W.H., Reid, D.S., Largman, C., Lawrence, H.J., and Humphries, R.K. (1994). Differential expression of homeobox genes in functionally distinct CD34+ subpopulations of human bone marrow cells. Proc Natl Acad Sci U S A *91*, 12223-12227.

Sawai, C.M., Babovic, S., Upadhaya, S., Knapp, D., Lavin, Y., Lau, C.M., Goloborodko, A., Feng, J., Fujisaki, J., Ding, L*., et al.* (2016). Hematopoietic Stem Cells Are the Major Source of Multilineage Hematopoiesis in Adult Animals. Immunity *45*, 597-609.

Schepers, K., Campbell, T.B., and Passegue, E. (2015). Normal and leukemic stem cell niches: insights and therapeutic opportunities. Cell Stem Cell *16*, 254-267.

Schodel, J., Oikonomopoulos, S., Ragoussis, J., Pugh, C.W., Ratcliffe, P.J., and Mole, D.R. (2011). High-resolution genome-wide mapping of HIF-binding sites by ChIP-seq. Blood *117*, e207-217.

Schofield, C.J., and Ratcliffe, P.J. (2005). Signalling hypoxia by HIF hydroxylases. Biochem Biophys Res Commun *338*, 617-626.

Schofield, R. (1978). The relationship between the spleen colony-forming cell and the haemopoietic stem cell. Blood cells *4*, 7-25.

Semenza, G.L. (2000). Surviving ischemia: adaptive responses mediated by hypoxia-inducible factor 1. J Clin Invest *106*, 809-812.

Serrano, N., Cortegano, I., Ruiz, C., Alia, M., de Andres, B., Rejas, M.T., Marcos, M.A., and Gaspar, M.L. (2012). Megakaryocytes promote hepatoepithelial liver cell development in E11.5 mouse embryos by cell-to-cell contact and by vascular endothelial growth factor A signaling. Hepatology *56*, 1934-1945.

Shima, H., Takubo, K., Iwasaki, H., Yoshihara, H., Gomei, Y., Hosokawa, K., Arai, F., Takahashi, T., and Suda, T. (2009). Reconstitution activity of hypoxic cultured human cord blood CD34-positive cells in NOG mice. Biochem Biophys Res Commun *378*, 467-472.

Shimshek, D.R., Kim, J., Hubner, M.R., Spergel, D.J., Buchholz, F., Casanova, E., Stewart, A.F., Seeburg, P.H., and Sprengel, R. (2002). Codon-improved Cre recombinase (iCre) expression in the mouse. Genesis (New York, NY : 2000) *32*, 19-26.

Simsek, T., Kocabas, F., Zheng, J., Deberardinis, R.J., Mahmoud, A.I., Olson, E.N., Schneider, J.W., Zhang, C.C., and Sadek, H.A. (2010). The distinct metabolic profile of hematopoietic stem cells reflects their location in a hypoxic niche. Cell Stem Cell *7*, 380-390.

Singh, R.P., Franke, K., Kalucka, J., Mamlouk, S., Muschter, A., Gembarska, A., Grinenko, T., Willam, C., Naumann, R., Anastassiadis, K*., et al.* (2013). HIF prolyl hydroxylase 2 (PHD2) is a critical regulator of hematopoietic stem cell maintenance during steady-state and stress. Blood *121*, 5158-5166.

Slany, R.K. (2009). The molecular biology of mixed lineage leukemia. Haematologica *94*, 984-993.

Somervaille, T.C., Matheny, C.J., Spencer, G.J., Iwasaki, M., Rinn, J.L., Witten, D.M., Chang, H.Y., Shurtleff, S.A., Downing, J.R., and Cleary, M.L. (2009). Hierarchical maintenance of MLL myeloid leukemia stem cells employs a transcriptional program shared with embryonic rather than adult stem cells. Cell Stem Cell *4*, 129-140.

Song, H., Fares, M., Maguire, K.R., Siden, A., and Potacova, Z. (2014). Cytotoxic effects of tetracycline analogues (doxycycline, minocycline and COL-3) in acute myeloid leukemia HL-60 cells. PLoS One *9*, e114457.

Spangrude, G.J., Aihara, Y., Weissman, I.L., and Klein, J. (1988). The stem cell antigens Sca-1 and Sca-2 subdivide thymic and peripheral T lymphocytes into unique subsets. Journal of immunology (Baltimore, Md : 1950) *141*, 3697-3707.

Spencer, J.A., Ferraro, F., Roussakis, E., Klein, A., Wu, J., Runnels, J.M., Zaher, W., Mortensen, L.J., Alt, C., Turcotte, R*., et al.* (2014). Direct measurement of local oxygen concentration in the bone marrow of live animals. Nature *508*, 269-273.

Spivak, J.L., Considine, M., Williams, D.M., Talbot, C.C., Rogers, O., Moliterno, A.R., Jie, C., and Ochs, M.F.

Stavropoulou, V., Kaspar, S., Brault, L., Sanders, M.A., Juge, S., Morettini, S., Tzankov, A., Iacovino, M., Lau, I.J., Milne, T.A*., et al.* (2016). MLL-AF9 Expression in Hematopoietic Stem Cells Drives a Highly Invasive AML Expressing EMT-Related Genes Linked to Poor Outcome. Cancer Cell *30*, 43-58.

Stiehl, D.P., Wirthner, R., Koditz, J., Spielmann, P., Camenisch, G., and Wenger, R.H. (2006). Increased prolyl 4-hydroxylase domain proteins compensate for decreased oxygen levels. Evidence for an autoregulatory oxygen-sensing system. J Biol Chem *281*, 23482-23491.

Sugiyama, T., Kohara, H., Noda, M., and Nagasawa, T. (2006). Maintenance of the hematopoietic stem cell pool by CXCL12-CXCR4 chemokine signaling in bone marrow stromal cell niches. Immunity *25*, 977-988.

Taichman, R.S., and Emerson, S.G. (1994). Human osteoblasts support hematopoiesis through the production of granulocyte colony-stimulating factor. J Exp Med *179*, 1677-1682.

Takeda, K., Aguila, H.L., Parikh, N.S., Li, X., Lamothe, K., Duan, L.J., Takeda, H., Lee, F.S., and Fong, G.H. (2008). Regulation of adult erythropoiesis by prolyl hydroxylase domain proteins. Blood *111*, 3229-3235.

Takeda, K., Cowan, A., and Fong, G.H. (2007). Essential role for prolyl hydroxylase domain protein 2 in oxygen homeostasis of the adult vascular system. Circulation *116*, 774-781.

Takeda, K., Ho, V.C., Takeda, H., Duan, L.J., Nagy, A., and Fong, G.H. (2006). Placental but not heart defects are associated with elevated hypoxia-inducible factor alpha levels in mice lacking prolyl hydroxylase domain protein 2. Molecular and cellular biology *26*, 8336-8346.

Takeda, N., O'Dea, E.L., Doedens, A., Kim, J.W., Weidemann, A., Stockmann, C., Asagiri, M., Simon, M.C., Hoffmann, A., and Johnson, R.S. (2010). Differential activation and antagonistic function of HIF-{alpha} isoforms in macrophages are essential for NO homeostasis. Genes Dev *24*, 491-501.

Takubo, K., Goda, N., Yamada, W., Iriuchishima, H., Ikeda, E., Kubota, Y., Shima, H., Johnson, R.S., Hirao, A., Suematsu, M.*, et al.* (2010). Regulation of the HIF-1alpha level is essential for hematopoietic stem cells. Cell Stem Cell *7*, 391-402.

Tang, Q., Iyer, S., Lobbardi, R., Moore, J.C., Chen, H., Lareau, C., Hebert, C., Shaw, M.L., Neftel, C., Suva, M.L.*, et al.* (2017). Dissecting hematopoietic and renal cell heterogeneity in adult zebrafish at single-cell resolution using RNA sequencing. J Exp Med *214*, 2875-2887.

Teitell, M.A., and Mikkola, H.K. (2006). Transcriptional activators, repressors, and epigenetic modifiers controlling hematopoietic stem cell development. Pediatric research *59*, 33r-39r.

Till, J.E., and Mc, C.E. (1961). A direct measurement of the radiation sensitivity of normal mouse bone marrow cells. Radiation research *14*, 213-222.

Tsai, F.Y., Keller, G., Kuo, F.C., Weiss, M., Chen, J., Rosenblatt, M., Alt, F.W., and Orkin, S.H. (1994). An early haematopoietic defect in mice lacking the transcription factor GATA-2. Nature *371*, 221-226.

Unwin, R.D., Smith, D.L., Blinco, D., Wilson, C.L., Miller, C.J., Evans, C.A., Jaworska, E., Baldwin, S.A., Barnes, K., Pierce, A.*, et al.* (2006). Quantitative proteomics reveals posttranslational control as a regulatory factor in primary hematopoietic stem cells. Blood *107*, 4687-4694.

van Rhenen, A., Feller, N., Kelder, A., Westra, A.H., Rombouts, E., Zweegman, S., van der Pol, M.A., Waisfisz, Q., Ossenkoppele, G.J., and Schuurhuis, G.J. (2005). High stem cell frequency in acute myeloid leukemia at diagnosis predicts high minimal residual disease and poor survival. Clinical cancer research : an official journal of the American Association for Cancer Research *11*, 6520-6527.

Velasco-Hernandez, T., Hyrenius-Wittsten, A., Rehn, M., Bryder, D., and Cammenga, J. (2014). HIF-1alpha can act as a tumor suppressor gene in murine acute myeloid leukemia. Blood *124*, 3597-3607.

Velten, L., Haas, S.F., Raffel, S., Blaszkiewicz, S., Islam, S., Hennig, B.P., Hirche, C., Lutz, C., Buss, E.C., Nowak, D.*, et al.* (2017). Human haematopoietic stem cell lineage commitment is a continuous process. Nature cell biology *19*, 271-281.

Vukovic, M., Guitart, A.V., Sepulveda, C., Villacreces, A., O'Duibhir, E., Panagopoulou, T.I., Ivens, A., Menendez-Gonzalez, J., Iglesias, J.M., Allen, L.*, et al.* (2015). Hif-1alpha and Hif-2alpha synergize to suppress AML development but are dispensable for disease maintenance. J Exp Med *212*, 2223-2234.

Vukovic, M., Sepulveda, C., Subramani, C., Guitart, A.V., Mohr, J., Allen, L., Panagopoulou, T.I., Paris, J., Lawson, H., Villacreces, A.*, et al.* (2016). Adult hematopoietic stem cells lacking Hif-1alpha self-renew normally. Blood *127*, 2841-2846.

Wang, G.L., Jiang, B.H., Rue, E.A., and Semenza, G.L. (1995). Hypoxia-inducible factor 1 is a basic-helix-loop-helix-PAS heterodimer regulated by cellular O2 tension. Proc Natl Acad Sci U S A *92*, 5510-5514.

Wang, J.C., and Dick, J.E. (2005). Cancer stem cells: lessons from leukemia. Trends in cell biology *15*, 494-501.

Wang, Y., Liu, Y., Malek, S.N., Zheng, P., and Liu, Y. (2011). Targeting HIF1α eliminates cancer stem cells in hematological malignancies. Cell Stem Cell *8*, 399-411.

Weiss, M.J., and Orkin, S.H. (1995). GATA transcription factors: key regulators of hematopoiesis. Exp Hematol *23*, 99-107.

Weissman, I.L., Anderson, D.J., and Gage, F. (2001). Stem and progenitor cells: origins, phenotypes, lineage commitments, and transdifferentiations. Annual review of cell and developmental biology *17*, 387-403.

Wilson, A., Laurenti, E., Oser, G., van der Wath, R.C., Blanco-Bose, W., Jaworski, M., Offner, S., Dunant, C.F., Eshkind, L., Bockamp, E*., et al.* (2008). Hematopoietic stem cells reversibly switch from dormancy to self-renewal during homeostasis and repair. Cell *135*, 1118-1129.

Wilson, A., Laurenti, E., and Trumpp, A. (2009). Balancing dormant and self-renewing hematopoietic stem cells. Current opinion in genetics & development *19*, 461-468.

Wong, P., Iwasaki, M., Somervaille, T.C., So, C.W., and Cleary, M.L. (2007). Meis1 is an essential and rate-limiting regulator of MLL leukemia stem cell potential. Genes Dev *21*, 2762-2774.

Wulf, G.G., Wang, R.Y., Kuehnle, I., Weidner, D., Marini, F., Brenner, M.K., Andreeff, M., and Goodell, M.A. (2001). A leukemic stem cell with intrinsic drug efflux capacity in acute myeloid leukemia. Blood *98*, 1166-1173.

Wunderlich, M., Mizukawa, B., Chou, F.S., Sexton, C., Shrestha, M., Saunthararajah, Y., and Mulloy, J.C. (2013). AML cells are differentially sensitive to chemotherapy treatment in a human xenograft model. Blood *121*, e90-97.

Xie, Y., Yin, T., Wiegraebe, W., He, X.C., Miller, D., Stark, D., Perko, K., Alexander, R., Schwartz, J., Grindley, J.C*., et al.* (2009). Detection of functional haematopoietic stem cell niche using real-time imaging. Nature *457*, 97-101.

Yamada, Y., Warren, A.J., Dobson, C., Forster, A., Pannell, R., and Rabbitts, T.H. (1998). The T cell leukemia LIM protein Lmo2 is necessary for adult mouse hematopoiesis. Proc Natl Acad Sci U S A *95*, 3890-3895.

Yamamoto, R., Morita, Y., Ooehara, J., Hamanaka, S., Onodera, M., Rudolph, K.L., Ema, H., and Nakauchi, H. (2013). Clonal analysis unveils self-renewing lineage-restricted progenitors generated directly from hematopoietic stem cells. Cell *154*, 1112-1126.

Yamazaki, S., Iwama, A., Takayanagi, S., Eto, K., Ema, H., and Nakauchi, H. (2009). TGF-beta as a candidate bone marrow niche signal to induce hematopoietic stem cell hibernation. Blood *113*, 1250-1256.

Yoshihara, H., Arai, F., Hosokawa, K., Hagiwara, T., Takubo, K., Nakamura, Y., Gomei, Y., Iwasaki, H., Matsuoka, S., Miyamoto, K*., et al.* (2007). Thrombopoietin/MPL signaling regulates hematopoietic stem cell quiescence and interaction with the osteoblastic niche. Cell Stem Cell *1*, 685-697.

Zanjani, E.D., Ascensao, J.L., and Tavassoli, M. (1993). Liver-derived fetal hematopoietic stem cells selectively and preferentially home to the fetal bone marrow. Blood *81*, 399-404.

Zhang, J., Niu, C., Ye, L., Huang, H., He, X., Tong, W.G., Ross, J., Haug, J., Johnson, T., Feng, J.Q.*, et al.* (2003). Identification of the haematopoietic stem cell niche and control of the niche size. Nature *425*, 836-841.

Zhang, P., Iwasaki-Arai, J., Iwasaki, H., Fenyus, M.L., Dayaram, T., Owens, B.M., Shigematsu, H., Levantini, E., Huettner, C.S., Lekstrom-Himes, J.A.*, et al.*

Zhang, Y., Gao, S., Xia, J., and Liu, F. (2018). Hematopoietic Hierarchy - An Updated Roadmap. Trends in cell biology *28*, 976-986.

Zhang, Y., Payne, K.J., Zhu, Y., Price, M.A., Parrish, Y.K., Zielinska, E., Barsky, L.W., and Crooks, G.M. (2005). SCL expression at critical points in human hematopoietic lineage commitment. Stem cells (Dayton, Ohio) *23*, 852-860.

Zhao, M., Perry, J.M., Marshall, H., Venkatraman, A., Qian, P., He, X.C., Ahamed, J., and Li, L. (2014). Megakaryocytes maintain homeostatic quiescence and promote post-injury regeneration of hematopoietic stem cells. Nat Med *20*, 1321-1326.

Zhen, L., Shijie, N., and Shuijun, Z. (2014). Tumor PHD2 expression is correlated with clinical features and prognosis of patients with HCC receiving liver resection. Medicine *93*, e179.

Zhou, H.S., Carter, B.Z., and Andreeff, M. (2016). Bone marrow niche-mediated survival of leukemia stem cells in acute myeloid leukemia: Yin and Yang. Cancer biology & medicine *13*, 248-259.

Zijlmans, J.M., Visser, J.W., Laterveer, L., Kleiverda, K., Heemskerk, D.P., Kluin, P.M., Willemze, R., and Fibbe, W.E. (1998). The early phase of engraftment after murine blood cell transplantation is mediated by hematopoietic stem cells. Proc Natl Acad Sci U S A *95*, 725-729.

Zuber, J., Radtke, I., Pardee, T.S., Zhao, Z., Rappaport, A.R., Luo, W., McCurrach, M.E., Yang, M.M., Dolan, M.E., Kogan, S.C.*, et al.* (2009). Mouse models of human AML accurately predict chemotherapy response. Genes Dev *23*, 877-889.